Developing quantitative GTPase affinity purification (qGAP) to identify interaction partners of Rho GTPases

Dissertation

zur Erlangung des akademischen Grades

doctor rerum naturalium

(Dr. rer. nat.)

eingereicht im Fachbereich Biologie, Chemie, Pharmazie

der Freien Universität Berlin

vorgelegt von

FLORIAN ERNST RUDOLF BENJAMIN PAUL (DIPL.-BIOCHEM.)

Januar 2014

Die vorliegende Arbeit wurde von Oktober 2008 bis Januar 2014 am Max-Delbrück-Centrum für Molekulare Medizin unter der Anleitung von Prof. Dr. MATTHIAS SELBACH angefertigt.

1. Gutachter: Prof. Dr. MATTHIAS SELBACH
   Cell Signalling and Mass Spectrometry
   Max-Delbrück-Centrum, Berlin
2. Gutachter: Prof. Dr. UDO HEINEMANN
   Institut für Chemie / Biochemie
   Freie Universität Berlin / Max-Delbrück-Centrum, Berlin

Disputation am 8. Mai 2014

“Study hard what interests you the most in the most undisciplined, irreverent and original manner possible.” — Richard P. Feynman

Contents

Summary

Rho GTPases are central regulators of the actin cytoskeleton. Additionally, they have influence on gene expression, cell division and other biological processes. Classical Rho GTPases function as molecular switches, being active when GTP is bound and inactive in the GDP-bound state. The exchange of nucleotides, the GDP/GTP cycle, is subject to intense regulation. The multiple biological activities of Rho GTPases are mediated by numerous downstream effector proteins. However, a systematic experimental comparison of Rho GTPase interaction partners has not been performed.

This thesis describes development, validation and biological outcome of a new method to identify Rho GTPase effector proteins for both of the nucleotide-loaded forms. We named this assay quantitative GTPase affinity pull-down (qGAP). qGAP combines affinity purification with quantitative mass spectrometry. Recombinant Rho GTPases were purified and loaded with either GDP or GTPγS. The Rho GTPases were covalently coupled to a sepharose matrix and used for affinity purification. Quantitative shotgun proteomics was then used to compare the abundance of proteins interacting with the GDP- and GTPγS-loaded forms, to identify loading state-specific binders.

First, qGAP was applied to RhoA, Rac1 and Cdc42 to identify binding partners from cytoplasmic extracts of SILAC-labeled HeLa cells (SILAC-qGAP). Next, lysates from mouse brains were used to identify interaction partners of RhoA, RhoB, RhoC, RhoD, Rac1 and Cdc42 using label free quantification (LF-qGAP). In both variants of qGAP, groups of specific binders could be distinguished from hundreds to thousands of background binders. Interaction partners identified by qGAP where highly enriched with known Rho interaction partners when compared to an unbiased reference database. For LF-qGAP, the sensitivity was good (50%) and the specificity excellent (97%). If further studies show, that the newly identified interaction partners are true, the real sensitivity might be higher. Hierarchical clustering of biological replicate samples showed that qGAP data was highly reproducible. In total, LF-qGAP identified 291 mostly novel interactions. Eleven out of twelve tested novel interactions were confirmed by a newly developed, independent assay.

From the binding data a comprehensive Rho interaction network was constructed. We found the promiscuousness of binding partners to be higher than anticipated. The overlap allowed us to deduce similarities between the network and the phylogeny of Rho GTPases. Altogether, these data show that qGAP is a valuable novel method to study Rho GTPase biology.

Zusammenfassung

Rho GTPasen stellen zentrale Regulatoren des Aktin-Zytoskeletts dar. Zusätzlich können sie die Genexpression, Zellteilung und andere biologische Prozesse beeinflussen. Die klassischen Rho GTPasen sind molekulare Schalter. Wenn sie GTP gebunden haben befinden sie sich im aktiven, bei Bindung von GDP im inaktiven Zustand. Der Austausch dieser beiden Nukleotide, auch GDP/GTP-Zyklus genannt, wird streng reguliert. Die vielfältigen biologischen Aktivitäten der Rho GTPasen werden durch zahlreiche Effektoren vermittelt. Trotz ihrer Wichtigkeit wurde eine systematische Untersuchung dieser Interaktionspartner noch nicht durchgeführt.

In dieser Doktorarbeit sind die Entwicklung, die Validierung und die biologischen Ergebnisse einer neuen Methode zur Identifizierung von Rho GTPase Effektoren beschrieben. Diese Methode wurde von uns „quantitative GTPase affinity pull-down“ (quantitativer GTPasen Affinitäts Pulldown, qGAP) genannt. qGAP vereinigt die Affinitäts-Aufreinigung (Pulldown) mit quantitativer Massenspektrometrie. Dabei werden beide Nukleotid-Ladungszustände berücksichtigt. Zu diesem Zweck wurden rekombinante Rho GTPasen aufgereinigt und entweder mit GDP oder GTPγS geladen. Die Rho GTPasen wurden kovalent an eine Sepharose Matrix gekoppelt und für Affinitätsaufreinigung eingesetzt. Quantitative shotgun proteomics wurde verwendet, um die Menge von Proteinen zu vergleichen, die mit der GDP- und GTPγS-geladenen Form interagiert haben. Dadurch wurden Ladungs-spezifische Bindungspartner identifiziert.

Zunächst wurde qGAP mit RhoA, Rac1 und Cdc42 auf zytoplasmatische Extrakte von SILAC-markierten HeLa Zellen angewendet (SILAC-qGAP). Im nächsten Schritt wurden Lysate von unmarkierten Maus Gehirnen verwendet um Interaktionspartner von RhoA, RhoB, RhoC, RhoD, Rac1 und Cdc42 zu identifizieren (LF-qGAP). In beiden Varianten von qGAP konnten Gruppe von spezifischen Interaktionspartnern klar von hunderten bis tausenden von Proteinen unterschieden werden. Durch den Vergleich mit einer Interaktionsdatenbank wurde festgestellt, dass diese spezifischen Interaktionspartner klar mit bekannten Rho Effektoren angereichert waren. Für LF-qGAP war die Sensitivität gut (50%) und die Spezifizität exzellent (97%). Falls weitere Studien zeigen, dass die neuen Interaktionspartner wahr sind, könnte die tatsächliche Sensitivität höher liegen. Eine hierarchische Clusteranalyse der biologischen Replikate ergab, dass qGAP sehr reproduzierbar war. Insgesamt wurden mit qGAP 291, größtenteils neue Interaktionspartner identifiziert. Elf von zwölf getesteten neuen Interaktionen wurden durch eine neu entwickelte, unabhängige Methode validiert.

Die Bindungsdaten wurden verwendet um ein umfassendes Rho Interaktionsnetzwerk zu erstellen. Es wurde eine höhere Promiskuität zwischen Bindungspartnern gefunden als zuvor vermutet. Das Überlappen von Bindungspartnern erlaubte uns auf Ähnlichkeiten zwischen dem Netzwerk und der

Stammesgeschichte der Rho-GTPasen zu folgern. Zusammenfassend zeigen die Daten, dass qGAP eine wertvolle neue Methode zum Studium der Rho GTPasen Biologie darstellt.

1 Introduction

Protein-protein interactions (PPIs) are essential for almost every biological process. Specifically, cellular signal transduction depends on the dynamic interaction of proteins with each other. These cascades are highly regulated and influence gene expression, cell death and survival or cell communication among other processes. The activation state of a signaling cascade is key to its control.

Rho (Ras homologues) GTPases are particularly important molecules in cellular signal transduction. The membrane-anchored proteins are central regulators of the actin cytoskeleton, and determine the morphology and motility of eukaryotic cells[1–3]. Furthermore Rho proteins have implications for cell polarity, cell division, gene regulation and apoptosis. Their activity is tightly controlled by the GDP/GTP cycle: GTP-bound Rho proteins are active, hydrolysis of the nucleotide to GDP renders them inactive.

PPIs have been systematically studied with the help of a broad range of tools. Most prominently, the yeast two-hybrid approach was used in large scale screening. Good scalability and easy handling made it a very popular method for the discovery of interactions. On the other hand, yeast two-hybrid suffers from a high false positive rate and the cellular background of interactions is not taken into account. In recent years affinity purification followed by quantitative mass spectrometry (q-AP/MS) has become a powerful alternative to identify PPIs.

The objective of this thesis is the systematic analysis of interaction partners of selected Rho GTPases. To this end, a quantitative proteomic approach is developed and employed. Interaction partners of Rho GTPases are identified in lysates from cell culture and whole organ samples. The quantification is performed with a stable-isotope and a label-free approach. The goal is to provide the scientific community with a comprehensive Rho GTPase interactome for the selected Rho proteins.

In the following introduction, the family of Rho GTPases is described and details about its members and their regulation are presented. Next, the cellular function of Rho GTPases and their relevance for diseases is outlined. Then, the fundamentals of quantitative mass spectrometry-based proteomics are explained with focus on the technologies to study PPIs. Finally the objectives of the thesis are delineated.

1.1 Rho GTPases

1.1.1 The GDP/GTP cycle

The Rho family is part of the superfamily of Ras (Rat sarcoma) GTPases, which are regulated via the GDP/GTP cycle: Inactive Rho proteins bind GDP, the nucleotide is released with the help of guanine exchange factors (GEFs) and is replaced by GTP[4] (see Figure 1.1). The Rho^{GTP} form represents the active form of the GTPase, it binds to downstream effectors that mediate the biological activity. Rho proteins possess a low intrinsic GTP hydrolysis rate that is enhanced by GTPase activating proteins (GAPs). GTP hydrolysis returns the enzyme to its inactive, GDP bound state, thus closing the GDP/GTP cycle[5]. This 'on' versus 'off' function renders Rho GTPases perfect bimolecular switches and offers multiple ways of regulation. Additionally, the activity of Rho GTPases can be modulated by guanine dissociation inhibitors (GDIs). GDIs extract Rho^{GDP} from the membrane, thereby reducing the Rho molecules that participate in the GTP cycle[6]. Rho proteins that are regulated by the GDP/GTP cycle are commonly called 'classical' Rho GTPases whereas 'atypical' Rho proteins (e.g. RhoU/Rnd) are in most cases not able to hydrolyze the nucleotide. Rho proteins are targeted by several bacterial toxins such as CNF1 and CNF_Y (cytotoxic necrotizing factor 1 and Y) from *E. coli*. These toxins circumvent the GDP/GTP cycle by constitutively activating Rho GTPases.

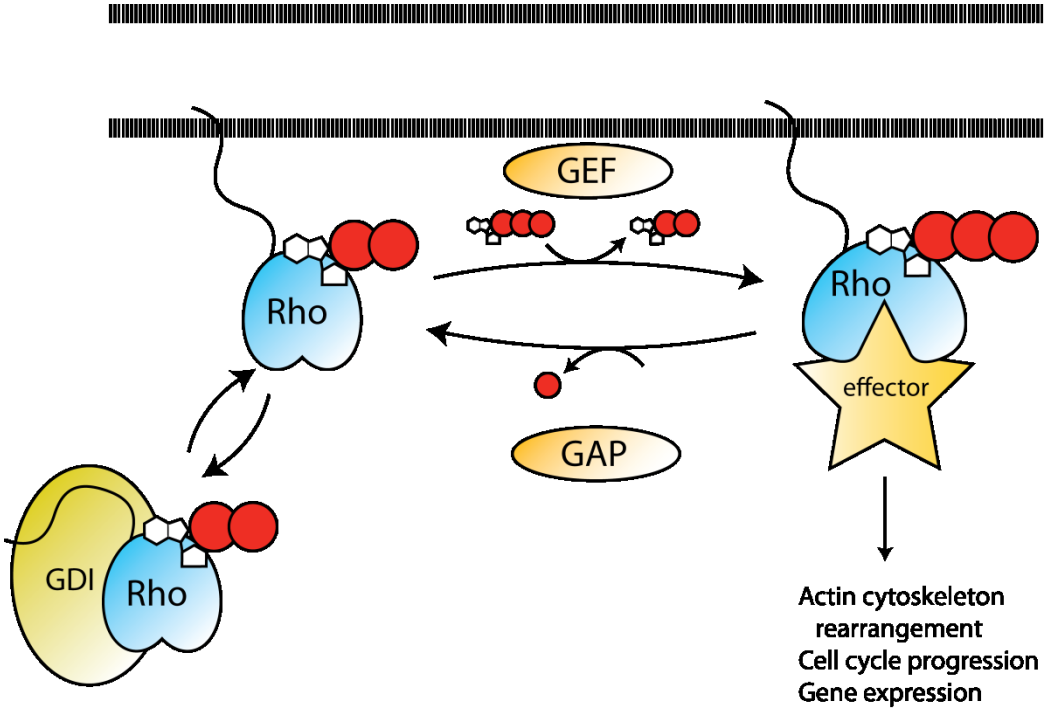

Figure 1.1: The GDP/GTP cycle is a main characteristic of classical Rho GTPases. Rho^{GDP} and Rho^{GTP} (symbolized with two or three phosphates as red dots) are located at the plasma membrane (symbolized with two dashed lines). Rho GTPases function as molecular switches between an on and off state. GEF proteins regulate Rho activation in a spatio-temporal manner. Rho^{GTP} binds to downstream effectors and influences a large number of cellular processes. GAP proteins terminate Rho signaling by facilitating GTP-hydrolysis. GDIs extract Rho^{GDP} from the membrane and create a cytosolic pool of Rho GTPases.

1.1.2 Rho GTPases as part of the Ras superfamily

The proto-oncogene Ras was the first member of the Ras superfamily discovered from two cancer-causing viruses and named the whole class. The Ras superfamily consists of the five branches Ras, Rho, Arf, Rab and Ran[7]. Occasionally the Rap, Rheb, RGK, Rit and Miro groups are classified as distinct families, with the latter closely related to the Rho family. The protein families are characterized through shared biological functions like cell proliferation (Ras), cytoskeletal dynamics (Rho), membrane trafficking (Rab)[8], vesicular transport (Arf) and nuclear transport (Ran) and sequence or structural similarities. For example, the 3-turn α-helix is a typical characteristic of Rho proteins. Within the 150 proteins of the Ras superfamily, the family of Rho GTPases covers 20 proteins (Figure 1.2).

All members of the Ras superfamily are small or monomeric GTPases possessing a conserved core G domain. The G domain binds guanine nucleotides and has in most cases the ability to hydrolyze and exchange the nucleotide[7,9]. In a few cases GTP has no detectable turnover (Rnd subfamily) or was evolutionary replaced by ATP (RhoBTB3[10]). The G domain fold is formed by a six-stranded mixed β-sheet with five helices on both sides, rendering it a typical α,β-nucleotide binding domain. The typical G domain consists of a set of conserved G box elements (GDP/GTP binding motif), which are, starting at the amino-terminus: G1 GxxxxGKS/T; G2, T; G3, DXXGQ/H/T; G4, T/NKXD; and G5, C/SAK/L/T [11] with an overall lengths of 160-180 amino acids. The guanine nucleotide is bound to the purine binding signature of the G1 box (named P-loop or Walker A motif). Magnesium serves as an essential cofactor.

To elucidate changes between the GDP- and GTP-bound states, the structures of Ras^{GPPNHP} (a non-hydrolyzable GTP analogue) and Ras^{GDP} were compared. It was suggested, that two flexible regions of Ras named switch I and II (located in the G2/G3 boxes respectively) are undergoing conformational rearrangement. This is accomplished by the formation of hydrogen bonds between the γ-phosphate of GTP and conserved threonine and glycine residues subsequently allowing the protein to bind downstream effectors. The comparison of the Ras^{GPPNHP} and Ras^{GDP} structures also allowed concluding on the mechanisms of GTP hydrolysis: A conserved glutamine is essential for GTP hydrolysis and probably functions as base. The C-terminal isoprenylation is responsible for correct membrane insertion. It is another feature shared by the Ras superfamily members.

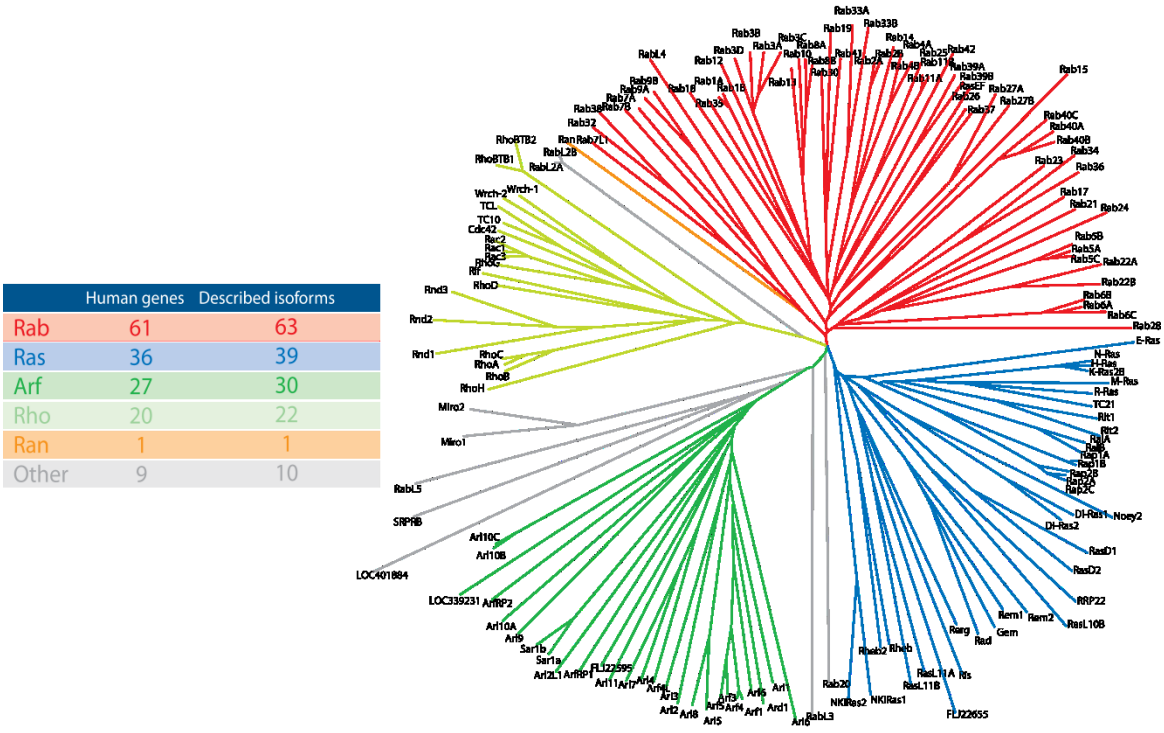

	Human genes	Described isoforms
Rab	61	63
Ras	36	39
Arf	27	30
Rho	20	22
Ran	1	1
Other	9	10

Figure 1.2: The superfamily of Ras proteins. Ras proteins share the G domain and influence cellular signaling, trafficking, gene expression and the cytoskeleton amongst other processes. In contrast to the heterotrimeric G proteins, Ras proteins act as small monomeric GTPases. Ras proteins are subdivided into Rab, Ras, Arf, Rho and Ran families (adapted with permission from Wennerberg et al., Journal of Cell Science, 2005[7]).

1.1.3 The family of Rho GTPases

Rho GTPases are 20 - 40 kDa in size and consist of the G domain and short N- and C-terminal extensions. RhoA, Rac1 and Cdc42 are the best-characterized members of the Rho GTPase family. RhoA was the first member of the family to be described as a Ras related protein in *Aplysia*[12]. In general RhoA is located in the central and rear regions of mammalian cells where it promotes the assembly and activity of contractile actin-myosin stress fibers and the formation of focal contacts[13]. Furthermore, RhoA suppresses the formation of cellular protrusions. Rac1 is linked to the expansion of lamellipodia[14] and Cdc42 to the creation of filopodia[15,16]. In the following, the term 'Rho' is generally used to represent any Rho GTPase (also Rac1 or Cdc42). It is to be distinguished from the specific protein RhoA or the Rho subfamily (RhoA, RhoB and RhoC).

Rho proteins are present in all eukaryotic species, with five members in *S. cerevisiae*, ten in *C. elegans*, eight in *D. melanogaster* and eleven in *A. thaliana*. The unique Rho GTPase subfamily ROP (Rho-related GTPase from plants) represents the only family of small GTPase involved in signal transduction in plants. ROPs share the highest sequence homology with Rac proteins and mediate both-, pathways that are plant specific and conserved in all eukaryotes. In mammalian systems 20 Rho proteins are present, accompanied by two members of the sister family of Miro GTPases. Miro

GTPases (Mitochondrial Rho) are ~70 kDa proteins with the typical G domain and two Ca^{2+}-binding EF hands. Rho genes display a high degree of conservation between species. For example, the mammalian Cdc42 is partly able to rescue deletions in *S. cerevisiae* Cdc42[17].

The mammalian Rho family of GTPases can be categorized into four classical and four atypical subfamilies (Figure 1.3). The atypical Rho GTPases do not follow the common GEF- and GAP- dictated activation scheme. In the following paragraphs, the members of the four classical subfamilies of Rho GTPases (Rho, Rac, Cdc42/TC10 and RhoD/Rif) and their main differences are briefly described.

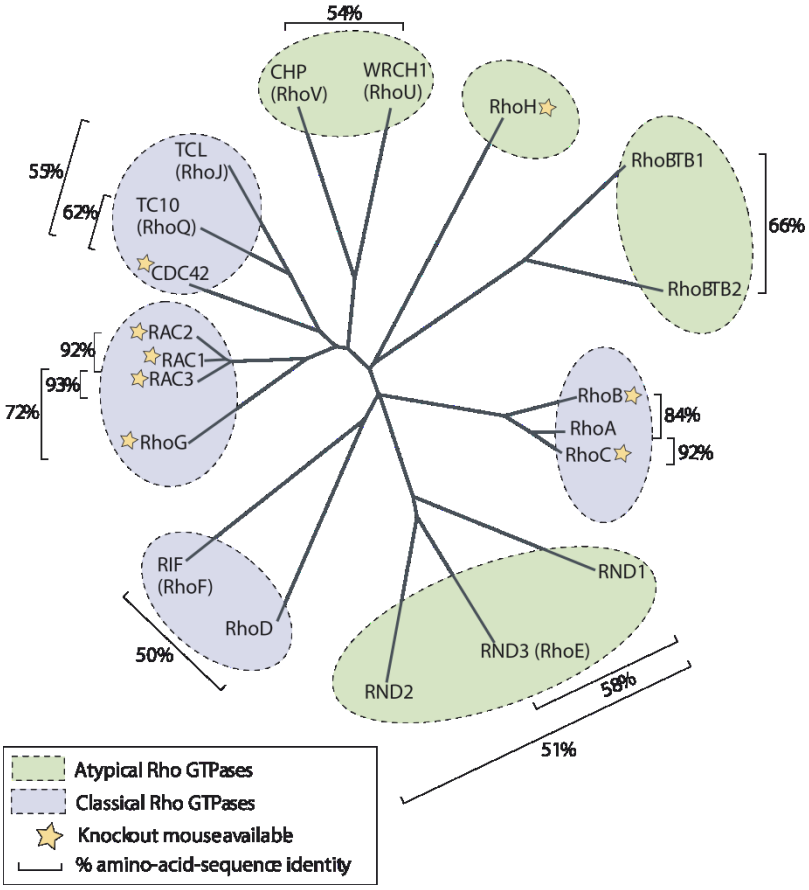

Figure 1.3: The family of Rho GTPases consists of four classical (Rho, Rac, Cdc42/TC10, RhoD/Rif) and four atypical (RhoU/RhoV, RhoH, RhoBTB and Rnd) subfamilies. The figure displays an unrooted phylogentic tree based on amino-acid alignment by ClustalW. Classical Rho GTPases are regulated by the GDP/GTP cycle. The Rac1 and Cdc42 subfamily are most closely related within the classical GTPases. Atypical Rho GTPases do mostly not possess detectable GTP hydrolysis capability and are rather regulated by expression. The amount of amino-acid-sequence identity within subfamilies was calculated by EMBOSS pairwise alignment (reproduced with permission from Heasman et al., Nature Reviews Molecular Cell Biology, 2008[18]).

The Rho subfamily within the Rho family consists of the three members RhoA, RhoB and RhoC sharing 85% sequence identity. All three possess the ability to induce stress fibers in cells[13,19]. Despite

the high sequence homology the proteins seem to have different cellular functions. Whereas RhoA-knockout mice have not been reported RhoB-null and RhoC-null mice have no major developmental defects[20,21]. RhoB in contrast to the other two members contains a palmitoylation site and seems to more specifically bind to Rho GDI 3[22]. RhoB plays a role in endosomal trafficking whereas RhoC is highly upregulated in metastatic cancer and therefore may more strongly regulate cellular locomotion[23].

All members of the Rac1 family are able to stimulate the formation of lamellipodia and membrane ruffles[14,24]. Beside Rac1, Rac2 and Rac3 the splice variant Rac1b with an increased intrinsic exchange rate was described[25]. A Rac2-specific production of reactive oxygen species by NADPH-oxidase[26] plays a role in hematopoietic cells[27]. Rac3 is more distinctly localized to the plasma membrane compared to Rac1 and is often present in breast cancer cell lines[28]. RhoG regulates NGF (nerve growth factor) stimulated neurite outgrowth[29].

The Cdc42 subfamily comprises members Cdc42, TC10 (RhoQ) and TCL (RhoJ). As common biological function all members stimulate the formation of filopodia by WASP (Wiscott-Aldrich syndrome protein)[30]. The effector proteins and biological properties between the Cdc42-related proteins overlap in large parts. The most interesting difference is an additional palmitoylation of TC10 preventing recognition by Rho GDI 1[31]. TC10 and TCL expression are upregulated during nerve regeneration[32].

The RhoD/Rif family is less investigated than the other subfamilies. RhoD and Rif share only a 48% sequence similarity. RhoD was shown to regulate transport of early endosomes[33] and the disruption of focal adhesions and disassembly of actin stress fibres[34]. Rif promotes the formation of Cdc42-independent filopodia[35].

The general concepts of the GDP/GTP cycle and regulation by GEF and GAP proteins are not applicable to the four subfamilies of RhoH, RhoU, RhoBTB and Rnd. Therefore, these proteins are commonly called ‘atypical’ Rho GTPases[36]. Atypical Rho GTPases are rather controlled on the level of expression and degradation[37]. Of the atypical Rho GTPases, the Rnd proteins are best characterized. Their affinity to GTP is a hundred times higher then to GDP and no intrinsic GTPase activity has been detected[38,39]. RhoH binds also constitutively GTP and inhibits Rho functions. This was shown for Cdc42/Rac1/RhoA-dependent activation of NF-κB and $p38^{MAPK}$ [40]. The subfamily of RhoU (Wrch-1, Wnt-1 responsive Cdc42 homolog) and RhoV (Chp, Cdc42 homologous protein) are able to hydrolyze GTP but exhibit high intrinsic exchange ability. RhoU is therefore mostly present in the GTP form[41]. RhoU is upregulated by Wnt1 and induces Wnt1-like cell transformation[42]. RhoBTB proteins differ most from the other Rho members by possessing two exclusive domains: BTB1 and BTB2 (Broad

Complex/Tramtrack/Bric-a-brac)[43]. RhoBTB proteins are assumed to be tumor suppressors based on their lack of expression in breast cancer biopsies (RhoBTB2[44]).

In the following the regulation of Rho GTPases and their involvement in biological processes are briefly discussed. To facilitate recognition of proteins that we identified as specific interaction partners in this study they are highlighted in **bold**.

1.2 Regulation of Rho GTPases

The importance of the Rho GDP/GTP cycle for biological processes is reflected by the high number of known regulators. More than 80 GEFs, over 70 GAPs and 3 GDIs have been predicted or characterized[45,46]. Despite the high cellular GTP/GDP ratio of ~10-30 – fold GTP excess[47], the slow exchange of GDP to GTP marks the rate-limiting step of Rho activation. GEFs trigger Rho activation by stabilization of a nucleotide and magnesium free intermediate. The dissociation of bound nucleotide is increased and the subsequent binding of GTP is supported[4].

Dominant-negative (DN) variants of GTPases (e.g. $RhoA^{T17N}$) bind GEFs unproductively and prevent activation of the endogenous GTPase. The constitutively active (CA) GTPase mutants (e.g. $RhoA^{Q63N}$) are not able to hydrolyze GTP and remain in a permanently activated state. Both protein variants are valuable tools in molecular biology to study GTPase function.

1.2.1 Guanine nucleotide exchange factors

Rho GEFs with a DH (Dbl homology) domain constitute with 71 members the largest class of direct Rho activators followed by Dock-related GEFs (downstream of Crk-180 homologue or dedicator of cytokinesis) with 11 members in the human genome[48].The oncogene Dbl (alternative name: MCF2) was the first GEF identified for Rho GTPases[49,50]. Dbl is a transforming gene from diffuse B-cell-lymphoma cells, this emphasizes the disease-relevant role of Rho regulation. Dbl and its *S. cerevisiae* homolog Cdc24 represented the initial members of the Dbl-GEF family. All members share a domain of 200 residues, the Dbl homology (DH) domain. In addition most members contain an adjacent 100 amino acid Pleckstrin homology (PH) domain. PH domains bind phosphoinositides and are suggested to function as membrane anchors. The PH domains localize DH-GEFs to the plasma membrane and regulate their GDP-exchange activity through allosteric mechanisms. DH domains consists of three conserved domains (CR1-CR3) comprising 10-15 α-helices and 3_{10}-helices forming an helical bundle that has been compared in appearance to a chaise longue[51]. The DH-PH combination is proposed to be a functional unit since the DH-PH fragment has higher nucleotide exchange ability than the respective DH domains alone[52]. As another function, PH domains mediate protein interactions (Dbl-Ezrin[53], **Trio**-filamin[54]). DH-GEFs contain additional domains like BAR, SH2, SH3. These domains

render Dbl GEFs multi-module regulators and specify spatio-temporal localization, protein interactors and activation.

Dock proteins form the second group of Rho GEFs. Dock-like GEFs consists of a DHR1 and DHR2 (Dock homology region-1 and -2) architecture[55]. The DHR regions involve a lipid binding C2 domain and parts of a suprahelical Armadillo (Arm) array employed to bind other (Arm-containing-) proteins. At the N-terminal region proline-binding SH3- or PH-domains are often located. Dock proteins are specific GEFs proteins for Rac (**Dock1** (alternative name: **Dock180)**, Dock8 subfamily)[55,56] and Cdc42 (**Dock9**/Zizimin subfamily)[57]. Studies suggest an involvement of Dock GEFs in actin regulation. For example, integrin signaling leads to Rac activation by **Dock1** resulting in cell spreading and migration[58,59].

Rho GEFs underlie different ways of regulation. Common are phosphorylation as observed for Vav by Lck[60,61,62], or specific subcellular localization found for the GEF Ect2. Ect2 is regularly found in the nucleus during interphase but is then dynamically moved to microtubules during cell division[63].

The patterns of GEF-driven Rho GTPase regulation are manifold. Rho GEFs can directly tether Rho effector proteins and link them to the specific GTPase. This can include negative feedback loops for fine tuning of Rho GTPase activity. For example the tripartite complex **Rho GEF 6** (synonymously **PixA** or **COOL2**)-**PAK**-Cdc42 is important for chemotaxis[64–66]. Higher order complexes in which Rho GEFs operate as scaffold to link several proteins have been described for **Tiam1**-JIP2-spinophilin mediated Rac1 activation leading to activation of MAPK[67]. The mutual activation of Rho GTPases is also mediated by GEF proteins. Active Rac1 binds Dbs thereby activating RhoA[68].

1.2.2 GTPase activating proteins

The low intrinsic hydrolysis rate of Rho GTPases is increased by Rho GAP proteins[69,70]. GAP proteins insert a conserved arginine into the active site of Rho GTPases. A water molecule proximal to the γ-phosphate group is orientated resulting in GTP hydrolysis and phosphate release. This was shown for Rho GAP 1 in complex with RhoA[71] and Cdc42[72,73]. Instead of simple termination of the signal GAP proteins regulate Rho activity in accurate spatio-temporal manner[45].

The RhoGAP domain, synonymously BH (Bcr homology) domain, is of 170 residues length. It forms an antiparallel nine α-helical bundle and is sufficient for GAP function[74]. Some Rho GAPs show tissue specific expression. For example the brain-specific protein **Grit** (alternative names: **Rho GAP 32**, gene name: **Arhgap32**) is involved in neuritogenesis[75]. GAPs can be specific for one GTPase (Rho GAP 6 on RhoA) or act on several GTPases (**Rho GAP 5**)[76].

The GAP activity itself doesn't seem to be necessary in all cases for biological function as shown for the Rho GAP α1-chemaerin[77]. The regulation of GAP proteins involves several mechanisms as phosphorylation, shown for **Rho GAP 35** (alternative name: **Grlf1**) by Src[78], or direct protein-interactions. The latter was revealed for PRC1 that binds to the GAP domain of Rac GAP 1, thereby regulating GAP activity down in metaphase[79]. The RhoGAP domain is often combined with one or several other domains, like PH, SAM, BAR.

1.2.3 Guanine dissociation inhibitors

The third class of Rho regulators, GDI proteins, bind to the GDP-bound GTPases but sequester them from the membrane and inhibit the release of the nucleotide[80,6]. The mode of action of GDI proteins is a unique regulation mechanism for Rho and Rab GTPases and not described for other families of the Ras superfamily. In mammals three Rho GDIs are described (Rho GDI 1-3)[81]. **Rho GDI 1** is the most abundant GDI and regulates several Rho GTPases including RhoA, Rac1 and Cdc42[82]. Rho GDI 2 is mostly expressed in hematopoietic cells[83] and RhoGDI3 is related to Golgi complex and other cellular membranes[84]. Rho GDIs create a cytosolic pool of inactivated Rho, comprising 90 - 95% of all Rho proteins in resting cells[85,86]. On the other hand, Rho GDIs allow instant deployment of Rho GTPases into the membrane after a stimulus.

Rho GDIs were attributed to be negative regulators of Rho GTPases by removing them from the GDP/GTP cycle. Recently it becomes clear that GDIs also function as chaperones and protect mature Rho GTPases from proteasomal degradation[86]. Studies for Rac1 during HGF (hepatocyte growth factor) stimulation[87] and Cdc42[88] give strong evidence that **Rho GDI 1** acts as a membrane shuttle necessary for Rho GTPases to reach the plasma membrane. Since Rho proteins are only stable bound either to the plasma membrane or Rho GDI, the total level of Rho GTPase molecules seems to be limited by the amount of Rho GDI molecules. The amount of Rho GDI is roughly equivalent the sum of the three major Rho GTPases[31] implying that changes in one of the GTPases could shift the whole equilibrium between them. Contradictory to their high influence on Rho regulation, only mild phenotypes were observed in yeast cells lacking Rdi1 (the ortholog of Rho GDI in *S. cerevisiae*) and **Rho GDI 1**-knockout mice[89,90].

1.2.4 Subcellular localization

Another level of regulation is given by the subcellular localization determined by the C-terminal region of Rho proteins. At least two signals influence the proper recruitment of Rho proteins to the plasma membrane or endomembranes. First a carboxyl-terminal C-20 geranylgeranylation or C-15 farnesylation at the CAAx tetrapeptide motif (C: cysteine, A: aliphatic amino acid and x terminal amino acid)[91,92] is of importance. Mutation of the cysteine residue of the CAAx motif results in Rho

inactivation by mislocalization to the cytosol. After attachment of the isoprenoid group the GTPases are translocated to the endoplasmatic reticulum and the AAx-tripeptide is removed by protease Rce1[93,94]. The C-terminus is next methylesterified at the carboxyl group by Icmt[93,95]. Second palmitoylation at cysteine residues upstream of the isoprenoid moiety (for RhoB and TC10) or lysine/arginine rich regions are essential sequence elements.

Like most other proteins, Rho GTPases are further regulated by posttranslational modifications. For example phosphorylation of RhoA on Ser188 regulates the affinity of Rho GDI binding[96].

1.3 General concepts of Rho GTPase signaling

The most prominent biological function of Rho GTPases is the regulation of the actin cytoskeleton[97]. Thereby, Rho GTPases influence morphology and migration of eukaryotic cells[1,98]. Additionally, Rho proteins play an important role in biological processes such as gene expression, proliferation, cell cycle and enzymatic activities. The broad spectrum of actions goes hand in hand with the high number of identified effectors for each GTPase.

1.3.1 Cell polarity

Rho GTPases affect polarity and the overall cell morphology. Experiments from *S. cerevisiae* provided first insight that Cdc42 is linked to cell polarity. Cdc42p (the yeast homolog of Cdc42) deficient yeast cells were not able to establish a defined site for daughter cell growth[99]. Further evidence came from *C. elegans* where the division of the zygote is arranged via an anterior/posterior axis. Genetic analysis revealed that this process is maintained by protein products of six par genes (PAR-1 -6, partitioning defective) in concert with the atypical protein kinase C (PKC-3)[100]. PAR-1 and PAR-2 are localized at the posterior and PAR-3, **PAR-6** and **PKC** at the anterior end. Inhibition of CDC-42 delocalizes all PAR proteins[101,102]. In mammalian cells $Cdc42^{GTP}$ engages **Par6** to stimulate the kinase activity of atypical PKC[103–105].

1.3.2 Actin cytoskeleton

The development of typical basal/apical epithelial cell morphology is mainly driven by formation of adherens junctions and tight junctions. Adherens junctions are strong links between neighboring cells and they are formed upon cadherin-mediated cell-cell contacts. Cdc42 and Rac1 are recruited to the contact sites and filopodia and lamellipodia are formed[106–108]. **IQGAP1** and the GEF **Tiam-1** regulate Rac1 activity in this context[109,110]. Tight junctions form a physical barrier against lipid and small molecule diffusion. A Par3-**Par6**-**aPKC** complex regulated by Cdc42 is needed for formation of tight

junction structure. This points out that the Par3/**Par6**/**PKC** mechanism is evolutionary conserved for cells obtaining polarity[111–113].

Directed cellular movement is driven by actin polymerization and filament elongation at the leading edge in combination with actin-myosin filament retraction in the rear parts of the cell body[2,3,98]. The events at the front of the cell are directly linked to the Rho-controlled formation of actin-related cellular protrusions: lamellipodia (Rac1)[14], filopodia (Cdc42)[15,16], invadopodia (Cdc42) and membrane blebs (RhoA, Rac1)[3]. RhoA function has been linked to the rear part of the cell in formation of contractile actin-myosin filaments (stress fibers) needed for retraction[13] (see also Figure 1.4).

Lamellipodia are dynamic microfilament rich sheet like structures at the cell front followed by a more stable region called the lamella[114]. Lamellipodia can extend long distances and are able to pull cells through tissues[115,116]. The Arp2/3 complex initiates the formation of branched actin networks by binding to the sites of actin filaments and nucleates actin polymerization[117,118]. Arp2/3 activity is enhanced by the WAVE complex. WAVE is a pentameric complex with the members **Abi1/2** (Abelson Interacting Protein), PIR121 (Sra/**CYFIP**), Nap1 and HSPC300[118]. Rac1 binds the WAVE complex by **IRSp53** (**BAIAP2**) and induces Arp2/3 mediated actin polymerization[119]. The formin family of proteins (e.g. **DIAPH1**) promotes unbranched actin lengthening by protecting the barbed ends of actin from capping for example mDia1 activated by RhoA[120]. The WH2 domains, that binds actin monomers is present in several proteins that support nucleation for example the **WIPF** family.

Filopodia are finger-shaped exploratory protrusions of the cell consisting of parallel bundles of actin filaments[121]. The formation of filopodia is driven by Arp2/3 complex, Fascin, **IRSp53**, formins and **N-WASP** are all coordinated by Cdc42[122–125].

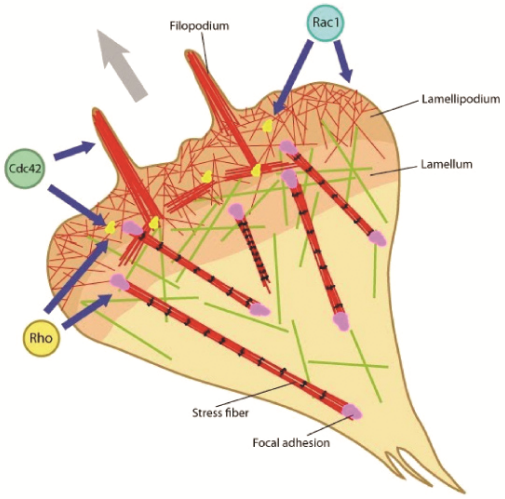

Figure 1.4: Organization of the actin cytoskeleton by Rho GTPases. Cdc42 and Rac1 are located at the leading edge of a moving cell and organize filopodia and lamellipodia respectively. RhoA regulates contraction of actin-myosin filaments in the rear part of the cell body. Cdc42 and RhoA regulate assembly of focal adhesions (yellow), (reprint with permission from Ladoux B, Nicolas A, Rep. Prog. Phys., 2012[126])

Membrane blebs are minor plasma membrane protrusions that form after local detachment of the membrane from the actin cytoskeleton by hydrostatic pressure from the cytoplasm. The function of Rho GTPases lays in the retraction of membrane blebs by RhoA induced actomyosin contraction mediated by **ROCK**.

1.3.3 Gene expression

Rho GTPases route gene expression through several pathways: SRF, JNK, NF-κB and MAPK/ERK[127]. These pathways deploy a complicated interplay and the exact functions of Rho GTPase are in most cases far from understood. As an exception, the influence of Rac1/Cdc42 on the ERK1/2 pathway is well described. This pathway is initiated by binding of an extracellular mitogen to a transmembrane receptor. The signal is transduced via **Grb**/Sos and the Ras-Raf-MEK-MAPK/ERK phosphorylation cascade to the transcription factors c-Myc, ETS, AP-1 and others. ETS and AP-1 activate transcription of CyclinD1[128]. Rac1 and Cdc42 bind to **PAK** serine/threonine kinases that are able to phosphorylate and activate RAF and MEK followed by ERK1/2 activation[129,130]. Rac1 and Cdc42 are likely to determine the duration and the magnitude of the ERK signal.

1.3.4 Enzymatic activity and cell cycle

Rho GTPases regulate the production of reactive oxygen species (ROS) and several reactions in lipid metabolism. Rac1 binds p67phox and stimulates production of ROS via the NADPH oxidase complex in phagocytic cells[131]. RhoA and Rac1 regulate **PI4P 5-kinase** (phosphatidylinositol 4-phosphate 5-kinase), PLC (phospholipase C) and other enzymes in lipid metabolism[132,133]. **Inppl1**, a protein that dephosphorylate phosphoinositides binds to RhoA[134].

Depending on cell type Rho GTPases have critical regulation functions during the cell cycle. The transcription of CyclinD1 was already mentioned. RhoA, Rac1 and Cdc42 have been shown to be essential for G1 progression[135,136], probably caused by the Rho-controlled CyclinD1 expression[137]. During mitosis actin-myosin filaments are orienting the centrosomes, a process in which **Rock** plays a role[138]. Cdc42 is important for correct microtubule attachment to the kinetochore, where mDia3, a Cdc42 effector is located[139]. Finally during cytokinesis the contractile ring consisting of actin and myosin II filaments is located to the cleavage furrow by RhoA with **Rock**, **Citron** kinase and **mDia**[140]. Taken all these points together, Rho GTPases are involved in many processes that are mediated by numerous interaction partners (some of them and their interplay is depicted in Figure 1.5).

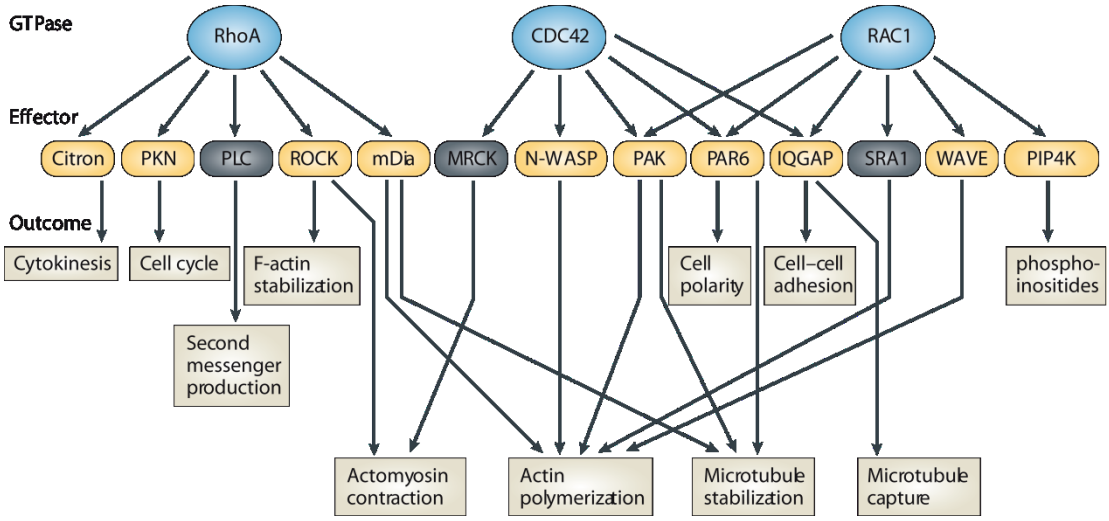

Figure 1.5: Overview of main Rho effector proteins and crosstalk between Rho GTPases. Rho GTPases regulate a broad spectrum of cellular processes. These effects are mediated by effector proteins that are partly shared between the Rho GTPases. Some of the effector proteins were identified in qGAP later (yellow) (adapted with permission, from Iden and Collard, Nature Reviews Molecular Cell Biology, 2008[141]).

1.4 Disease relevance of Rho GTPases

The expression or activity of Rho GTPases are frequently altered in cancer[142]. Based on their broad cellular activities like cell cycle control and regulation of the actin cytoskeleton, Rho proteins play a role in tumorigenesis, invasion and metastasis[127]. Activated forms of RhoA, RhoG, Rac1, Cdc42 and TC10 are capable to transform fibroblasts but with a lower impact than Ras oncogenes[143–145]. RhoA expression is increased in progressed breast cancer and testicular germ-cell tumors[146]. RhoC shows high expression levels in inflammatory breast cancer[147].

Increased activation of Rho GTPases is induced by growth factors in the tumor environment or altered GEF proteins. Interestingly a faster GDP/GTP cycle seems to have higher transforming ability than changes in expression, reflecting the cyclic nature of the biological processes controlled by Rho GTPases. A Cdc42 mutant with a faster GDP to GTP exchange is more efficient in transformation than a GTPase-defective mutant[148]. Rho proteins support tumor invasion by the disruption of cell polarity and cell-cell junctions, increased motility and the degradation of the extracellular matrix[127]. Finally Rho proteins support metastasis, RhoA and Rock enable cells to cross the vascular endothelium[149,150] and RhoC overexpression leads to expression of angiogenic factors and elevates the capability of melanoma cells to colonize the lung[151,152]. In contrast, RhoB deploys pro-apoptotic and cancer suppressive roles[153]. Metastasis and tumor growth can be inhibited by ectopic expression of RhoB[154]. In various aggressive cancer types RhoB expression is decreased[155]. It has been postulated that RhoB acts mainly by competitive binding to RhoA/RhoC targets.

Rho proteins are modified by various bacterial toxins[156,157]. The mode of action comprises glucosylation (Toxin A and B of *C. difficile*), ADP-ribosylation (C3 exoenzymes) and deamidation (CNF1 and CNF_Y (Cytotoxic Necrotizing factor) from *E. coli*) among others[158–161]. Rho proteins deamidated by CNF toxins are able to bind GTP but cannot hydrolyze the nucleotide and remain constitutively active. CNF toxins are valuable tools to modify the activation state of Rho GTPases in eukaryotic cells. CNF1 activates RhoA, Rac1 and Cdc42, whereas CNF_Y is a specific activator of RhoA.

1.5 Mass spectrometry for Protein identification

Proteomics evolved as discipline to study protein structure and function in a large-scale manner. ESI LC/MS (electrospray ionization liquid chromatography mass spectrometry) is one approach of the large proteomics toolbox[162,163]. In combination with bioinformatic data evaluation it is capable to determine the sequence and modifications of peptides and whole proteins. Elaborated labeling techniques and advanced computational strategies allow determining the relative and absolute amounts of proteins.

In general, two strategies of sequence determination, 'top down' (undigested protein) and the more popular 'bottom up' using digested, mostly tryptic peptides are applied. Peptides are in most cases more soluble than an intact protein and a protein modified at different residues leads to a combinatorial high number of subpopulations exacerbating detection. Most mass spectrometers are most efficient in obtaining information from peptides of 20 amino acids sequence length. In the following all descriptions refer to the 'bottom up' approach.

For a typical experiment, protein samples are fractioned by SDS-PAGE or isoelectric focusing to decrease sample complexity and to allow more identifications. Proteins are digested, the peptide sample is desalted[164] and loaded onto a microscale capillary column with a HPLC (high-performance liquid chromatography) device. At the tip of the column the peptides are vaporized and ionized by application of a strong electric potential. This process is called electrospray ionization (ESI) and offers a mild ionization of peptides[165]. Subsequently, peptides are eluted from the column by reversed-phase HPLC and injected into the mass spectrometer. Low flow rates in nanoliter scale allow a high resolution in peptide separation prior to ionization, then termed nanospray. For most applications the mass spectrometer detects positively charged ions, for peptides achieved by protonation of the amino groups by acidic pH. The MS is then operated in the positive (+)-mode.

Different types of mass spectrometers have been developed; for peptide detection five mass spectrometric principles have proven to be most applicable: TOF (time of flight) mass analyzers, quadrupole mass filters, linear ion traps, the FT-ICR (Fourier transform ion cyclotron resonance)

analyzers and the Orbitrap family of mass spectrometers[166,167]. The Orbitrap is a mass analyzer with an inner spindle-like electrode surrounded by an outer coaxial electrode. Together they form an electrostatic field in which ions are dynamically trapped[168]. These ions create an image current that is detected and then converted by Fourier transformation into the frequency and finally the mass spectra[169]. The Orbitrap exists in combination with other mass spectrometers as in the LTQ-Orbitrap with a linear ion trap[170,171] or with mass filters as in the Q-Exactive with a quadrupole[172]. Both kinds of instruments have been employed in the work presented. The steps of mass spectrometric sample preparation and measurement are summerized in Figure 1.6.

For study of peptides the m/z (mass to charge) ratio of the intact peptide (precursor or parent ion) is measured first (MS or MS1 mode). In a second step the precursor is broken into fragment ions (or product ions) that contain information on the order of amino acids in the primary sequence (MS/MS or MS2 mode). This fragmentation step is generally performed by collision with gas particles in either CID (collision induced dissociation) or by HCD (higher-energy collisional dissociation). The performance of a mass spectrometer in detection of peptides relies mostly on resolution, sensitivity, sequencing speed and accuracy of the peptide peaks and the dynamic range, the ratio between the largest and smallest peak within a given spectra. With working resolutions of 60,000 at m/z = 400 a mass accuracy of below 5 ppm and a dynamic range of 5,000 are achieved, rendering peptide identification very reliable. For the Q Exactive device, the full peptide signal and the fragments produced in the octapole are both measured within the Orbitrap. The signals are detected and transformed into the RAW-data format for further procession.

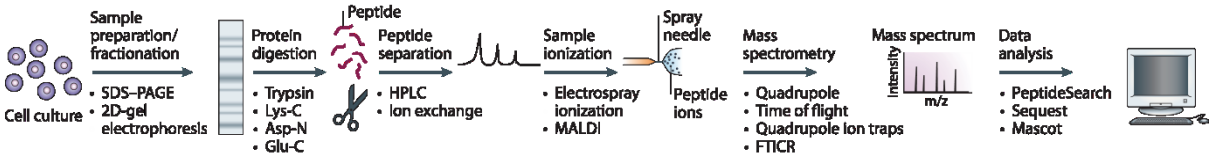

Figure 1.6: Scheme of a typical experiment in bottom up LC-MS. Proteins are isolated, fractionated and digested. The peptide sample is ionized and injected into the mass spectrometer. Peptides are detected and fragmented. The recorded mass spectra are analyzed. Peaks are assigned to peptides and these are assembled to proteins (reproduced with permission, from Steen and Mann, Nature Reviews Molecular Cell Biology, 2004[173]).

1.5.1 Quantitative mass spectrometry

Biological questions regularly ask for quantitative comparison of proteins. Populations of different peptides cannot be quantified by their peptide intensity via MS. Instead, the intensity of the same peptide can be compared and ratios can be calculated. To calculate the ratio of intensities of the same peptide between different MS runs is one possibility, named label free quantification. Alternatively, the ratio of the same peptide within one spectrum is calculated. This is achieved by using peptides containing isotopes of different molecular weight. The peptides are subjected to chemical or metabolic labeling beforehand. For chemical labeling, peptides are conjugated with tags

of different isotope composition. Mostly applied are the iTRAQ[174] and ICAT[175] technologies. The metabolic labeling in contrast is performed during the cultivation of cells or by feeding the animal.

Recently, SILAC (stable isotope labeling by amino acids in cell culture) has become the most popular metabolic labeling approach. It is used to compare proteins from two or three different cell populations to each other by introduction of stable isotopes (^{2}H, ^{13}C and ^{15}N) into amino acids. In most experiments light-labeled cells are compared to heavy-labeled ones. One cell populations was supplemented with unlabeled L-lysine and arginine (0|0) and the other population with heavy L-lysine ($^{13}C_6$, $^{15}N_2$) and heavy L-arginine ($^{13}C_6$, $^{15}N_4$). During the experiment the protein samples from both populations are mixed. The tryptic digest of the sample contains both forms of one peptide differing in 8 Da (lysine) or 10 Da (arginine). Labeling has been used to approach a growing number of biological topics and is most accurate in peptide ratios in the order of one magnitude. The labeling of model organisms as C elegans, D melanogaster[176] and mouse has broadened the application range of SILAC.

The label free approach is a quantitative method for MS that seeks to compare the relative abundance of peptides between different mass spectra. Often SILAC-labeling is cost extensive or not possible for certain organisms. For label free quantification, samples are measured with comparable conditions, in detail on the same mass spectrometer with the same setup and subsequently to each other in time to reduce artificial influences. The total ion currents of peptides are measured, integrated and compared between MS runs. Since minor changes in the mass spectrometric run conditions can lead to tremendous variations in peptide intensity, label free is less accurate in determining relative peptide amounts compared to label techniques. By usage of biological replicates the overall certainty of determined peptide ratio is increased.

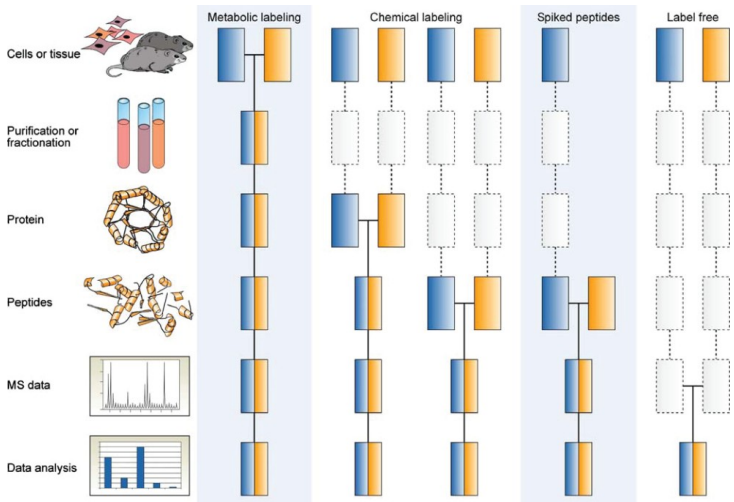

Figure 1.7: Comparison of quantification strategies in mass spectrometry. Blue and yellow represent experimental conditions. Horizontal lines indicate when samples are combined. Dashed lines indicate points at which experimental variation can occur (reproduced from Bantscheff et al., Anal Bioanal Chem, 2007[177]).

1.5.2 Protein Identification and Quantification

The MaxQuant software platform offers a straight-forward, flexible and reproducible identification and quantification for Orbitrap output files (RAW data files)[178,179]. It takes advantage of the high-resolution data provided by the Orbitrap devices. The description given below follows in large parts the MaxQuant analysis framework and includes references to alternative approaches.

In brief, MaxQuant extracts information about MS1 (survey scans) and MS2 (fragment scans) from RAW data files. The peptide masses are calculated in an intensity-weighted way. Fragment scans are compared to *in silico* calculated spectra of a tryptic digestion of the respective proteome (so called 'data matching') [180]. The database search of MS peaks is performed against a reversed nonsense database to estimate random hits (target decoy database)[181,182]. Peptides are reported with a score that estimates the significance of the identification[183,184]. The peptides are assembled to protein groups, containing one or more proteins. This can be the case if isoforms or paralogs share peptide sequences. Then the unambiguous assignment of the shared peptide to one protein is not possible. For quantification, the peak area of the peptide isotope pattern is calculated. For SILAC, the intensities of a SILAC pair within one spectrum can be directly calculated as ratio of intensities. The protein ratio is then determined as median of all peptide ratios[185,186]. Protein ratios are normalized to the median off all protein ratios to compensate for differences in protein loading.

1.6 Protein Interactions and q-AP/MS

Most biological processes are mediated by interacting proteins. Signal cascades, cellular machineries and transport complexes are some examples. All these processes are based on either transient or permanent protein-protein interactions (PPIs). Furthermore, the creation of protein interaction networks helps to understand the links between molecular interplay and to obtain a global view of biological processes at the systems level[187–189].

To discover PPIs a number of biochemical and biophysical methods are available. The methods have different strengths and weaknesses with regard to their sensitivity and specificity and differ in the readout systems. Common methods are: co-immunoprecipitation, pull-down assays, tandem affinity purification (TAP)[190], traditionally evaluated by Coomassie-stained SDS-PAGE or western blot. Alternatives are proximity ligation assay (PLA)[191,192], surface plasmon resonance, isothermal titration calorimetry (ITC)[193,194] or fluorescence resonance energy transfer (FRET)[195] among others.

Screening approaches offer the advantage that a high number of potential interaction partners are identified within a single experiment. The yeast two-hybrid system, the phage display, the blot overlay assay, TAP and quantitative affinity purification followed by mass spectrometry (q-AP/MS) are commonly used screening assays. The yeast two-hybrid has been the most popular approach for

long time. In eukaryotic organisms, transcription factors are modular and divided into DNA-binding and activation domain. For the yeast two-hybrid system the DNA-binding domain is genetically linked to one protein (bait) and the activation domain to a potential binding protein (prey)[196]. If binding between bait and prey occurs, a reporter gene is expressed and detected. The yeast two-hybrid can be easily carried out with standard laboratory equipment, it is scalable and can be automated[197]. On the other hand yeast two-hybrid has rate of false positive hits reaching up to 70%[198]. The environment of the yeast nucleus in which the interaction takes place may differ to the normal surrounding of the investigated proteins. Modifications as phosphorylation or GTP/GDP loading can also not be investigated.

The phage display screening method is able to detect protein/peptide - protein/peptide/DNA interactions[199]. The DNA of the protein is conjugated to the pIII or pVIII gene of M13 filamentous phage, expressing the minor or major coat protein. Libraries containing large numbers of phages expressing the coat proteins linked to the protein of interest are created this way. The phage library is incubated with a microtiter plate with immobilized protein sequences on the surface; binding phages are eluted, proliferated and finally sequenced. The phage display suffers as well from non-native binding conditions and the absence of modifications.

q-AP/MS combines classical biochemical approaches for PPI identification with quantitative mass spectrometry[200–203]. Interaction partners of proteins are purified by co-immunoprecipitation or pull-down then identified and quantified by mass spectrometry. The remarkable sensitivity of Orbitrap mass spectrometers reaches down to the attomolar[204] range in peptide concentration and leads to identification of hundreds of proteins in q-AP/MS experiments. The advances of quantitative MS have provided tools to specifically distinguish between interaction partners and background contaminants for isotope-labeled and for label free experiments. Thereby the need for stringent purification steps that often led to a loss of transient or weak interaction was overcome. As general principle, the experiment is compared with a suitable control that shares most biochemical properties. This was successfully illustrated by pull-down experiments with phosphorylated versus unphosphorylated peptides where specific interaction partners of the phosphorylated form were searched for[205]. Abundances of identified proteins are compared between experiment and control and are expected to be equal for contaminants but higher for specific interaction partners. For experiments with transfection vectors in cell cultures, the empty vector has been used as control.

Affinity purification protocols use bait proteins that are either (over-) expressed within the cell or purified proteins that are used to ‘fish’ from a cell lysate. Co-immunoprecipitation of a tag-free protein at endogenous expression level represents the experimental gold standard for PPI studies. In laboratorial praxis it can happen that the expression level of the protein of interest is low or a

suitable antibody is not available. These problems are circumvented by overexpression of a (tagged) protein. However, overexpression of a protein can influence the overall expression profile of a cell and lead to false positive identifications. Quantitative immunoprecipitation combined with knock-down (QUICK) was developed as elegant alternative[206]. The protein of interest is knocked down in the control cell population and another cell population is left untreated. The protein of interest and its interaction partners are expected to be present in the untreated sample only.

In case of exogenous baits, recombinant proteins or synthesized peptides can be immobilized and incubated with cell or tissues lysate to 'fish' for interaction partners. As a control, the cell lysate is incubated with empty beads. An advantage of this approach is that bait-induced changes in cellular protein expression levels are avoided. Moreover, the amount of recombinant protein is easily controllable and even cell lines that are difficult to transfect can be used for PPI screening. In addition, complex tissues can be subjected to pull-downs. However, the detected interactions form not within the cell but post-lysis. This can lead to the loss of higher order complexes that need temporal assembly steps in the living cell. Exogenous and endogenous expression of the bait protein are compared in Figure 1.8.

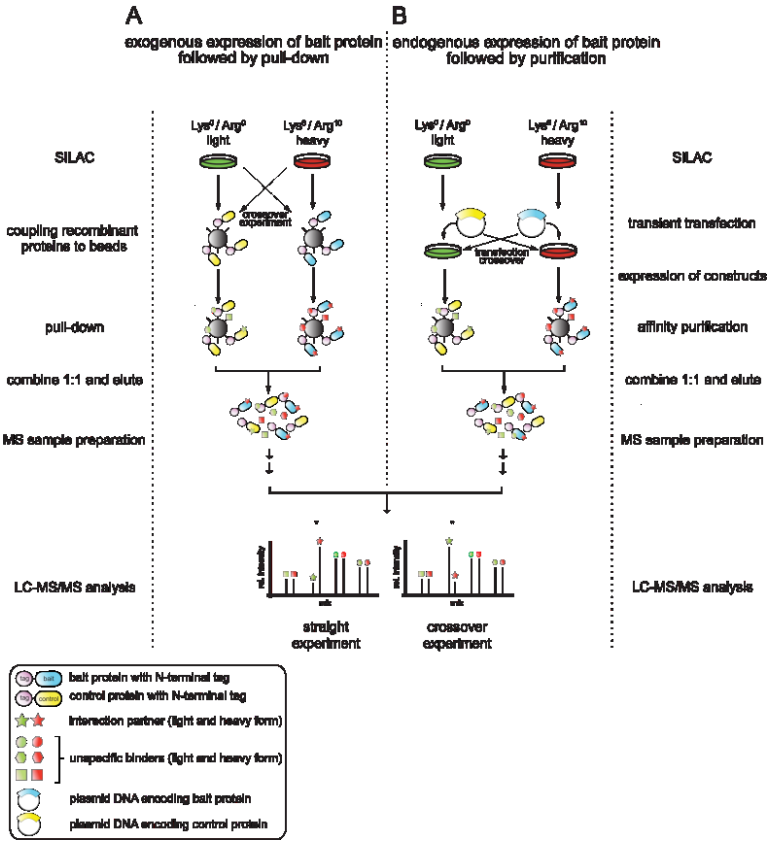

Figure 1.8: Experimental workflow for SILAC-based interaction proteomics. As a general principle the protein of interest/bait (blue) is compared to a control (yellow). (A) Pull-down approach with (exogenous) recombinant protein. The bait protein is incubated with heavy labeled cell lysate, the control with light labeled cell lysate. In a crossover experiment, to control for differences in protein expression, the labels are swapped. (B) Expression of bait protein in the cell (endogenous) followed by cell lysis an immunoprecipitation of the bait-interactor complexes. Mass spectrometry is performed on the straight (forward) and crossover (reverse) sample (Reprint from Paul et al., Methods, 2011).

1.6.1 Identification of Rho GTPase interaction partners

The identification of binding partners helped to assign biological functions to Rho GTPases. For example, co-precipitation experiments with recombinant Dbl, Cdc42 and RhoA showed, that Dbl binds preferentially to the nucleotide-depleted and GDP-bound forms of RhoA and Cdc42 compared to their GTPγS-loaded equivalent[207]. A GAP assay monitoring the accelerated release of ^{32}P from [γ-^{32}P]GTP-bound RhoA, Rac1 and Cdc42 proved GTPase activation capability for **Rho GAP 5** (p190-B)[208]. In parallel the activity of a protein as GEF can be measured by dissociation of preloaded [^{3}H]GDP, shown for **Rho GEF 6** (alternative name: Cool-2) with Rac1 and Cdc42[209]. In the same paper, the physical interaction of GST-Cdc42 with **Rho GEF 6** was shown by co-transfection of COS-7 cells followed by pull-down on GST-beads. The authors also showed by pull-down experiments with several Rac1 nucleotide forms that **Rho GEF 6** binds preferentially to activated $Rac1^{GMPPCP}$ and with lower affinity to $Rac1^{GDP}$ or nucleotide-free Rac1. This finding stands in contrast to the previous knowledge of Dbl-GEF proteins binding preferentially the GDP-bound GTPase. A yeast two-hybrid system expressing a mouse cDNA library was employed to discover the binding of Rho and Rac1 to Citron. The interaction was validated with an overlay assay. To achieve this, recombinant Citron peptides were subjected to SDS-PAGE, blotted and probed against $RhoA^{[35S]GTP\gamma S}$ [210]. The same strategy was applied for the discovery that Rhotekin binds strongly to RhoA and RhoC, weakly to RhoB and not to Rac1 and Cdc42[211]. Search for the missing mediator of Rac1-WAVE1 activation led to the discovery of IRSp53 by yeast two-hybrid screening with the proline-rich region of WAVE1 as bait[212]. The yeast two-hybrid was optimized and specified for the activated versions of Rho GTPases. Purification of effectors via nucleotide-bound Rho affinity columns followed by shotgun mass spectrometry was performed for the identification of SHIP2 and ACAT1 as $RhoA^{GTP}$ interaction partner[134]. The impact of Trio-regulated Rho- and Rac-activity on the JNK and p38 pathway for proliferative signals in GNAQ and GNA11 mutated ulvean melanoma was investigated by a genome wide RNAi screen[213].

1.7 Objectives

Rho GTPases play a central role in a plethora of biological processes. Despite intensive work on RhoA, Rac1 and Cdc42 their role in processes like gene expression or cell cycle control, is still not completely understood. Moreover, little is known about other classical Rho GTPases like RhoD. In addition, it becomes more and more clear, that even within the subfamilies of Rho GTPases large differences in biological function exist. For example, it has been assumed for long that the proteins of the Rho subfamily, RhoA, RhoB and RhoC, may have mostly overlapping effects. In contrast to this assumption, it has been recently revealed that RhoA and RhoB show opposite effects on cell survival and apoptosis.

The function of Rho proteins is best revealed by identification of their effector proteins. Studies focused so far mainly on individual Rho-effector interactions. To date, no single screening approach provided the scientific community with a picture of the Rho GTPase interactome. Valuable networks for some of the Rho/Ras/Arf/Rab/Ran GTPases have been created from curated metadata and granted insight into the GTPase interplay[214]. However, these data are compiled from different sources of unknown quality. A detailed network of Rho GTPase effectors, based on a single comprehensive study, would allow obtaining a global picture of Rho GTPase biology. Such a network would reflect crosstalk between Rho GTPases and, in the best case, reveal new Rho binding proteins. The understanding of Rho GTPases, especially so far uncharacterized proteins like RhoD, would be deepened.

The main goal of this thesis is to establish **q**uantitative **G**TPase **a**ffinity **p**urification (qGAP). qGAP represents a method to identify (Rho) GTPase interaction partners by relative quantification of binders of the Rho^{GDP} compared to the binders of the Rho^{GTP} state. In brief, qGAP combines classical pull-downs with quantitative mass spectrometry by metabolic labeling (SILAC-qGAP) or in a label free manner (LF-qGAP). qGAP is validated by calculation of known Rho binding partner enrichment, by determining the specificity and the sensitivity. Some of the newly identified interaction partners are validated by an independent experimental approach. This approach, a combination of proximity ligation assay with cytotoxic necrotizing factors, was established during the thesis. qGAP is then used to obtain a global picture of Rho binding partners by construction of interaction networks for the GTP- and GDP-bound form. We included RhoA, RhoB, RhoC, RhoD, Rac1 and Cdc42 in our experiments.

2 Materials & Methods

2.1 Materials

2.1.1 Chemicals

Chemicals were purchased from: Carl Roth GmbH (Karlsruhe, GER), Sigma-Aldrich (Steinheim, GER), Invitrogen/life technologies (Carlsbad, USA), Merck KGaA (Darmstadt, GER), Pierce (Holmdel, USA), GE Healthcare (Little Chalfont, UK) and Isotec (Miamisburg, USA).

2.1.2 Media and buffers

Microbiology

LB (lysogeny broth) medium

10 g Bacto tryptone (BD, Franklin Lakes, USA), 5 g Bacto yeast extract (BD), 5 g NaCl, ad 1 l distilled water, adjusted to pH 7.4; for plates 1.5% (w/v) agar was added.

Ampicillin

100 mg/µl stock solution in distilled water, sterilized by filtration, aliquots were stored at -20 °C.

Kanamycin

10 mg/µl stock solution in distilled water, sterilized by filtration, aliquots were stored at -20 °C.

Chloramphenicol

34 mg/µl stock solution in ethanol, sterilized by filtration, aliquots were stored at -20 °C.

IPTG (Isopropyl β-D-1-thiogalactopyranoside)

1 M stock solution in distilled water, sterilized by filtration, aliquots were stored at -20 °C.

Molecular biology

TAE running buffer

40 mM Tris-HCl (pH 8.5), 40 mM acetic acid, 1 mM EDTA

5× DNA loading buffer

63 mM Tris-HCl (pH 6.8), 2% [w/v]SDS, 10% [v/v] glycerol, 0.01% [w/v] bromphenol blue

Protein purification

Lysis buffer

50 mM HEPES (pH 7.5), 200 mM NaCl, 5 mM $MgCl_2$, 2.5 mM DTT, 1 µg/ml DNAse I, 1 tablet Complete Mini-EDTA free protease inhibitors (Roche, Penzberg)

Equilibration buffer

20 mM HEPES (pH 7.5), 150 mM NaCl, 5 mM $MgCl_2$, 2.5 mM DTT

Washing buffer

20 mM HEPES (pH 7.5), 300 mM NaCl, 5 mM $MgCl_2$, 2.5 mM DTT

Elution buffer

50 mM HEPES (pH 7.5), 150 mM NaCl, 5 mM $MgCl_2$, 2.5 mM DTT, 20 mM glutathione

SEC buffer

20 mM HEPES (pH 7.5), 150 mM NaCl, 5 mM $MgCl_2$, 2.5 mM DTT

Cell cultivation, fractionation and lysis

Extraction buffer A (ExtA)

10 mM HEPES (pH 7.9), 1.5 mM $MgCl_2$, 10 mM KCl, 1 tablet Complete Mini-EDTA free protease inhibitors (Roche, Penzberg)

Extraction buffer B (ExtB)

10 mM HEPES (pH 7.9), 1.5 mM $MgCl_2$, 10 mM KCl, 0.2% NP-40, 1 tablet Complete Mini-EDTA free protease inhibitors (Roche, Penzberg)

Lysis buffer for adherent cells and mouse brains

50 mM Tris-HCl (pH 7.4), 150 mM NaCl, 1% Triton X-100, 1 mM EDTA, 1 mM EGTA and 1 tablet Complete Mini-EDTA free protease inhibitors (Roche, Penzberg)

Alternative lysis buffer for mouse brains

50 mM Tris-HCl (pH 7.4), 150 mM NaCl, 1.2% n-Octyl-β-D-glucopyranoside (Sigma-Aldrich), 1 mM EDTA, 1 mM EGTA and complete protease inhibitors (Roche)

Protein chemistry

SDS running buffer

40 ml 20× NuPAGE MES SDS running buffer for Bis/Tris gels (Invitrogen, Karlsruhe, Germany) in 760 ml distilled water.

Transfer buffer

25 mM Tris-HCl (pH 8.5), 190 mM glycine, 10% [v/v] methanol, 0.1% [w/v] SDS

Stripping buffer

68 mM Tris-HCl, (pH 7.5), 2% [w/v] SDS, 0.8% [v/v] β-mercaptoethanol

10× TBS

200 mM Tris base, 1.4 M NaCl, adjusted to pH 7.4

TBS-T

0.1% [v/v] Tween-20 in TBS

Blocking solution

1× TBS-T supplemented with 5% [w/v] non-fat dry milk powder

Sample preparation and LC-MS

All MS relevant solutions were prepared in LiChrosolv (HPLC grade) water or acetonitrile.

ABC buffer

50 mM ammonium bicarbonate (NH_4HCO_3) in water (with a final pH of 8.0)

Destaining buffer

25 mM ammonium bicarbonate in 50% [v/v] ethanol (EtOH).

Reduction buffer

10 mM dithiothreitol (DTT) in ABC buffer

Alkylation buffer

55 mM iodoacetamide in ABC buffer

Extraction buffer

3% [v/v] trifluoroacetic acid (TFA), 30% [v/v] acetonitrile (ACN)

Denaturation buffer, urea/thiourea (U/T)

6 M urea, 2 M thiourea in 10 mM HEPES (pH 8.0)

Buffer A* (sample buffer)

5% [v/v] acetonitrile, 3% trifluoroacetic acid

Buffer A

5% [v/v] acetonitrile, 0.1% [v/v] formic acid in water

Buffer B

0.1% [v/v] formic acid in 80% acetonitrile

2.1.3 Enzymes/Proteins

- BamH I restriction enzyme – New England Biolabs Inc.
- Not I restriction enzyme – New England Biolabs Inc.
- Xho I restriction enzyme – New England Biolabs Inc.
- T4 DNA ligase blue/white cloning qualified - Promega

2.1.4 Antibodies

Table 2.1: Antibodies used for proximity ligation assay.

Name (clone)	Host species	Working dilution PLA	Company
ACAT1 (HPA004428)	Rabbit	1:400	Atlas antibodies
C1Orf198 (HPA004798)	Rabbit	1:400	Sigma
Cdc42 (B-8)	Mouse	1:400	Santa Cruz
Cdc42 (P-1)	Rabbit	1:300	Santa Cruz
IQSEC3	Rabbit	1:400	Atlas antibodies
Mzt2 (C-14)	Rabbit	1:200	Santa Cruz
Opa1 (55772)	Mouse	1:400	Abcam
Rac1 (23A8)	Mouse	1:500	Upstate
Rac1 (20571-1-AP)	Rabbit	1:300	Proteintech
RhoA (26C4)	Mouse	1:400	Santa Cruz
RhoA (119)	Rabbit	1:300	Santa Cruz
Rock2 (1E12)	Rabbit	1:200	Abnova
SESTD1 (LS-B5489)	Rabbit	1:1,000	LS Bio

Table 2.2: Antibodies used for western blotting.

Name (clone)	Host species	Working dilution western blotting	Company
PAK2 (2608)	Rabbit	1 : 1,000	Cell signaling
Opa1 (55772)	Mouse	1 : 1,000	Abcam
HRP conjugated anti-mouse	Sheep	1 : 10,000	GE Healthcare
HRP conjugated anti-rabbit	Donkey	1 : 20,000	GE Healthcare

2.1.5 Kits

- Qiaprep Spin Miniprep Kit (Qiagen)
- Plasmid Midi Kit (Qiagen)
- Gel extraction kit (Qiagen)
- PCR purification kit (Qiagen)

2.1.6 Bacteria strains

- *E. coli* TG1 K12, genotype supE, hsd -5, thi, -(lac-proAB), F'[traD36, proAB+, lacq, lacZ- M15] (Promega, Mannheim, D)
- *E. coli* (DE3) Rosetta, genotype F- ompT hsdsSB (rB- mB-) gal dcm (DE3) pRARE (CamR) (Novagen, Darmstadt, D) with pRARE containing the tRNA genes argU, argW, ileX, glyT, leuW, proL, metT, thrT, tyrU and thrU

Both strains were gifts from Prof. Oliver Daumke, MDC, Berlin, GER.

2.1.7 Plasmids

N-terminal GST-fusion proteins of RhoA, Rac1, Cdc42 were gifts from Prof. Alfred Wittinghofer (MPI, Dortmund, GER). N-terminal GST-fusion proteins of RhoB and RhoC were gifts from Prof Anne Ridley (Kings College, London, UK). Citrine-, mCherry- and CFP-fusion proteins of RhoA, $RhoA^{T19N}$, $RhoA^{Q63L}$, Rac1, $Rac1^{T17N}$, $Rac1^{Q61L}$, Cdc42, $Cdc42^{G12V}$ and $Cdc42^{T17N}$ were generous gifts from Dr. Oliver Rocks (MDC, Berlin, GER).

2.1.8 Cell lines

- HeLa cells: human cervical cancer cells were obtained from Promochem (Wesel, GER).

2.1.9 cDNA clones

- Full length RhoD of human origin (pCMV-SPORTS6, IRATp970E084D) was obtained from Imagenes (Berlin, GER).

2.2 Molecular biology methods

2.2.1 Primer design and Oligonucleotides

Primer design followed standard strategies[215], the potential formation of hairpins or dimers was ruled out by NetPrimer software from Premier Biosoft (Palo Alto, CA)[216]. Primers were purchased from Biotez (Berlin, GER).

2.2.2 Polymerase Chain Reaction

Amplification of DNA fragments was conducted using Pfu polymerase according to manufacturer's procedures.

2.2.3 DNA purification

PCR products were desalted with nucleospin columns from Qiagen (Hilden, GER) following manufacturer's procedures.

2.2.4 Restriction digest

Desalted PCR products were digested by restriction enzymes from New England Biolabs (Frankfurt a. Main, GER) according to manufacturer's procedures.

2.2.5 Agarose gel electrophoresis

Plasmids or DNA fragments were separated on 1% agarose gels, prepared and run following standard procedures.

2.2.6 DNA extraction

DNA bands were sliced out from agarose gels, melted and purified using the QIAquick Gel Extraction Kit, Qiagen (Hilden, GER) according manufacturer's procedures.

2.2.7 Ligation

Plasmids and amplified DNA fragments (inserts) were quantified by absorption measurement at 260 nm. 10 ng plasmid was ligated with a sixfold molar excess of insert using T4 DNA Ligase from New England Biolabs (Frankfurt a. Main, GER) following the manufacturer's procedures.

2.2.8 Transformation of chemically competent E. coli

Chemically competent bacteria were transformed with plasmids using the heat shock method. The plasmid was incubated with 50 µl of competent cells for 10 min, followed by a heat shock at 42 °C for 60 s in a water bath. Cells were incubated with additional 500 µl of LB medium for 45 min at 37 °C under constant agitation. Cells were streaked on LB agar plates containing the appropriate antibiotics. Plasmids were maintained and amplified in *E. coli* TG1 strain, protein expression was performed in *E. coli* (DE3) Rosetta strain.

2.2.9 Long term storage of E. coli *cultures*

For long-term storage of bacterial cultures, cryostocks were prepared by mixing 1 ml of a 5 ml LB overnight culture with 0.5 ml of sterile glycerol. Cryostocks were slowly frozen down and stored at -80 °C.

2.2.10 Plasmid preparation

E. coli cryostocks were used to inoculate 5 ml (miniprep) or 100 ml (midiprep) of LB medium. Cultures were grown over night and harvested by centrifugation (5,000 g, 10 min, 4 °C). Plasmids were purified with kits from Qiagen.

2.3 Biochemical Methods

2.3.1 Antibiotics

Bacteria transformed with pGEX plasmids were cultured at a final concentration of 100 µg/ml ampicillin. Rosetta strains were additionally treated with chloramphenicol at a final concentration of 34 µg/ml. Kanamycin was used at concentrations of 10 µg/ml in liquid culture and 50 µg/ml in agar plates.

2.3.2 Protein expression in E. coli

N-terminal GST-fusion proteins of RhoA, B, C, D, Rac1 and Cdc42 were expressed in *E. coli* (DE3) Rosetta. N-terminal GST-tagged CNF1 and CNF_Y were expressed in *E. coli* Tuner pLysS. 5 – 10 l TB prewarmed medium supplemented with the respective antibiotics were inoculated 1:1,000 with an overnight *E. coli* culture. Bacteria were grown at 37 °C with 180 rpm shaking to an OD_{600} of 0.4. Bacteria cultures were cooled down to 18 °C and protein expression was induced with 40 µM isopropyl β-D-1-thiogalactopyranoside, cultures were grown for at least 15 hours. Bacteria were sedimented by centrifugation (8,000 g, 4 °C for 20 min in JA-10 rotor) and pellets were resuspended in 20 ml lysis buffer per litre of bacterial culture. The suspension was stored at – 20 °C. For expression and solubility test the amount of bacteria culture was scaled down to 50 ml.

2.3.3 E. coli cell lysis and preparation of the cytosolic fraction

The bacteria suspension was thawed on ice and lysed by either passing it at least twice through a microfluidizer or by 6 × 10 seconds of sonication (UP200S, 0.85 amplitude, 0.5 s cycle time, sonotrode DRH-S2) with cooling steps in between. The lysate was cleared from debris by centrifugation (50,000 g, 4 °C, 45 min, JA-12 rotor) and filtered through a 0.2 µm pore size filter.

2.3.4 Glutathione affinity chromatography

Purification steps were conducted at 4 °C. For purification of GST-tagged Rho fusion proteins 1, 5 or 15 ml GSH sepharose columns were used at a flow rate of 1 ml/min. The column was washed with 6 column volumes (CV) water and equilibrated with 6 CV equilibration buffer (EB). The filtered bacteria lysate was applied, the column was washed with 30 CV washing buffer (WB) followed by 5 CV EB and finally eluted with 5 CV elution buffer (EluB). Protein solutions were concentrated and subjected to size exclusion chromatography or concentrated and stored without further purification (RhoB, RhoC and RhoD).

2.3.5 Size exclusion chromatography

Size exclusion chromatography was performed for RhoA, Rac1 and Cdc42. The protein solution was concentrated to 2 ml and centrifuged for 5 min at 20,000 g. The protein solution was applied to a Superdex 200 16/60 column pre-equilibrated with 2 CV EB. The purification was conducted at a flow rate of 1 ml/min with an Äkta Prime system. The peak fractions containing the protein of interest were pooled and concentrated (see 2.3.9).

2.3.6 Nucleotide loading

Nucleotide exchange was forced by EDTA-driven Mg^{2+}-depletion as described previously[217]. 200 µM of the respective Rho GTPase was incubated with 15 mM EDTA, 150 mM NH_4SO_4, and 10 mM of GDP or 2 mM GTPγS in 1 M HEPES (pH 7.5) over night at 4°C. The exchange reaction was stopped by addition of 30 mM $MgCl_2$, excess nucleotide was removed by Amicon concentrator or buffer exchange via fast protein liquid chromatography (FPLC).

2.3.7 Determination of protein-bound nucleotide

Determination of protein-bound nucleotide followed standard protocols[218]. The protein was diluted to a final concentration of 50 µM with SEC buffer, 20 µl were injected into a HPLC system equipped with a reversed-phase ODS-2 hypersil column at flow rates of 1.5 ml/min. The protein was denatured and absorbed at a nucleosil 100 C18 pre-column. Nucleotide intensities were detected by measuring A_{254} and compared to standard nucleotide solutions at concentrations of 50 µM. Loading efficiency was calculated by comparing the areas below the peaks.

2.3.8 Protein concentration determination

Protein concentration in purified protein solution or cell lysates was determined using the Bradford assay[219]. Alternatively for purified protein solution E_{280} was measured and concentration was determined using calculated extinction coefficients[220].

2.3.9 Protein concentration and storage

Protein solutions were concentrated with Amicon centrifugal devices (10 kDa cutoff). The purified Rho GTPases were aliquoted to 500 µg fractions (concentration 10 g/l), shock-frozen in liquid nitrogen and stored at -80 °C. GST-CNF1 and -CNF_Y were stored at -20 °C in 50 mM Tris (pH 7.5), 50% glycerol at concentration of 0.4 g/l.

2.3.10 Sodium dodecyl sulfate polyacrylamide gel electrophoresis (SDS-PAGE)

Protein samples were denatured in NuPAGE LDS sample buffer with 20 mM DTT and separated on NuPAGE Novex 4-12% Bis-Tris gels in an Xcell Sure Lock system (Invitrogen/life technologies). Seeblueplus2 (Invitrogen/life technologies) protein standard was used as molecular weight marker. Gels were run for 45 min (200 V, 100 mA, 30 Watt) and then subjected to fixation (40% [v/v] methanol, 10% [v/v] acetic acid) and stained (30% [v/v] methanol, 30% [v/v] NuPAGE stainer A with addition of 5% [v/v] stainer B after 5 min) for one hour. Protein gels were destained in water and scanned.

2.3.11 Western blotting

Proteins were transferred from the SDS-gel to PVDF membrane in an Xcell Sure Lock wet blotting system (Invitrogen/life technologies). The membrane was activated with methanol, blotting was performed with 1 mA per 1 cm² of membrane for 2 h. The membrane was blocked against unspecific protein binding with 1% BSA in 0.1% Tween-20 solution (blocking buffer) for 30 - 60 minutes. Incubation with primary antibody in blocking buffer was performed over night at 4 °C and continuous. The membrane was washed three times in TBS-T solution and incubated with HRP-conjugated secondary antibody for one hour at room temperature. After three washing steps in TBS-T the membrane was incubated with mixed Western Blot Chemiluminescence Reagent Plus for ECL immunostaining (Perkin Elmer) for one minute. The blot was exposed to X-ray films (GE Healthcare) in the dark. For sequential detection of proteins on the same blot, antibodies were removed by shaking in stripping buffer (37 °C, 15 min).

2.4 Cell cultivation, fractionation and lysis

2.4.1 Cell media/SILAC

Adherent mammalian cells were cultivated in Dulbeccos's Modified Eagle's Medium supplemented with GlutaMAX (DMEM GlutaMAX, High Glucose 4.5 g/l, Gibco) with 10% (v/v) fetal calf serum (FCS), (Invitrogen/life technologies), penicillin (100 U/ml) and Streptomycin (100 µg/ml). Media were cleaned by sterile filtration with 0.22 µm microfiltration systems (TPP, Trasadingen).

SILAC media was prepared from DMEM (High Glucose, 4.5 g/l) lacking L-arginine, L-lysine and L-glutamine ('SILAC-DMEM', PAA) supplemented with 10% (v/v) dialyzed FCS (Sigma-Aldrich), 4 mM L-glutamine, penicillin (100 U/ml), streptomycin (100 µg/ml) and the respective L-arginine and L-lysine amino acid. 'Heavy' (8|10) SILAC medium was prepared by addition of 28 mg/ml $^{13}C_6{}^{15}N_4$ L-arginine and 49 mg/l $^{13}C_6{}^{15}N_2$ L-lysine (Sigma Isotec). 'Light' SILAC medium was prepared by addition of corresponding amino acids with standard isotope distribution.

2.4.2 Cell cultivation

Cell lines were cultivated at 37 °C with 5% CO_2 and subjected to passage as required. To generate cell stocks ~10^6 cells were washed with PBS, detached by trypsin and centrifuged at 800 g, RT for 5 min. The supernatant was discarded and cells were resuspended in cell freezing medium (Gibco) and transferred to a cryotube. Cells were stepwise frozen using a freezing container (VWR, Darmstadt) filled with isopropanol first to -80 °C and afterwards in liquid nitrogen for long-term storage. The

thawing process was done in a waterbath at 37 °C, cells were resuspended in cell culture medium afterwards and centrifuged at 800 g at RT for 5 min. The cell pellet was resuspended again and dispensed on a culture dish.

2.4.3 Preparation of cytosolic extracts

Dishes with adherent cells were placed on ice, the medium was removed. Cells were washed once in PBS, harvested in 2 ml PBS with 5 mM $MgCl_2$ and then transferred to a pre-chilled 50 ml tube and centrifuged for 5 min at 400 g. Cells were washed twice, centrifuged and the volume of the pellet was determined. The cell pellet was resuspended in 5 volumes ice-cold buffer ExtA and incubated for 10 min on ice. After centrifugation, the volume of the pellet was determined for resuspension in 2 volumes of ice-cold buffer ExtB. Cells were transferred to a dounce homogenizer and lysed with 30 strokes with a pestle type B (tight). After centrifugation for 15 minutes at 4,600 g, the supernatant containing the cytosolic fraction was aliquoted and frozen in liquid nitrogen.

2.4.4 Transient transfection of mammalian cells

Plasmid DNA was mixed with polyethylenimine (PEI) transfection reagent (ratio DNA: PEI = 1 µg:4 µg for HeLa cells) in serum-free cell culture medium (DMEM). The setup was incubated for 15 min at RT for efficient binding of DNA to the polycation PEI. For a cell culture dish of 10 cm diameter, 5 – 15 µg DNA were dissolved in 1 ml serum-free medium. The transfection setup was directly applied onto the adherent cells. Cells were transfected at 50 – 70% confluency and harvested 24 hours post-transfection.

2.4.5 Lysis of adherent mammalian cells

For the lysis of adherent mammalian cells, the cell culture medium was removed and the dish was placed on ice. The cells were washed once in ice-cold PBS and then detached with cell scrapers (Corning Inc., Amsterdam, The Netherlands) in 1 ml PBS with 5 mM $MgCl_2$. Cells were sedimented at 1,000 g (4 °C, 5 min), washed twice in 2 ml PBS, resuspended in 150 µl lysis buffer, transferred to a dounce homogenizer and lysed with approximately 40 strokes. If necessary 2-10 U of benzonase (Merck) were added and the lysate was incubated on ice for 30 min to degrade DNA. The cell lysate was incubated on ice for 10 min and then centrifuged for 10 minutes at 20,000 g for 20 min.

2.4.6 Preparation of mice brain

Mouse brains were dissected from female BL/6 mice at an age of 12 weeks (kind gift of Dr. Ibanez-Tallon, MDC Berlin). Brains were either used as a whole (RhoB, RhoC, RhoD) or sliced into a hippocampal (Cdc42), cerebral (Cdc42, Rac1, RhoA) and remaining cerebrum fraction (Cdc42, Rac1,

RhoA). The tissue samples were lysed in lysis buffer (50 mM Tris-HCl (pH 7.4), 150 mM NaCl, 1% Triton X-100, 1 mM EDTA, 1 mM EGTA and protease inhibitors (Roche)) by application of 50 – 100 strokes in a dounce homogenizer on ice. The lysate was cleared from debris by two subsequent centrifugation steps at 20,000 g (4 °C, 20 min) and directly used for experiments.

2.4.7 Immunoprecipitation (GFP-fusion proteins)

GFP (green fluorescent protein) and related proteins (citrine, RFP, CFP) were immunoprecipitated by GFP-Trap (Chromotek). 15 µl of bead suspension was centrifuged (2 min, 1,000 g, 4 °C) and the storage solution was removed. Beads were washed once in lysis buffer, the cell lysate was applied and incubated for at least 30 min at 4 °C. The supernatant was removed, the beads were washed twice in 800 µl lysis buffer and proteins were eluted in either 40 µl denaturation buffer or LDS-loading buffer.

2.4.8 Pull down assay

For pull down assays cell lysates were freshly prepared from adherent HeLa cells or mice brains.

SILAC experiments were conducted as label swap experiments; in a forward experiment GTP-bound Rho GTPases were incubated with heavy labeled cell lysate and GDP-bound Rho GTPases were incubated with light labeled cell lysate. The reverse experiment was performed with swapped labels. A SILAC experiment included four pull downs, the two pull downs of the forward experiment ($Rho^{GTP\gamma S}$ + heavy lysate and Rho^{GDP} + light lysate) and the two pull downs of the reverse experiment ($Rho^{GTP\gamma S}$ + light lysate and Rho^{GDP} + heavy lysate) were mixed during the wash steps after incubation with the lysate.

Experiments from mice brains were conducted as triplicates resulting in six single pull downs per Rho GTPase. Each pull down was measured separately by mass spectrometry.

Sepharose beads with an active NHS (N-Hydroxy-Succinimide) group were used for covalent coupling of recombinant proteins. Storage solution was removed from bead slurry by centrifugation (1,000 g, 2 min). Beads were washed in ice-cold equilibration buffer and incubated with the recombinant protein for at least two hours at RT. The beads were subsequently washed in buffer A, B and incubated in buffer A for 30 min. After wash steps with buffer B, A and again B the cell lysate was added to the beads and incubation was performed for 30 min at 4°C. The supernatant was removed, the beads washed in pull down wash buffer twice and bound proteins were eluted with 200 µl denaturation buffer by shaking at 1,400 rpm on an Thermo shaker (Eppendorf) for 15 min.

2.4.9 Protein ethanol precipitation

Samples with volumes of 300 µl or less were mixed with 70 µl of 2.5 M sodium acetate (pH 5.0) and 1 µl Glycoblue (Ambion) and filled to 2 ml with ethanol. The samples were briefly mixed and incubated over night at 4 °C and centrifuged at 20,000 g and 4 °C for at least 30 min. The supernatant was removed and the protein pellet was air dried.

2.4.10 Proximity ligation assay

The proximity ligation assay was used for *in situ* validation of protein protein-interactions. HeLa cells were seeded on poly-L-lysine coated 18 well µ-slides (ibidi, Martinsried, Germany) for one day in standard cell culture medium (450 cells/well). After 24 hours the medium was replaced by starvation medium (0.2% FCS) and cells were cultivated for another 24 hours. Cells were then either incubated for one hour with cytotoxic necrotizing factor (CNF1 or CNF_Y) with a final concentration of 0.4 µg/ml or left untreated. Cells were briefly washed in PBS, fixed with 4% PFA (paraformaldehyde) and permeabilized with 0.1% Triton X-100 in PBS. Cells were washed in PBS and unspecific binding of antibodies was blocked by incubation in PBS containing 1% BSA, 0.05% Tween20 for 20 min. Reagents for PLA were obtained from Olink Bioscience (Duolink® in situ orange starter kit). The primary antibody solution was applied for one hour at 37 °C in a humidity chamber. Antibodies were combinations of one from mouse and one from rabbit donors. The two PLA probes were mixed, diluted 1:5 in antibody diluent buffer and incubated for 20 min. The primary antibody was removed from the chamber slide. The slide was washed once; the PLA probe solution was added and incubated for 1 hour at 37 °C. The probes were removed, the slide was washed twice for 5 min under gentle agitation and the Ligation-Ligase solution was added to each sample and incubated in a pre-heated humidity chamber for 30 min at 37 °C. For amplification the slide was washed twice for 2 min and the Amplification-Polymerase solution was added and incubated for 100 min in a pre-heated humidity chamber for 80 min at 37 °C. Finally the slides were washed, dried and In Situ Mounting Medium including 4',6-diamidino-2-phenylindole (DAPI) was added. Nonspecific signals were assessed by single primary antibody staining.

2.4.11 Microscopy and processing of images

Images were taken with a Leica TCS SP5 confocal microscope (Leica Microsystems, Wetzlar, Germany) using a 63× objective and Leica LAS AF software. Standard parameters were: Pinhole of 2.5 AE, Resolution of 2048 × 2048 pixels, line average of 4. Pictures were processed with ImageJ (version 1.44, Bethesda, USA) using the LOCI plugin. Pictures were imported without autoscale, threshold was set with a minimum of 30 and a maximum of 255 and ‘analyze particles’ function was used for counting of spots.

2.5 Mass spectrometry

2.5.1 In solution digestion

Protein pellets were solubilized in 20 µl denaturation buffer (U/T buffer) by gentle shaking of the vial. Heating steps were avoided, consequently all steps were performed at room temperature. Disulfide bridges were reduced by addition of 1 µl DTT solution per 50 µg protein and incubated for 30 minutes. Alkylation of cysteine residues was performed in the dark with 1 µl iodoacetamide solution per 10 µl digestion setup. The proteins were digested in a first step by addition of 1 µg LysC protease per 50 µ protein for three hours. The sample was diluted 4 fold in ABC buffer and digested in a second step with 1 µg trypsin per 50 µg protein and incubated over night with gentle shaking. Trypsin activity was stopped by acidifying the sample with 10 µl of a 10% trifluoroacetic acid solution to obtain a pH of 2.5 or lower.

2.5.2 In gel digestion

For MS analysis from stained SDS-gels, bands were sliced out and chopped into blocks of 1 mm edge length. The gel slices were subsequently washed in buffer ABC/EtOH for 20 min, in buffer ABC for 20 min and in buffer ABC/EtOH for 20 min. The slices were twice dehydrated by shaking in ethanol for 10 min. For reduction gel pieces were rehydrated in DTT solution for 45 min at 56 °C. The supernatant was removed and the gel pieces washed in ABC buffer for 20 min and afterwards dehydrated twice. Ethanol was removed by vacuum centrifugation and trypsin solution was added for rehydration of gel pieces. To compensate for evaporation, ABC buffer was added to cover the gel pieces. The digestion setup was incubated at 37 °C over night. The digestion was stopped by addition of 2 µl TFA, peptides were extracted by incubating the gel pieces first with extraction solution and second by dehydration in acetonitrile. The supernatants were combined, concentrated and subjected to stage-tip purification.

2.5.3 Stage-tip purification

The stage tip purification was performed as previously described[164], with LC/MS grade chemicals. For application of liquids the columns were centrifuged at 5,000 g. Desalting columns were prepared from C18 Empore filters and pipette tips. The column was conditioned by 50 µl methanol and washed with 100 µl buffer A*. The peptide sample was brought to a concentration of 3% TFA and 5% acetonitrile and applied to the column. The column was washed with 100 µl washing buffer and stored at 4°C. Prior to MS measurement the peptides were eluted in 60 µl buffer B into an autosampler plate and concentrated in a speedvac device to a volume of approximately 2 µl and filled up to 8 µl with buffer A*.

2.5.4 Liquid-chromatography mass spectrometry (LC-MS)

LC-MS was performed with an EASY-nLC system (Thermo Scientific) coupled online to a Q Exactive Orbitrap (Thermo Fisher) for cerebrum and whole brain samples and to a LTQ-Orbitrap-Velos (Thermo Fisher) for hippocampus and cerebellum samples. For SILAC samples LC-MS was performed with an Eksigent NanoLC-1D Plus system coupled to an Orbitrap XL. 5 µl peptide samples were loaded onto a fritless microcolumn[221] (75 µm inner diameter packed in-house with ReproSil-Pur C18-AQ 3-µm resin, Dr. Maisch GmbH). Peptides were eluted with an 8-60% acetonitrile gradient and 0.5% formic acid. Runs were performed as four hours gradients at a flow rate of 200 nl/min. Peptides were ionized at currents of 2 – 2.5 kV. Samples were analyzed with 4 hours gradients. The Q-Exactive Orbitrap device was operated in the data dependent mode with a standard TOP10 method. One full scan (m/z range = 300 – 1650, R = 70,000, target value: 10^6 ions, maximum injection time = 20 ms) was used to detect precursor ions. The 10 most intense ions with a charge state greater than one were selected for fragmentation (R = 17,500, target value 10^6 ions, isolation window = 3 m/z, maximum injection time = 60 ms). Dynamic exclusion time for fragmented precursor ions was set to 30 s[222]. The Velos Orbitrap device was operated in the data dependent mode with a standard TOP20 method. One full scan (m/z range = 300 – 1700, R = 60,000, target value: 10^6 ions) was used to detect precursor ions. The 20 most intense ions with a charge state greater than one were selected for fragmentation (target value 3,000 ions, isolation window = 2 m/z). Dynamic exclusion time for fragmented precursor ions was set to 60 s[222].

2.6 Data processing and analysis

2.6.1 MaxQuant

MS raw data files were analyzed with the MaxQuant software platform (version 1.3.0.5) that allows identification and quantification of proteins. Standard settings were used, the ‘match between run’ function allowing for peak identification by comparison with adjacent MS runs was, if possible, activated. Proteins were searched against ‘uniprot human’ or ‘uniprot mouse’ database (version June 2012). For SILAC experiments with HeLa cell culture the multiplicity was set to ‘2’ and heavy labels ‘Arg10’ and ‘Lys8’ were chosen, min. ratio counts was set to ‘1’. For experiments with mouse brains the multiplicity was set to ‘1’ and label-free quantification was activated with ‘LFQ min. ratio count’ set to ‘2’.

2.6.2 Perseus

Text files produced by MaxQuant were evaluated with the Perseus software (versions 1.3.0.4 and 1.4.0.0).

For SILAC experiments the protein.txt was uploaded and the 'ratio H/L normalized' values of forward and reverse experiment were selected as expression values. The matrix was filtered for columns 'Only identified by site', 'Contaminant' and 'Reverse hits'. The logarithms of 'ratio H/L normalized' to the base of two for the forward and reverse experiment were calculated and plotted. To correct for differences in protein expression, the logarithms of 'ratio H/L normalized' were multiplied, a product of >4 was suggested to point on enrichment of the protein due to differences in the lysates. The 'Significance A' for forward and reverse experiment were calculated, proteins being significant for both experiments were considered to be outliers binding to either the GDP- or GTP-bound Rho GTPase.

For label-free experiments the protein.txt was uploaded and 'LFQ Intensity' for each experiment was selected as expression value. Proteins were filtered as described above. Only proteins with ratios in both experiments were considered. The logarithms of 'LFQ intensity' to the base of two were calculated. For each Rho GTPase triplicate the LFQ intensities were grouped in either GDP or GTP experiment. Proteins were required to possess 3 valid values in one of the two groups otherwise there were filtered out. Missing values were replaced by normal distribution (width 0.3, down shift 1.8). A two sided t-test was performed with an FDR of 5% and an s0 of 0.5[223]. Results were plotted in a volcano plot. Significant hits were plotted in a network.

2.6.3 Cluster analysis of gene ontology (GO) terms

To test identified interactors for enrichment in GO terms the online DAVID tool was used[224]. The respective list of interactors was compared against a human background if not stated differently. Significant count threshold was set to 1 and the EASE score (modified Fisher's exact test probability) cutoff was set to 1. The p-values mentioned in this thesis are not Benjamini-Hochberg corrected.

2.6.4 Alignment of protein sequences

Protein sequences of Rho GTPases in the fasta format were obtained from uniprot[225]. Amino acid sequences of Rho GTPases were aligned with the ClustalW online tool[226] using standard settings.

3 The quantitative Rho GTPase affinity pull-down (qGAP)

We aimed to combine quantitative mass spectrometry with standard biochemical methods to establish a screening method for Rho GTPase interaction partners: The quantitative Rho GTPase affinity pull-down (qGAP). qGAP considers the nucleotide loading state of the GTPase. For the development of this interaction screening we chose the Rho members RhoA, RhoB, RhoC, RhoD, Rac1 and Cdc42 as targets covering the four subfamilies of classical Rho GTPases with nucleotide hydrolysis ability. RhoA, Rac1 and Cdc42 have been characterized in detail and were used as standards to assess the quality of the qGAP method. qGAP was developed based on classical pull-down approaches.

An overview of the qGAP principle is shown in Figure 3.1. First, recombinant N-terminal GST-tagged Rho GTPases were purified. The proteins were loaded with either GDP or GTPγS and excess nucleotide was removed. GTPγS is a GTP analogue with slower hydrolysis kinetics[227,228]. The GST-tag was not cleaved off to allow for a higher surface and thereby for a more efficient binding of the GTPase to the NHS matrix in the next step. The qGAP affinity matrix was then used to screen lysates for Rho interaction partners, either from SILAC labeled cells or from label free whole tissue samples. The qGAP matrix was washed and binding partners to Rho^{GDP} or Rho^{GTP} eluted, subjected to in solution digest and peptides measured via mass spectrometry. Additionally different coupling and immunoprecipitation strategies were tested as alternatives and compared (see sections 3.1.2 and 3.3).

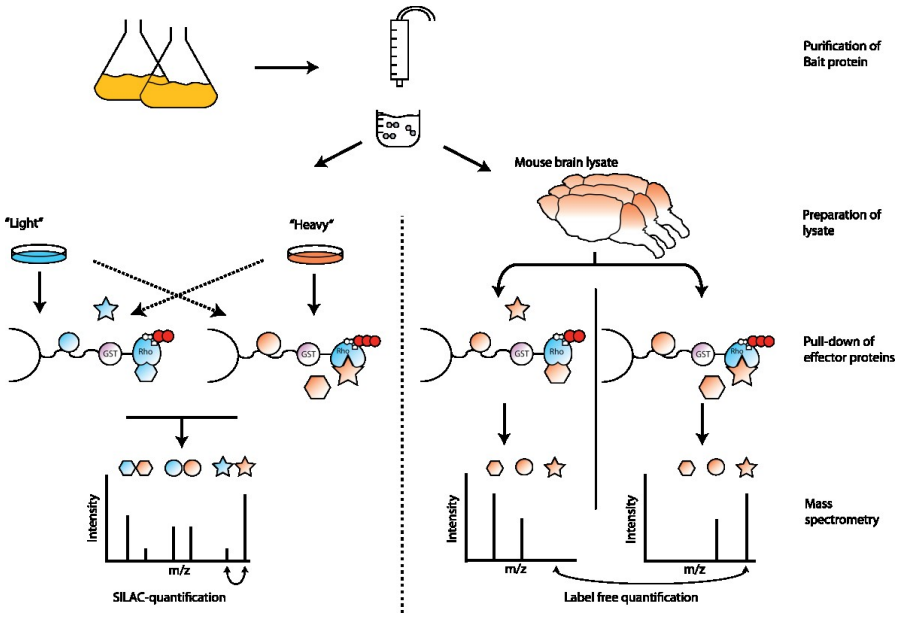

Figure 3.1: Experimental scheme for SILAC-qGAP (left) and label free, LF-qGAP (right). Both procedures require the purification of GST-Rho proteins and their binding to sepharose. For SILAC-qGAP label swap experiments are symbolized by dashed arrows. H and L pull-down from $Rho^{GTPγS}$ and Rho^{GDP} are mixed after the experiment. In contrast for label free experiments, from mouse brain, the $Rho^{GTPγS}$ and Rho^{GDP} pull-downs are measured separately.

3.1 Development of qGAP

3.1.1 Purification of Rho GTPases

In the first step of qGAP development we purified and loaded GST-fusion proteins of RhoA(F25N), RhoB, RhoC, RhoD, Rac1 and Cdc42. All constructs were full length apart from Rac1 (amino acids 1 – 187) and Cdc42 (1 – 178). For Rac1 and Cdc42 the prenylation site had been removed for better solubility. RhoA(F25N) carries a mutation that increases solubility[229]. For simplicity the RhoA(F25N) is termed RhoA in this work. The six Rho GTPases were expressed in *E. coli*. Cells were harvested and lysed by using a microfluidizer or a sonicator. The proteins were purified by Glutathione affinity chromatography and size exclusion chromatography. Exemplary results of steps are shown in Figure 3.2A.

GST-RhoA, -Rac1 and -Cdc42 purifications resulted in high yields (between 10 – 20 mg per liter culture), whereas GST-RhoB, -RhoC and -RhoD resulted in smaller yields (< 1 mg/l). For the latter three proteins no size exclusion chromatography was performed. Proteins were loaded with either GDP or GTPγS, the loading efficiency was then measured after removal of excess nucleotide by analytical HPLC (Figure 3.2B). The loading efficiency was typically between 82 and 90%.

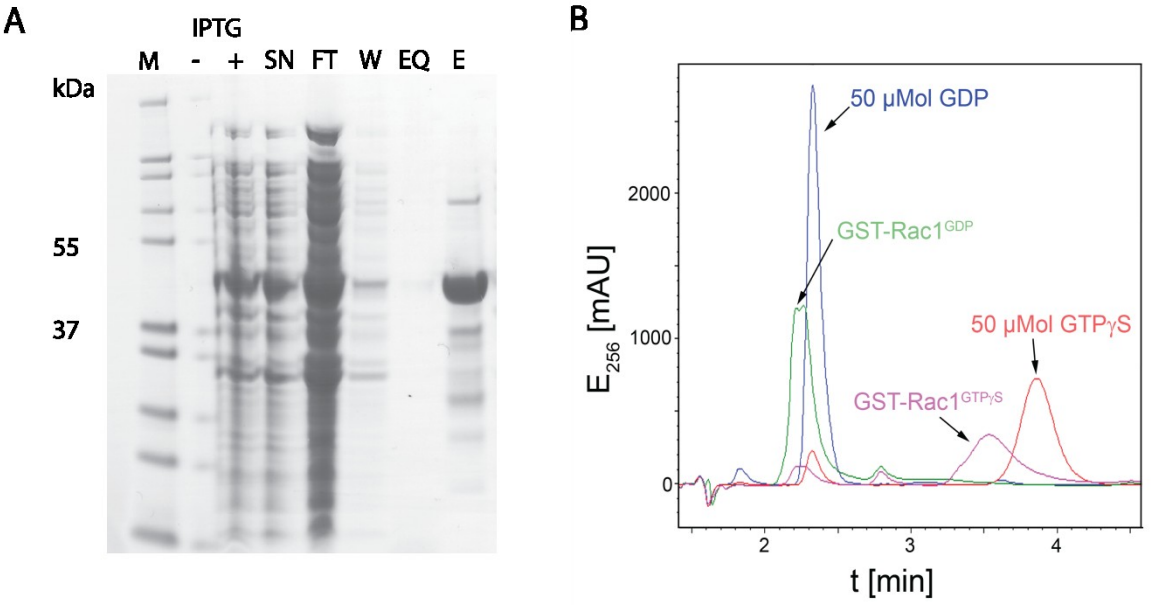

Figure 3.2: Typical purification and nucleotide loading results for GST-Rac1. (A) Coomassie-stained SDS-PAGE of various samples from GST-Rac1 purification: M: Marker, expected size of GST-Rac1 ~48 kDa, -/+ IPTG: whole cell bacterial lysate before and after induction, SN: supernatant of cell pellet, FT: flow-through of glutathione sepharose column, W: wash of column with wash buffer, EQ: wash of column with equilibration buffer, E: Elution. (B) Superimposed elution profiles from analytical HPLC: GDP/GTPγS: 50 µMol of nucleotide standards, GST-Rac1$^{GDP/GTP\gamma S}$: GST-Rac1 with the respective nucleotide bound, the area below the curves represents the amount of nucleotide.

SDS-PAGE gels were Coomassie-stained and Rho protein containing bands were sliced out and subjected to in-gel digestion and mass spectrometry to verify the sequence on the protein level. For

all GTPases more than 90% of the sequence was covered. Undetected parts were tryptic peptides of less than six amino acids in length and therefore not expected to be found.

3.1.2 Test of different coupling strategies for qGAP affinity matrix

For an interaction screen the purified Rho GTPases need to be bound to a solid phase matrix. Thus, in a second step of qGAP method-development, we tested several strategies for coupling the Rho proteins to a sepharose matrix. We tested if reversible binding to glutathione beads is sufficient or if a covalent crosslinking step is necessary. For this we compared (A) binding to glutathione matrix and (B) binding to glutathione matrix followed by covalent crosslinking with dimethylpimelimidate[230] and (C) direct covalent crosslinking to an N-hydroxysuccinimide (NHS) matrix[231,232] (Figure 3.3A-C). The three different approaches have different advantages and disadvantages: The usage of a glutathione matrix has the advantage that the GST-Rho fusion protein is bound in a directed way towards the matrix. GST functions as a linker and the Rho protein should be free to interact with effectors. However, without crosslinking recombinant Rho GTPases could also be eluted. This is problematic since peptide signals of GST and Rho GTPases would be the most prominent signals in the mass spectra and potentially interfere with identification of effector proteins. In contrast, usage of the NHS matrix would link the Rho protein randomly in an undirected way towards the matrix, but only effector proteins are expected in the eluate. By using directed binding to a glutathione matrix followed by covalent crosslinking with DMP, we hoped to combine both advantages. However, DMP may block binding sites on the GTPase during the coupling step.

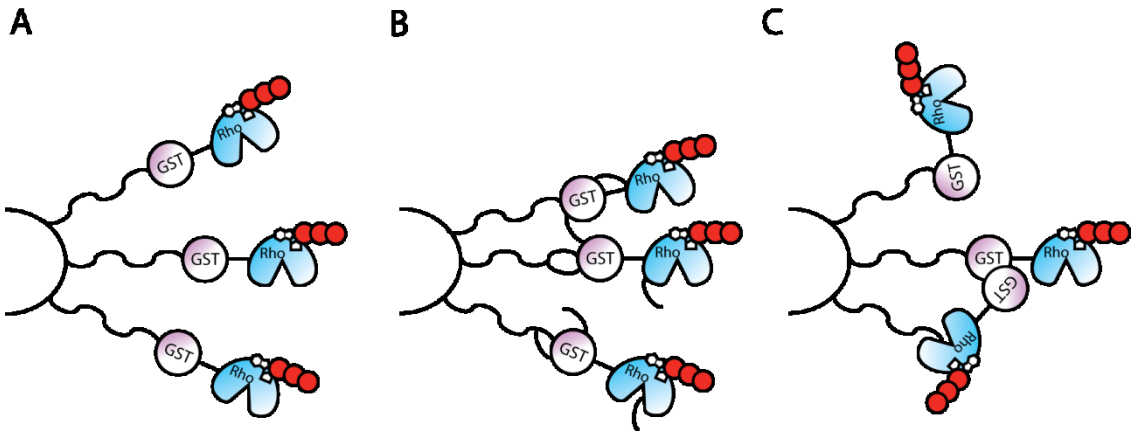

Figure 3.3: Three coupling strategies of GST-Rho proteins to sepharose. (A) GST-Rho fusion proteins are reversibly bound to glutathione-sepharose. (B) GST-Rho fusion proteins are bound to glutathione sepharose and covalently crosslinked by dimethylpimelimidate. (C) Fusion proteins are covalently coupled in an undirected way in a one-step binding to sepharose.

To compare effectors specific for the GDP and GTPγS forms of Rho GTPases we used the SILAC technology in the HeLa cell culture system[233]. Rho GTPase effectors are expected to be mainly located in the cytoplasm[234]. After subcellular fractionation cytoplasmic extracts of 'light' or 'heavy'

labeled HeLa cells were used for the pull-down. The affinity matrix with the GTPγS form of the respective Rho GTPase was incubated with the heavy and the GDP form with the light labeled cell lysate. Proteins were eluted, mixed and measured by MS. A specific interaction partner of the $Rho^{GTP\gamma S}$ state is expected to show a high heavy to light ratio of its peptide peak intensities (see Figure 3.1). These 'heavy to light ratios' are further normalized and as a general praxis the logarithms to the base of two ('log_2 fold changes' or 'L2FC') are calculated.

The evaluation of different coupling strategies was done with $Cdc42^{GTP\gamma S}$ against $Cdc42^{GDP}$. The identified proteins were sorted by their 'normalized heavy to light ratio'. As a rough estimation of the quality of the pull-down, known effector proteins from the literature, which were among the top 30 hits for each experiment, were counted. In Figure 3.4 the results of different coupling strategies are summarized in a Venn diagram.

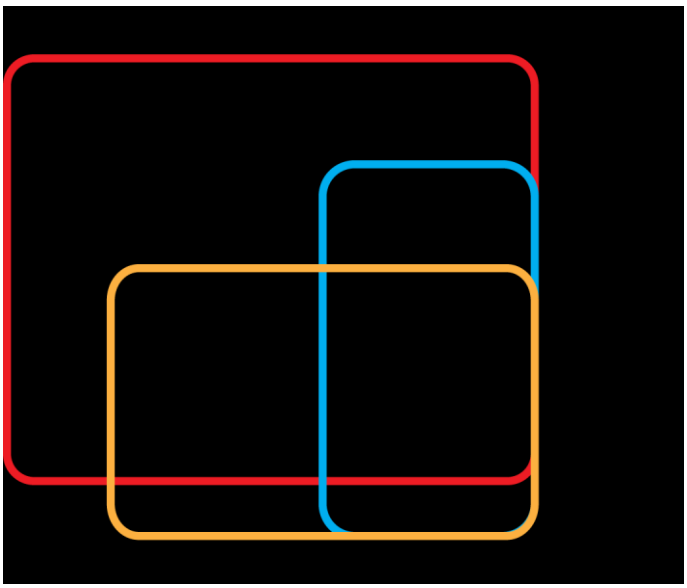

Figure 3.4 Venn diagram with $Cdc42^{GTP\gamma S}$-binding proteins in different coupling strategies. Proteins from H-labeled cells were pulled down with $Cdc42^{GTP\gamma S}$ and proteins from L-labeled cells with $Cdc42^{GDP}$. The number of literature-described proteins among the top 30 hits of the protein list sorted by normalized H/L ratios is mentioned.

In total 22 literature-described interaction partners were identified by the three coupling strategies. Compared to the other strategies, NHS coupling identified most Cdc42 interaction partners (20 of 22). DMP crosslinking identified ten interaction partners and GST coupling identified seven. Interestingly, only 2 proteins were not detected with the NHS pull-down. These were WIPF1 and WIPF2, both were not identified at all in the NHS experiment.

It was concluded that crosslinking with NHS matrix promises to be most successful.

3.2 Systematic identification of Rho GTPase interaction partners using qGAP

3.2.1 Interaction partners of Rho GTPases in Cell culture

For systematic identification of Rho GTPase binding partners from SILAC-labeled HeLa cells, the label swap strategy was applied: To compensate for potential differences in protein expression levels between light- and heavy-labeled cells, a forward and a reverse experiment were conducted. The forward experiment was performed as described in 3.1.2. Additionally in the reverse experiment the affinity matrix with the GTPγS-form of the respective Rho GTPase was incubated with the light and the GDP-form with the heavy labeled cell lysate (isotope or label swap)[235].

For each Rho GTPase we were able to identify several proteins as interaction partners by quantitative mass spectrometry, showing clear differences in intensities between heavy and light states (example spectra Figure 3.5A-E). As an example for $RhoA^{GTP\gamma S}$-, our assay identified the known interaction partner Pkn2. The serine/threonine-protein kinase N2 (Pkn2) is activated by autophosphorylation after $RhoA^{GTP}$ binding and mediates specific signal transduction processes as a RhoA induced transcriptional activation of the serum response factor[236]. Peptides of Pkn2 show higher intensity in the heavy form ($RhoA^{GTP\gamma S}$ pull-down) compared to the light form ($RhoA^{GDP}$ pull-down) in the forward experiment (Figure 3.5A). In the reverse experiment the light form of the respective peptide has higher ion intensity then the respective heavy form (Figure 3.5B). For $RhoA^{GDP}$-, we identified Rho GDI 1 as an interaction partner. Rho GDP-dissociation inhibitor 1 (Rho GDI 1) binds $RhoA^{GDP}$ and inhibits GDP dissociation and RhoA activation[237]. Light peptides of Rho GDI 1 have higher intensity in the forward experiment whereas heavy peptides of Rho GDI 1 are more prominent in the reverse experiment (Figure 3.5D and E). Glyceraldehyde-3-phosphate dehydrogenase (GAPDH), a protein not linked to RhoA biology, is detected with similar abundances in the two nucleotide pull-downs (reverse experiment shown Figure 3.5C). GAPDH represents a typical unspecific binder. The unspecific binders are either matrix-binding background or bind to both nucleotide species with similar affinity.

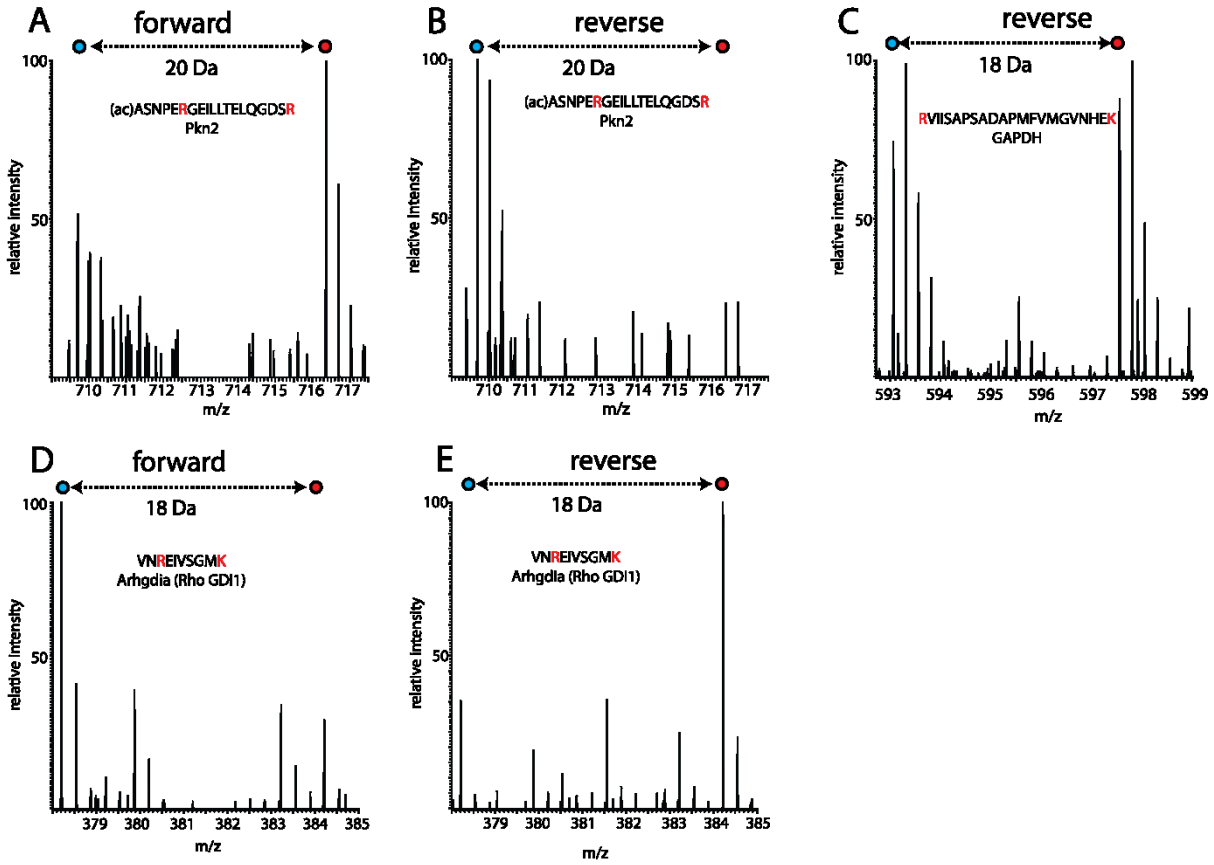

Figure 3.5: Mass spectrometry survey scans (MS1) for SILAC-qGAP. Survey scans show abundance difference for heavy (red: monoisotopic peak of the heavy peptide) and light (blue: monoisotopic peak of the light peptide) peptides. Differentially labeled amino acids are colored in red. Depicted are RhoA Interaction partners Pkn2 (A) and (B) and Rho GDI (Arhgdia) (D) and (E). The background binder GAPDH has same H and L intensities (C), only reverse experiment shown.

For each Rho GTPase pull-down 1,100 – 1,200 proteins were quantified for their heavy to light intensity ratios. A critical point is to distinguish significant Rho binders from unspecific background. Proteins with a difference in abundance between the heavy or light lysate could falsely be considered as specific interaction partners of the GTPγS- or GDP-form if only the forward or reverse experiment was considered. By performing the complete label swap experiment, these proteins can easily be identified since they appear in both experiments with either positive or negative $\log_2$ fold change of heavy to light ratios. The product of their $\log_2$ fold changes is always positive. Since these proteins should be removed before calculation of the significance, all proteins with a product of $\log_2$ fold changes from the forward and reverse experiment greater than 4 were excluded (usually a maximum of ten proteins). The value 4 was employed because it worked best to separate protein background around the origin from proteins with differences in abundance between the heavy or light lysate.

Next, the significant outliers within the distribution of $\log_2$ fold changes were calculated for the forward and reverse experiment (example for Cdc42 Figure 3.6). When a protein is a statistical outlier it can be assumed that this protein is a biological interactor of the respective Rho GTPase. The significance was calculated dependant on the protein intensity (“significance B” in the software

package Perseus) with a Benjamini-Hochberg FDR < 5%[178]. All proteins were plotted with their protein intensities (summed peptide intensities) against the $\log_2$ fold change of normalized H/L ratios.

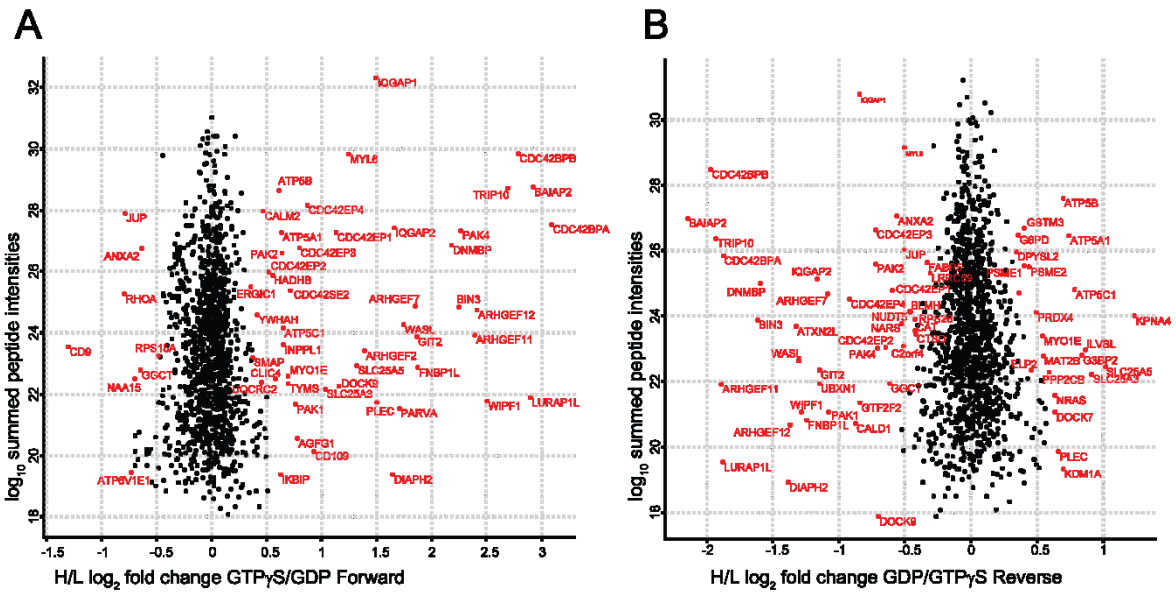

Figure 3.6: Significant interaction partners of Cdc42 in SILAC-qGAP. Proteins from H- and L-labeled cells were pulled down with $Cdc42^{GTP\gamma S}$ and $Cdc42^{GDP}$ in a forward (A) and reverse experiment (B). Proteins that were calculated as significant outliers for the respective experiment are labeled in red. The results from the forward and reverse experiment were later united to a single graph (see Figure 3.7, example for Cdc42 in panel (C)).

Proteins were considered as $Rho^{GTP\gamma S}$-specific binders if their $\log_2$ fold change of normalized ratios was a significant outlier and positive for the forward experiment and a significant outlier and negative for the reverse experiment. For Rho^{GDP}, specific binders had to be significant outliers with swapped algebraic signs for their $\log_2$ fold change of normalized ratios.

We found loading-state dependent interaction partners for RhoA, Rac1 and Cdc42 (Figure 3.7). These were clearly distinguishable from several hundred proteins that were not binding specifically to one of the two nucleotide states. Most proteins were specific binders for the GTPγS-bound Rho GTPase (second quadrant), in accordance with the GTP-bound state being the active form that binds to downstream effector proteins. Interaction partners of Rho^{GDP} are expected to have opposite $\log_2$ fold changes (fourth quadrant). Background binders are expected to be located around the origin. Within the group of specific binding partners, most proteins are literature-known or homologs of literature known Rho GTPase binding partners, thereby proving the functionality of the assay (for details on enrichment see section 3.2.3).

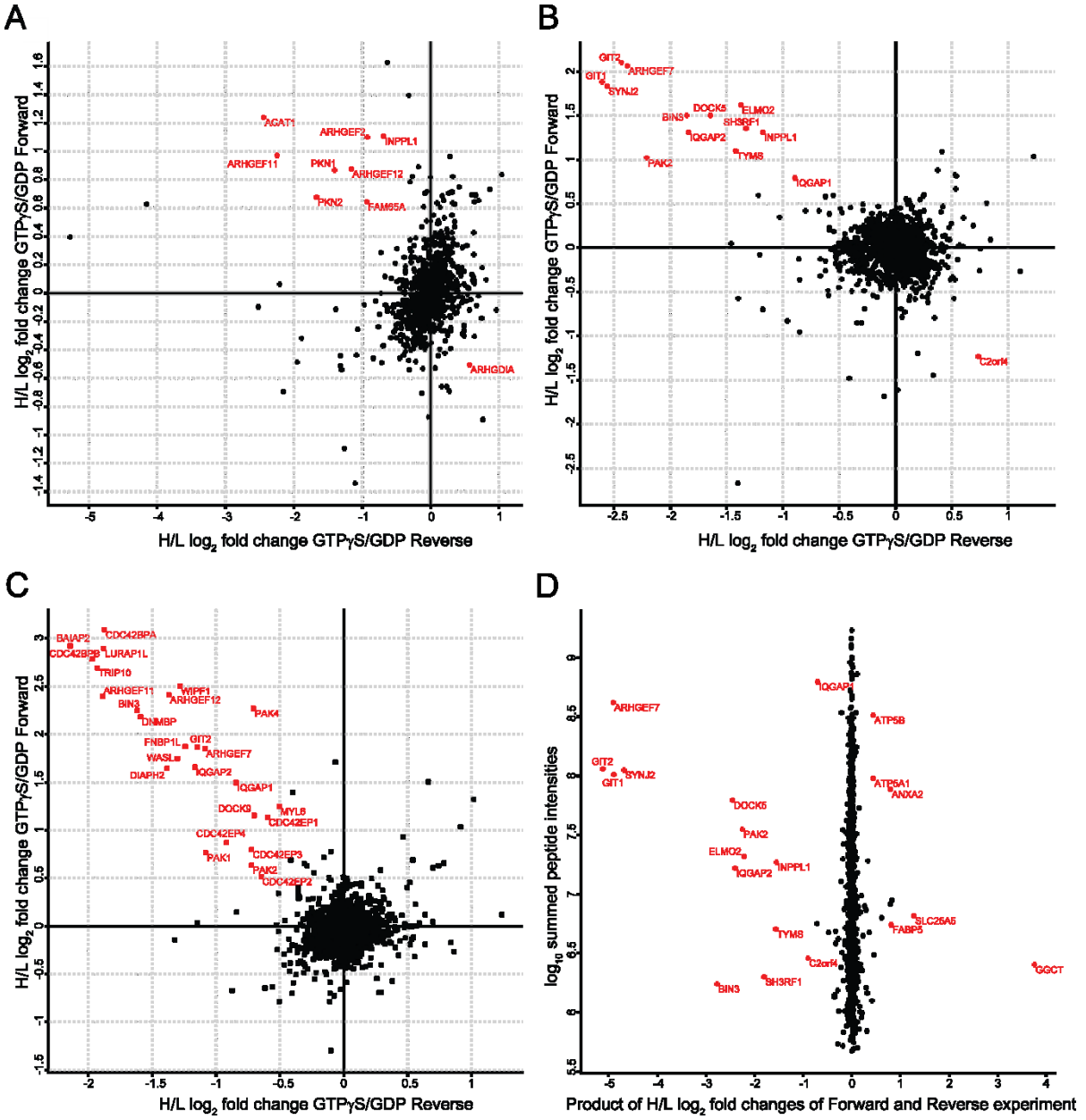

Figure 3.7: qGAP from SILAC-labeled HeLa cells. Cytoplasmic fractions of H and L labeled HeLa cells were used for pull-downs with the GTPγS- and GDP-form of Rho GTPases as described in **Figure 3.1**. Scatter plot summarizing results for (A) RhoA, (B) Rac1 and (C) Cdc42 pull-downs. Significant interactors are marked with their official gene names labeled in red. In all cases significant outliers form a cloud in the secon quadrant. (D) Alternative display of the Rac1 pull-down. The overall summed peptide intensities of the forward and reverse Rac1 pull-down plotted against the product of $\log_2$ fold changes of the forward and reverse experiment. Notably, significant interaction partners are spread over the whole range of intensities.

For Cdc42, we identified different classes of effectors such as GEFs (Rho GEF 2, -7, -11 and -12, depicted with their gene name Arhgef) GAPs (IQGAP1 and -2), effector proteins such as serine-threonine kinases (PAK1 and -4) and the scaffold protein BAIAP2 (Figure 3.7C). This shows that the assay is able to recognize a broad range of different effector types. Moreover, also Rac1 and RhoA experiments (Figure 3.7A, B) resulted in identification of canonical effectors as Rho^{GTP} specific interaction partners, for example, Dock1, Dock2, Synaptojanin (all three $Rac1^{GTP}$ binders), PKN2 and Rock2 (both $RhoA^{GTP}$ binders). Aside from Rho GDI 1 (gene name: ARHGDIA) for $RhoA^{GDP}$ and MEMO1

for Rac1^{GDP}-, all interaction partners were bound to the GTPγS-form of the respective Rho protein. 49 proteins were showed to be significant interactors in SILAC-qGAP: 26 binding partners for Cdc42, 14 for Rac1 and nine for RhoA. From the data the conclusion was drawn that the novel q-AP-MS based screen can enrich Rho GTPase effector proteins (see section 3.2.3 for the enrichment of literature-known binding partners among the significant interactors).

Interestingly, identified interaction partners of Rac1 (Figure 3.7D) spanned more than two orders of magnitude in summed peptide intensity. This suggests that qGAP is able to identify interaction partners over a broad range of abundance within the pull-down eluate.

3.2.2 Interaction partners for Rho GTPases in Brain lysates

We next addressed the capability of qGAP to specifically enrich Rho GTPase interaction partners from non-labeled tissue samples (label free or LF-qGAP). SILAC had been successfully established for numerous model organisms[176,238]. However, cost and time intensive labeling complicates these experiments for animal models. Recently, label-free quantification was introduced for identification of interaction partners of endogenously expressed GFP-fusion proteins[239]. Tissue experiments promise a broader expression profile of proteins including interaction partners, which may not be present in cell culture. Mouse brain was chosen due to the fact that five of the six investigated Rho GTPases are expressed in this tissue (only RhoC seems to be expressed in macrophages or glandular cell types)[240]. In addition, different cell types are present in brain, which should lead to a large number of potential binding proteins being available in the lysate. In order to determine whether different tissue types present different binding profiles, mouse brains were dissected into a hippocampus, the remaining cerebrum and a cerebellum fraction. Experiments were performed with cerebrum and cerebellum fractions for RhoA and Rac1, and all three tissue types for Cdc42.

RhoA, Rac1 and Cdc42 have been in the focus of research for long time (for simplicity they are further called ‘canonical Rho GTPases’). This data was then extended by a second row of experiments in which whole brain lysates were used for interaction studies of RhoB, RhoC and RhoD. The latter three Rho GTPases (further termed ‘uncharted Rho GTPases’) have not been studied that intensively yet. The obtained quantitative data was used to assess the power of LF-qGAP and to construct the first comprehensive network of Rho GTPase interactions.

For a label free quantification experiment, pull-down experiments from the GDP- and GTPγS-form of Rho GTPases were performed and separately measured. The protein intensities were normalized and compared to each other (Figure 3.1 right). Peptide signals of Rho binders are expected to exhibit different peptide intensities in Rho^{GTPγS} and Rho^{GDP} MS runs. To clearly distinguish between specific

interaction partners and background binders, each pull-down was performed in triplicates. This allows determination of the significance of differences of mean intensities between the $Rho^{GTP\gamma S}$ and Rho^{GDP} MS runs by using a Student's t-test. Both pieces of information, the log_2 fold change of normalized intensity ratios of a protein between the $Rho^{GTP\gamma S}$ and Rho^{GDP} run, and its significance represented by the p-value, are summarized in volcano plots. A protein was considered to be a specific interaction partner of either the GDP- or GTPγS-form of a Rho GTPase with respect to both properties[223]. Visually the GTPγS-specific interaction partners are found in the upper right and the GDP-specific binders in the upper left corner of a volcano plot.

We were able to identify and quantify 2,300 proteins in an analysis containing pull-downs from hippocampus (Cdc42), cerebellum (Cdc42, Rac1, RhoA) and remaining cerebrum (Cdc42, Rac1, RhoA). For the experiments of RhoB, RhoC and RhoD from whole brain lysates, 3061 proteins were identified and quantified.

For the six Rho GTPases we observed 381 significant outliers (=interactions) over all experiments (Figure 3.8A-F). Some proteins were repeatedly identified interaction partners for a Rho GTPase (e.g. Pak1 was an interaction partner for Cdc42 in all three tissues). Filtering these multiple hits we identified a total number of 291 Rho GTPase interactions (Table 6.1). Significant binders possessed log_2 fold changes of -5.4 to -1.1 for GDP- and 1.1 to 10.2 for GTPγS-specific interactors.

As expected, the number of identified interaction partners was considerably higher in LF-qGAP compared to SILAC-qGAP. As an example, for the single RhoA-Cerebrum experiment 42 interaction partners were identified whereas in the SILAC pull-down for RhoA only nine proteins were determined significant interactors (for detailed comparison see section 3.2.7). Classes of proteins with different molecular functions were identified as interaction partners (Table 3.1). The molecular functions showed links to Rho GTPase biology.

Table 3.1: Selected examples of molecular functions for identified Rho GTPase interaction partners in LF-qGAP. The listed terms were identified with the DAVID online tool. Interaction partners are involved in a broad range of molecular functions. The selected examples are functions that are linked to Rho GTPase biology.

Molecular function	Example proteins
Guanine exchange factors	Rho GEF1, -2, -6, -7, -11, -12, -17, -18, Kalirin, Plekhg5, Prex1, Tiam2, Trio, Akap13, Abr, Dock9
GTPase activating proteins	Rho GAP 5, -32, -35, PI3K regulatory subunit
Dissociation inhibitors	Rho GDI 1 (ARHGDIA)
Protein kinases	PAK1-4, -6, -7, Pkn1, Rock1, -2
Scaffold proteins	Baiap2, Pard6a, Sh3RF1

Additionally, proteins of higher order molecular complexes such as the WAVE complex (Abi1, 2, Brk1, Cyfip2, Nckap1, WASF1, 3) and WASP complex (FNBP1, FNBPL1, TRIP10, WASL) were identified. The identified Rho interaction partners cover a broad range of biological processes as listed in Table 3.2. The regulation of the actin cytoskeleton, of focal adhesions or of adherens junctions are typically linked to Rho GTPases.

Table 3.2: Selected examples of biological processes for identified Rho GTPase interaction partners in LF-qGAP. The listed terms are based partly on the gene ontology term "Biological process" as well as the "KEGG pathways" and were identified with the DAVID online tool.

Biological process	Example proteins
Regulation of actin cytoskeleton	GIT1, NCKAP1, Brk1, PAK1-4, -6, -7, WASF1, Baiap2
Focal adhesion	Rock1, Grb2, Grlf1, Ppp1ca
Adherens junctions	N-WASP, IRSp52, WAVE
Axon guidance	Rock1, -2, PAK, PlexinB1, -2, LARG (Rho GEF 12)
Cell division	Anilin, Pard6a, Septi4, Rho GEF 2, PIK3 cat sub
Cell polarity	LGL, Pard6a, PKCiota

The given examples for molecular and biological properties of identified interaction partners demonstrate the presence of proteins that are related to Rho biology (see also section 3.2.3).

Importantly, proteins known to fulfill specific functions in neurons, for example, neuronal differentiation (Rho GAP 32) or neuronal shape and growth (Kalirin) were also identified. Some of the interactions may be indirect, for instance the interaction of LLGL to Cdc42 is mediated by PARD6A[105]. The interaction of Lurap1 could be mediated by Cdc42bpa or Cdc42bpb (alternative names: MRCKα/β)[241]. In both examples the potential mediators of the indirect interactions were identified as specific interaction partners as well.

Similar to the SILAC experiments we found that most interaction partners bound specifically the GTPγS-form of Rho proteins. Exceptions were the dissociation inhibitor Rho GDI 1 (Arghdia) and some GEF proteins (Rho GEF 17, Kalirin, Tiam2). However, it is important to note that most of the Rho GEF proteins bound to the GTPγS-form of the respective Rho GTPase (Rho GEF 1, -2, -6, -7 (labeled with their gene name Arhgef in Figure 3.8) and Akap13). This behavior was unexpected, but is supported by a recent study[242].

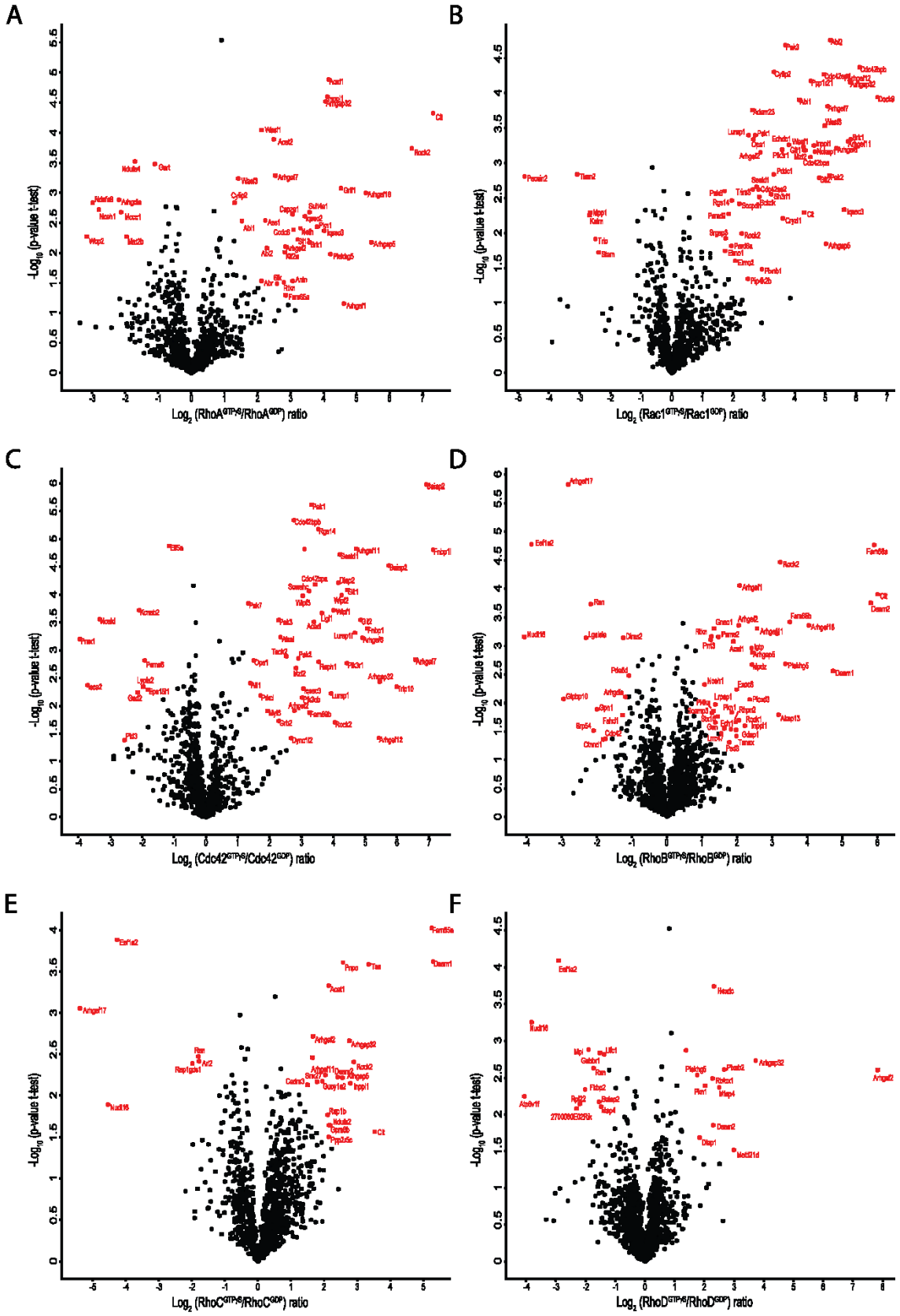

Figure 3.8: LF-qGAP from brain lysates for six Rho GTPases. Volcano plots displaying the difference of means of intensities between the GTPγS and GDP pull-down (log_2 ratio of intensities) and the significance of the change of the difference of means ($-log_{10}$ p-value). Cerebrum pull-downs for (A) RhoA, (B) Rac1, (C) Cdc42. Pull-downs from whole brain lysates for (D) RhoB, (E) RhoC, (F) RhoD. Significant outliers (=interactors) are labeled in red with their official gene names. GTPγS-specific interactors are expected in the upper right corner, interactors of the GDP-form in the upper left corner.

3.2.3 Enrichment of Rho binding proteins by qGAP

To estimate the quality of LF-qGAP, we aimed to determine the sensitivity, specificity and reproducibility. The comparison of the data with confirmed literature is necessary to determine probabilities, Type I and II errors (false positives and negatives). For the canonical Rho GTPases a good coverage of the biological interactions by available databases is to be expected.

The "**H**uman **I**ntegrated **P**rotein-**P**rotein **I**nteraction r**E**ference" database (HIPPIE), a recently developed metadatabase was used as a standard[243]. HIPPIE combines interaction data from 10 source databases (HPRD, BioGRID, IntAct etc.) and 11 individual high throughput studies. We expected HIPPIE to represent a solid standard for interaction partners of canonical Rho GTPase *in vivo*. However, it should be noted that part of the data included in HIPPIE resulted from yeast two-hybrid assays, which are prone to identify false positives. Compared to manual studies of the literature numerous known Rho interactors were not included in HIPPIE. Despite these drawbacks HIPPIE still seems to be the most comprehensive non-biased database for Rho GTPase interaction partners.

As a first step to estimate the quality of qGAP, the enrichment of known Rho binding proteins in significant qGAP hits was calculated. A total number of 552 interactions are listed in HIPPIE for the six Rho GTPases (11th October 2013). Most of the interactions are noted for the canonical GTPases (482 total, 128 for RhoA, 180 for Rac1 and 174 for Cdc42) and a lower number for the uncharted GTPases (70 total, 34 for RhoB, 20 for RhoC, 16 for RhoD).

The enrichment of HIPPIE-listed Rho interaction partners among the significant qGAP hits was calculated with the help of the cumulative hypergeometric probability using the formula:

$$p(X \geq k) = \sum_{y=0}^{k} \frac{\binom{K}{y}\binom{N-K}{n-y}}{\binom{N}{n}}$$

N Population size (total number of interaction partners listed in HIPPIE: 13477)

K Successes in population (number of interaction partners for the respective Rho GTPase)

n Sample size (number of significant hits in the respective experiment)

k Successes in sample (overlap between significant hits and HIPPIE-listed interaction partners)

p (X ≥ k) Probability to identify at least the number of overlapping proteins

The hypergeometric test is used to calculate probabilities for sampling without replacement. Low probabilities indicate an enrichment of HIPPIE-listed interaction partners in the SILAC-qGAP hits. The

HIPPIE database does not differentiate between interaction partners of the GDP- and GTP-forms of GTPases. Therefore, the significant GDP- and GTPγS-specific hits for a Rho GTPase from qGAP were pooled. We first investigated SILAC-qGAP data for RhoA, Rac1 and Cdc42. After filtering we obtained 49 specific interactions from which 32 were annotated in HIPPIE. To estimate the quality of the enrichment the cumulative probability by hypergeometric testing was calculated (results in Table 3.3).

Table 3.3: Results of SILAC-qGAP and enrichment in HIPPIE interaction partners. Identified interaction partners from SILAC-qGAP were checked for presence in the HIPPIE metadatabase (overlap). With hypergeometric testing the cumulative probability was calculated. Low cumulative probabilities indicate that SILAC-qGAP identifies known interaction partners for the respective Rho GTPase.

	Interactions SILAC-qGAP	**Overlap with HIPPIE (k)**		**Cumulative probability p (X ≥ k)**
RhoA	9	6	(66.7%)	$5.4 \cdot 10^{-11}$
Rac1	14	6	(42.85%)	$1.4 \cdot 10^{-8}$
Cdc42	26	20	(76.9%)	$1.2 \cdot 10^{-35}$
total	49	32	(65.3%)	$6.9 \cdot 10^{-35}$

As the hypergeometric test shows, the identified binding partners are with high significance (p-value ($X \geq k$) = $1.4 \cdot 10^{-8}$ for Rac1 to $1.2 \cdot 10^{-35}$ for Cdc42) enriched in Rho GTPase interaction partners. Interestingly, almost all of the significant binding partners found by qGAP that were not listed in the HIPPIE database were either described in other literature sources as Rho binders (Inppl1, Acat1, Memo1), had homologs listed in HIPPIE (Fam65A, Dock5, Elmo2) or are likely indirect interaction partners (Git1, Git2). Only Thymidylate synthase (Tyms) has not been linked to Rho biology so far. This indicates that qGAP identifies almost exclusively known Rho GTPase interaction partners from SILAC samples. It should also be noted that a few binding partners have been described only recently (Bin3, Lurap1L, Acat1, Inppl1)[134,241,244].

The calculation of the cumulative hypergeometric probability was also applied to LF-qGAP (Table 3.4). Of 291 identified Rho GTPase interactions 60 were found in the database (20.6%). The calculated probabilities are significant with a range between 0.02 for RhoD and $7.3 \cdot 10^{-25}$ for Cdc42. Comparing the enrichments between SILAC- and LF-qGAP, better values were achieved for RhoA and Rac1 in the label free study. The canonical Rho GTPases have better enrichment scores than the uncharted RhoB, C and D. This can be explained by the much higher overall number of HIPPIE-listed interaction partners for the canonical Rho GTPases (ratio 7:1).

Table 3.4: Enrichment of Rho binding partners in significant qGAP hits. Significant qGAP hits were tested for known Rho binding partners by cumulative hypergeometric testing. The HIPPIE database was used as reference. . Low cumulative probabilities indicate that LF-qGAP identifies known interaction partners for the respective Rho GTPase.

Rho GTPase^{Nucleotide}	Interactions LF-qGAP	Overlap with HIPPIE (k)		Cumulative probability p (X ≥ k)	Overlap literature total	
$RhoA^{GDP}$	13	1	(7.7%)	$1.3 \cdot 10^{-12}$	2	(15.4%)
$RhoA^{GTP\gamma S}$	38	10	(26.3%)		15	(39.5%)
$Rac1^{GDP}$	9	3	(33.3%)	$2.5 \cdot 10^{-19}$	5	(55.6%)
$Rac1^{GTP\gamma S}$	56	15	(26.8%)		26	(46.4%)
$Cdc42^{GDP}$	12	0	(0%)	$7.3 \cdot 10^{-25}$	0	(0%)
$Cdc42^{GTP\gamma S}$	60	22	(36.7%)		29	(48.3%)
$RhoB^{GDP}$	14	2	(14.3%)	$3 \cdot 10^{-9}$	2	(14.3%)
$RhoB^{GTP\gamma S}$	38	4	(10.5%)		9	(23.7%)
$RhoC^{GDP}$	6	0	(0%)	$7.2 \cdot 10^{-4}$	0	(0%)
$RhoC^{GTP\gamma S}$	21	2	(9.5%)		3	(14.3%)
$RhoD^{GDP}$	12	0	(0%)	0.02	0	(0%)
$RhoD^{GTP\gamma S}$	12	1	(8.3%)		1	(8.3%)
total	291	60	(20.6%)	$5.13 \cdot 10^{-26}$	92	(30.3%)

The significant hits contained literature known proteins that were not listed in HIPPIE. When interaction partners described in the literature were included in addition to those described in HIPPIE, the overlap was clearly higher (30.3%). A large part (225 of 291, 77%) of the specific interactions was GTPγS-specific going hand in hand with the GTP-bound Rho GTPase representing the active state. The number of interaction partners described in the literature is higher for the group of GTPγS-specific binders (83 of 225, 36.9%) compared to GDP-specific interactors. Among the GDP-specific interaction partners, only nine were described in the literature. This could either indicate that the false positive rate is higher in the group of GDP-specific interaction partners or that Rho^{GDP} specific interactors have been studied less thoroughly than Rho^{GTP} interactors.

As an alternative to HIPPIE, the enrichment of known Rho effector domains within the group of significant outliers was calculated. First, Rho GTPases bind to distinct structural elements, e.g. the PAK-box binding domain (synonymously 'Cdc42/Rac interactive binding' (CRIB) region specific for Rac1 and Cdc42 interaction) and GEF/GAP domains. Secondly, the interaction partners are expected to contain domains that are necessary for their function, like binding to the actin cytoskeleton. The

list of all significant LF-qGAP outliers was analyzed with the online DAVID tool against mouse background (Table 3.5).

Table 3.5: Selected "Interpro" terms that were enriched in LF-qGAP hits. The list of identified qGAP interaction partners was tested for enrichment with the DAVID software. Note: not all proteins were annotated with Interpro terms.

Term	Number of proteins		P-Value
PAK-box/P21-Rho-binding	10	(6.1%)	$1.1 \cdot 10^{-14}$
Dbl homology (DH) domain	13	(8%)	$3.4 \cdot 10^{-13}$
Guanine-nucleotide dissociation stimulator, CDC24	11	(6.7%)	$2.7 \cdot 10^{-11}$
Pleckstrin homology	18	(11%)	$1.3 \cdot 10^{-10}$
Src homology-3 domain	15	(9.2%)	$4.8 \cdot 10^{-9}$
Rho GTP exchange factor	6	(3.7%)	$2.1 \cdot 10^{-8}$
Serine/threonine kinase Pak-related	5	(3.1%)	$8.3 \cdot 10^{-8}$
Pleckstrin homology-type	15	(9.2%)	$2.5 \cdot 10^{-7}$
Actin-binding WH2	6	(3.7%)	$5 \cdot 10^{-7}$
Serine/threonine protein kinase	14	(8.6%)	$5.9 \cdot 10^{-7}$

Among the enriched protein domains (Interpro database), typical Rho binding domains, such as GEF domains (DH with N-terminal PH-domain, GDS and Rho GTP exchange factor domains) and the Rho-binding PAK-box domain, were found. Additionally, sequences that are typically present in Rho effector proteins are enriched. For example, the WH2 motif is typically found in proteins that remodel the actin cytoskeleton and the Pak domain is found in kinases binding to Rho proteins.

For $RhoA^{GTP\gamma S}$, $Rac1^{GTP\gamma S}$ and $Cdc42^{GTP\gamma S}$ the significant hits were grouped to search for potential structural or biological links between interactors and Rho GTPases (**Figure 3.9**).

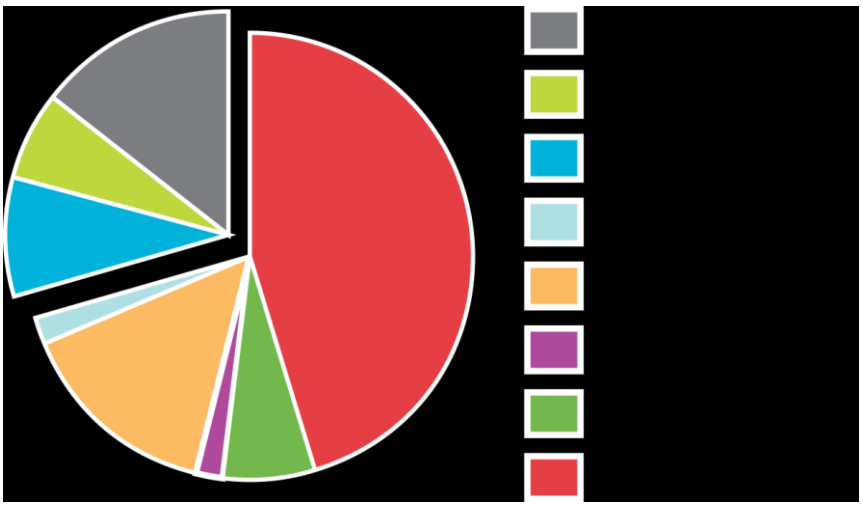

Figure 3.9: PIE chart grouping interactions of the GTPγS-specific binders of RhoA, Rac1 and Cdc42. 154 specific binders of the GTPγS-forms of the three GTPases were distributed into groups. The groups were chosen to explain the binding of the protein to the Rho GTPase.

Notably, nearly half of the interactions were described in the literature (45%). For the remainder, a large part of significant interactors (14.9%) is known to bind to another Ras GTPase than the one identified, most of them still to Rho GTPases (e.g. RhoA-Rock2 binding is known and Rac1-Rock2 binding was observed). This finding points to either promiscuous or indirect binding. Other identified interactors can be explained by either indirect binding (e.g. Lurap1 binds via Cdc42bpa), the presence of a Rho-binding domain (e.g. Cdc42bpa binding to Rac1 via CRIB domain) or the known binding of a homolog to a Rho GTPase (Fam65B-RhoA binding is described, the Fam65A-RhoA interaction was observed). 29.2% of the significant binders have not yet been related with Rho GTPases, but several (8.4%) have implications on the cytoskeleton (Kif2, Mzt2 and Septins). Unexpectedly a large number of metabolic proteins (10 proteins, 6.5%) were identified. Some of them were found to be interactors in several experiments, as for the interactions Cdc42-Acadl, Rac1-Echdc1 and RhoA-Acat1. The latter interaction is also supported by SILAC-qGAP and was recently reported[134]. All three interactions are involved in Coenzyme A-acyl metabolism.

3.2.4 Specificity, sensitivity and reproducibility of qGAP

To estimate the power of LF-qGAP, the sensitivity and specificity of the assay was calculated. The sensitivity reflects the capability to correctly identify true results and the specificity to identify false results:

$$sensitivity = \frac{n_{true\ positives}}{n_{true\ positives} + n_{false\ negatives}}$$

$$specificity = \frac{n_{true\ negatives}}{n_{true\ negatives} + n_{false\ positives}}$$

For this reason, the total number of 8506 protein identifications (summed over all experiments, repeatedly identified proteins) was mapped against the HIPPIE database (contribution of Dr. Henrik Zauber). Significant interactions were considered to be true positives if they were listed for the respective Rho protein, which hold true for 106 of 381. Additionally, 107 proteins from the non-significant protein background were listed in HIPPIE (false negatives).

Table 3.6: Contingency table for calculation of the specificity and sensitivity of LF-qGAP. True positives (upper right) and true negatives (lower left) are colored in green. False positives (upper left) and false negatives (lower right) are colored in red.

RhoA, B, C, D, Rac1, Cdc42	not HIPPIE interactor	HIPPIE interactor
significant	**275**	**106**
non significant	**8018**	**107**

Altogether LF-qGAP achieves a sensitivity of 0.5 and a specificity of 0.97. Notably these values do not change when only the canonical Rho GTPases are considered. Since not all literature-known interaction partners are part of HIPPIE, the calculation was repeated including additional literature-described interaction partners. Considering these additional true positives increases the sensitivity to 0.59. It has to be noted that, for practical reasons, the background was not checked for additional false negatives. This could have decreased the sensitivity of 0.59.

To estimate the reproducibility of qGAP, 42 individual LF-qGAP pull-downs (14 triplicates) were subjected to hierarchical clustering using their protein intensities (LFQ intensity). The experiments comprised experiments of the GTPases RhoA, Rac1 and Cdc42 from Hippocampus, Cerebrum and Cerebellum lysates. The clustering revealed that in almost all cases pull-downs from one triplicate experiment cluster together (Figure 3.10).

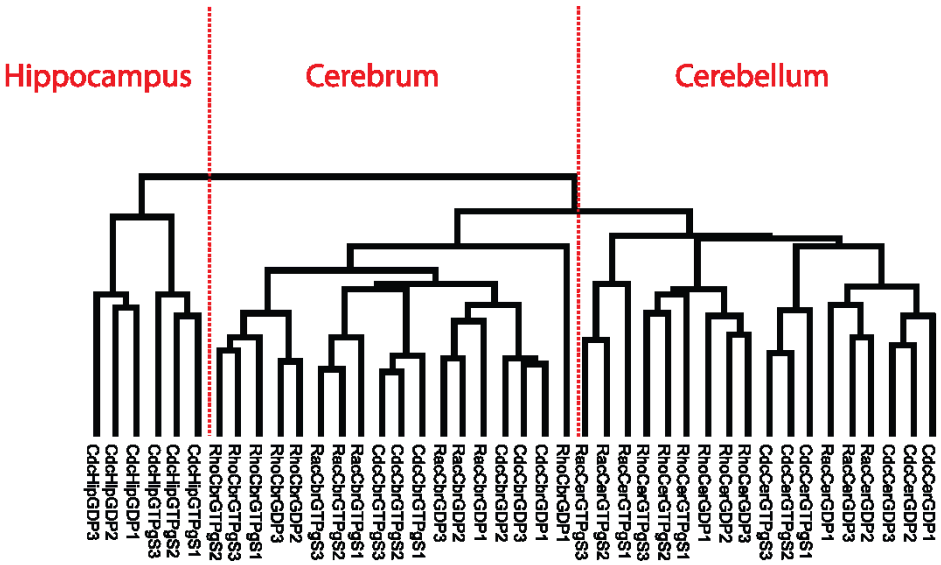

Figure 3.10: Dendrogram with hierarchical clustering of 14 triplicate experiments to estimate the reproducibility of qGAP. 'Hip': hippocampus, 'Cer': cerebellum, 'Cbr': cerebrum. Rho: RhoA, Rac: Rac1 and Cdc: Cdc42. 42 pull-downs (14 triplicates) were clustered based on their normalized protein intensities (LFQ intensity). In most cases the three triplicates of one experiment cluster together. This reflects the resemblance of the experiments and points to a high reproducibility of single qGAP pull-downs.

Moreover, pull-downs from the different lysate types cluster in three distinguishable branches in the dendrogram. Interestingly, in the 'Cerebrum branch' (abbreviation 'Cor', middle branch) samples of $Cdc42^{GTP\gamma S}$ and $Rac1^{GTP\gamma S}$ form a sub-branch and are more similar to each other than to their respective GDP-bound pull-downs. Only one experiment (RhoCorGDP1) does not cluster with the other two samples of the RhoA cerebrum experiment (explanation see discussion). Overall, clustering of individual LF-qGAP samples indicates that the data is highly reproducible.

3.2.5 Validation of identified interaction partners by Proximity Ligation Assay

In addition to indirect validation by *in silico* enrichment studies, an attempt was made to validate the novel interactions in a biological manner. For this reason, the proximity ligation assay[192,245] (PLA) was combined with specific activation of Rho GTPases using cytotoxic necrotizing factors CNF1 or CNF_Y[160,246]. PLA provides evidence for close association of proteins within cells with the readout of a fluorescence signal. For PLA, antibodies against the two proteins of interest are targeted with two organism-specific secondary antibodies that are labeled with oligonucleotides. If the target proteins are in close proximity the nucleotide sequences can be ligated and amplified. Upon addition of DNA-probes with a fluorescent label, their binding to these sequences can be detected. A common challenge in PLA experiments is to distinguish between a specific signal raised by the interaction of two proteins and background signal. To distinguish between Rho^{GTP}-specific interactions and background signals we employed the cytotoxic necrotizing factors.

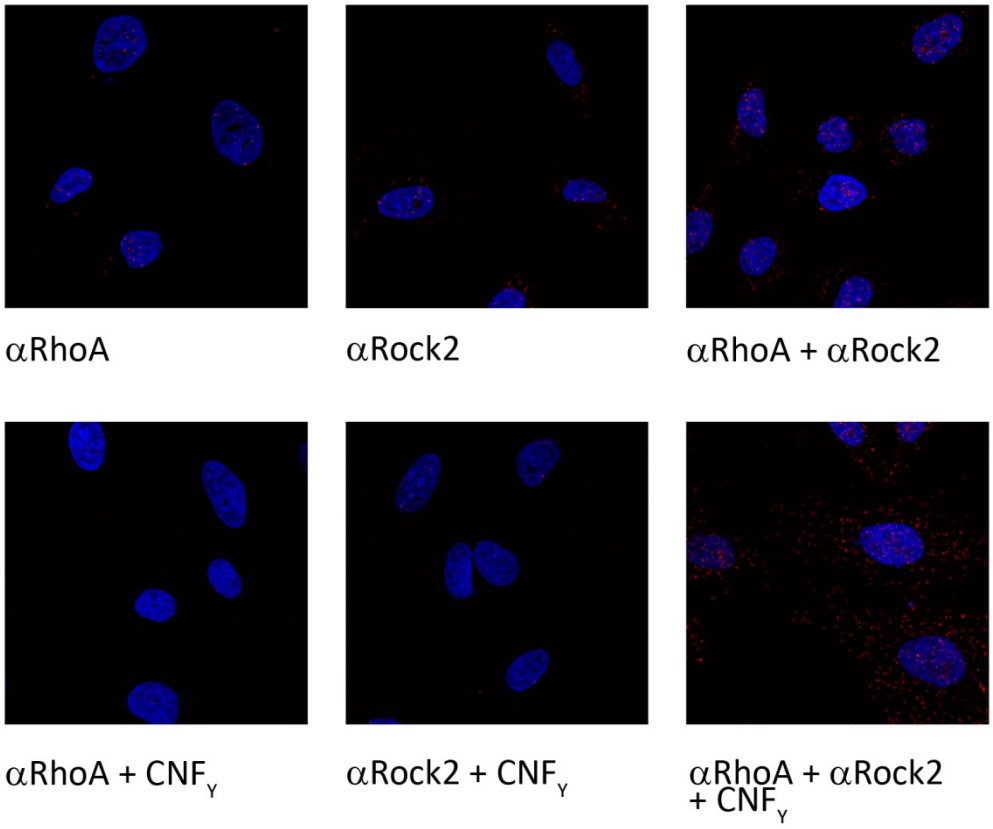

Figure 3.11: $RhoA^{GTP}$-Rock2 interaction increases after toxin treatment in HeLa cells. PLA experiment monitoring increased number of interactions of $RhoA^{GTP}$ with Rock2 after treatment with CNF_Y. PLA experiments were carried out identically apart from the combination of primary antibody. Single antibody experiments serve as background control. For validation of RhoA-Rock2 binding the untreated and toxin-treated (+ CNF_Y) samples are compared by quantification of the fluorescent signal. Notably, the background signal (left and middle panels) is low. Combination of RhoA and Rock2 antibodies reflects basal interaction between the two proteins. Upon addition of CNF_Y the amount of signals increases.

Cytotoxic necrotizing factors 1 and Y (CNF1 and CNF_Y) from *E. coli* activate RhoA (CNF_Y) or RhoA, Rac1 and Cdc42 (CNF1). These AB-type toxins autonomously enter various cell types. CNF toxins

deamidate the catalytic glutamine residue in Rho GTPases that is necessary for GTP hydrolysis. The Rho GTPases are then constantly locked in the GTP-bound form. Toxin-treated cells contain a higher amount of Rho^{GTP} and therefore, more interactions with Rho^{GTP}-specific binding partners are expected. With the combination of PLA and CNF toxins we created a novel assay that is able to detect and quantify *in situ* interactions of activated Rho GTPases with effector proteins. Both, Rho GTPases and effector proteins, are untagged and expressed at endogenous levels. The increase of interactions is quantifiable by an increased fluorescent signal in the toxin-treated cells.

Figure 3.11 shows microscopic pictures from a typical PLA experiment of RhoA-Rock2. Negative controls with one antibody only are left untreated (upper left and middle picture) or treated with CNF_Y (lower left and middle picture). The combination of both antibodies results in a fluorescent signal that is strongly increased by toxin treatment (upper and lower right pictures). Further examples are shown in Figure 3.12.

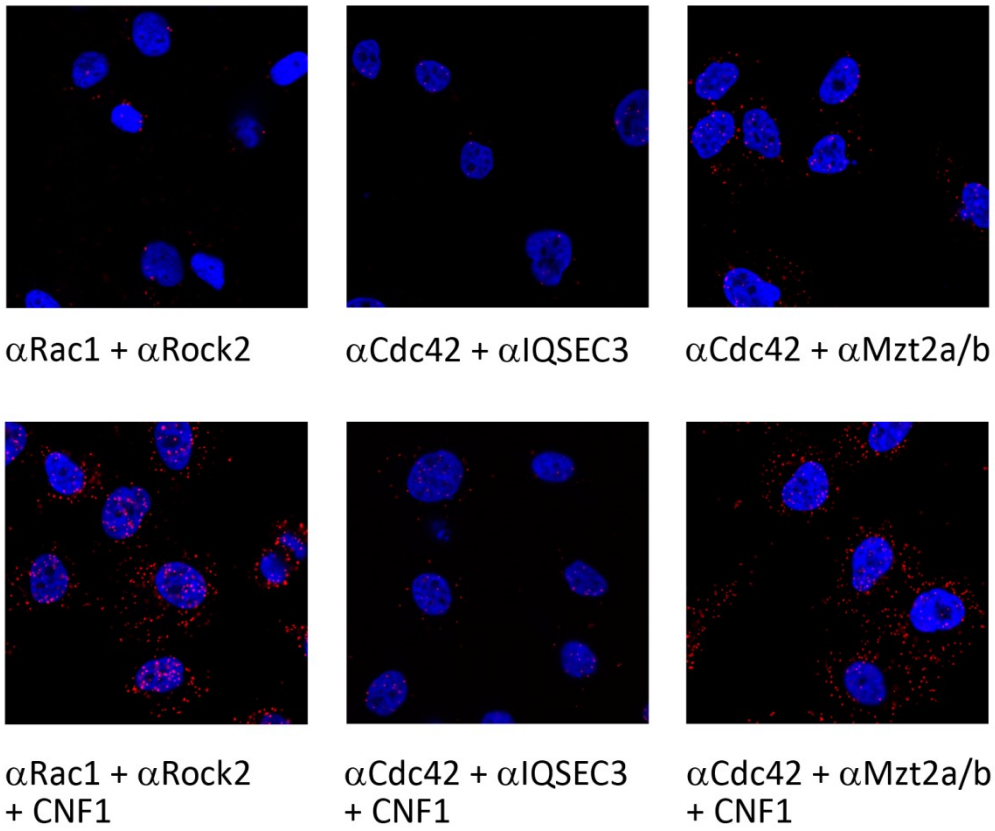

Figure 3.12: The combination of PLA with cytotoxic necrotizing factors CNF1 and CNF_Y is used to validate interactions for all three GTPases. Shown are examples for Rac1 and Cdc42. Experimental setup identical to Figure 3.11 apart from the combinations of antibodies and usage of CNF1. Upper three panels reflect basal interaction without treatment. Upon addition of cytotoxic necrotizing factors (lower three panels) the amount of signals increases.

14 interactions were examined by the PLA assay in HeLa cells. RhoA-Rock2 and Rac1-SESTD1 binding are described in the literature and served as positive controls[112,247]. The RhoA-Acat1 interaction had been reported in a previous screen, but has not been validated so far[134]. Eleven out of twelve novel

interactions could be validated by PLA with high significance ($p < 0.05$) (Figure 3.13). Only the interaction of Cdc42 with Opa1 seemingly decreased after toxin treatment. This interaction had been significant in all three LF-qGAP experiments of Cdc42 with $\log_2$ fold changes of 1.5 – 3.9.

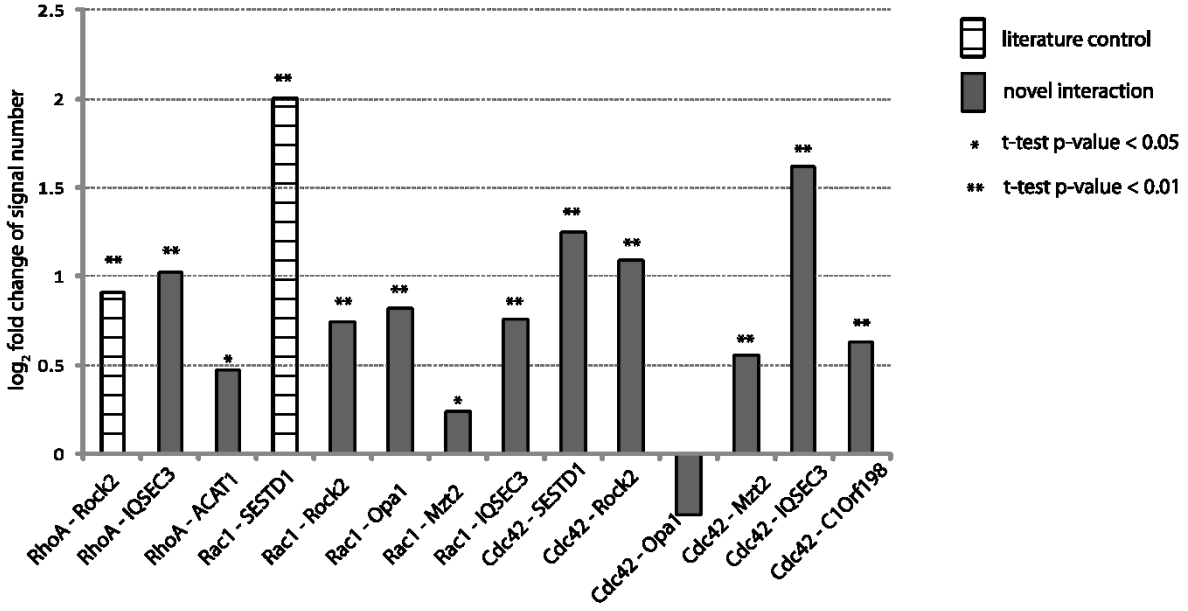

Figure 3.13: Validation of Rho interactions with PLA. Signals increase for eleven out of twelve novel interactions after treatment with toxin. RhoA experiments were performed with CNF_Y, Rac1 and Cdc42 experiments with CNF1. Each interaction was examined with at least two biological and five technical replicates. Signals were automatically quantified from pictures. The significance of signal increase was calculated with a one-sided homoscedastic t-test.

Taking these results together, it was possible to validate most of the tested interactions by an alternative, mass spectrometry independent approach. Since the PLA approach is performed *in situ* it is one step closer to the living system. The biological relevance of the interactions is discussed later.

3.2.6 Effector binding specificity towards GTPases

Most of the identified effectors were specific for a single GTPase, consistent with a high specificity of the interactions. However, it should also be mentioned that some interaction partners may have escaped detection in individual pull-down assays. Therefore, the true overlap between the GTPases may be higher. Some effectors specifically interacted with the GTPγS-form of several GTPases. Interestingly, this set included well-known proteins like Rock2 – a protein that is generally thought to interact with RhoA, B and C only. This might indicate that Rock2 is less specific than previously thought or that the interplay of interaction partners makes Rock2 and indirect interactor of Cdc42 and Rac1. Rock2 might simply be a false positive hit for Cdc42 and Rac1. However, our data seem

reliable since the Rock2-Rac2 and Rock2-Cdc42 interactions were validated with PLA (see Figure 3.13). To assess the binding specificity of overlapping interaction partners the GTPγS-form of respective GTPases were compared to each other via a t-test (Figure 3.14). Comparison of LF-qGAP results from RhoA^{GTPγS} vs Rac1^{GTPγS} and RhoA^{GTPγS} vs Cdc42^{GTPγS} showed that Rock2 indeed binds with highest specificity to RhoA, consistent with existing literature.[248] Citron and Rho GEF 2 are also most specific towards RhoA, whereas Abi1, -2, Wasf1, -3 and Nckap1 components of the Rac1-binding WAVE complex are more specific towards Rac1^{GTPγS}.

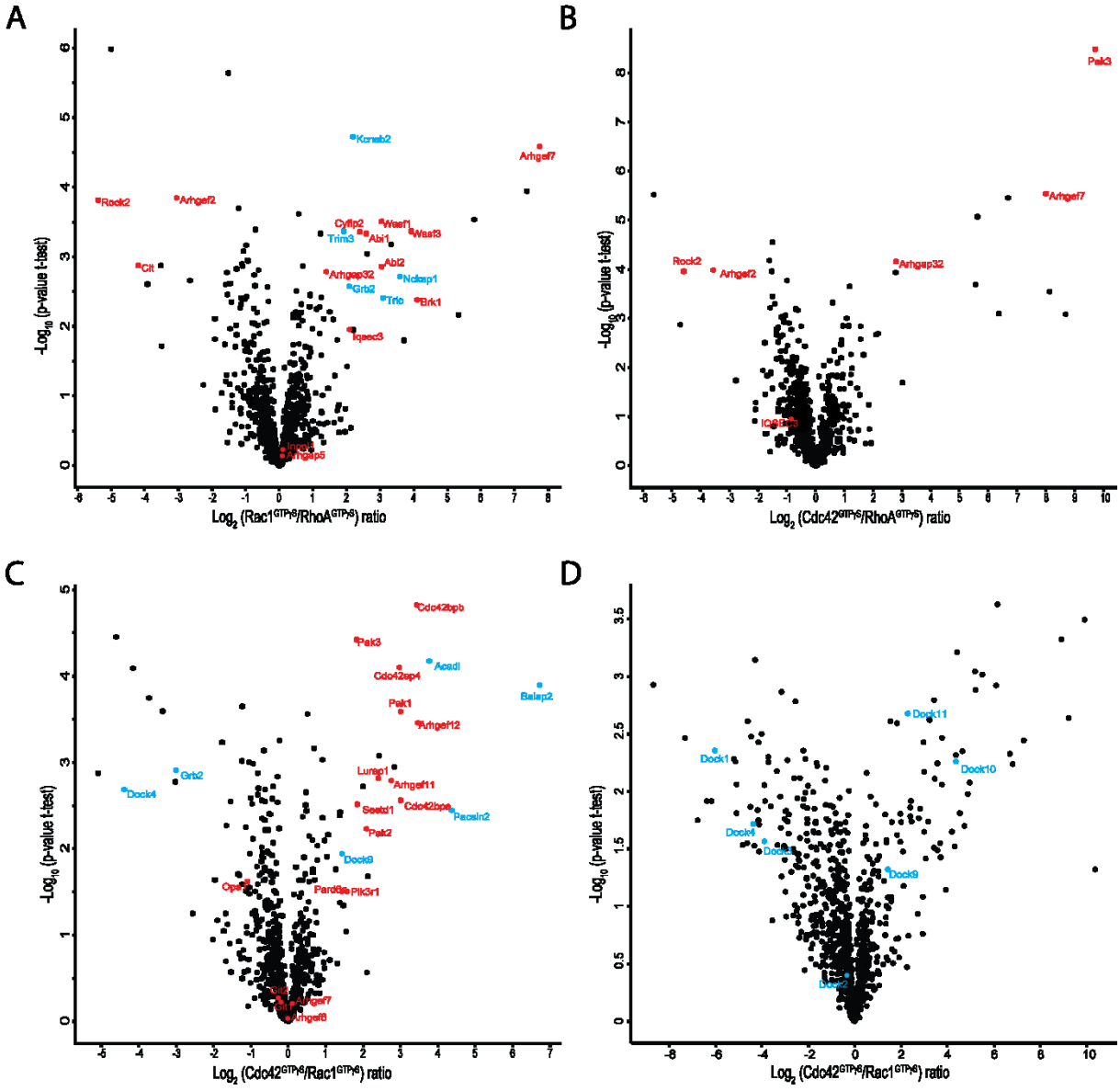

Figure 3.14: Comparison of protein binding affinity between the Rho GTPases. Label free protein intensities of GTPγS pull-downs were used to compare binding profiles of (A) Rac1^{GTPγS} against RhoA^{GTPγS} (B) Cdc42^{GTPγS} against RhoA^{GTPγS} and (C) Cdc42^{GTPγS} against Rac1^{GTPγS}. (D) Similar to (C) but less stringent filtering (3 valid values in at least one group). Proteins labeled in red were significant outliers in both of the respective GTPase assays. Proteins labeled in blue are noteworthy and explained in the text. The comparison of interaction partners between the Rho GTPases reveals that some interactors have a preference in binding (e.g. Rock2 to RhoA). In addition, the comparison reveals constitutive binders (e.g. Dock proteins).

The proteins Cdc42bpa, Cdc42bpb and Cdc42ep4 are most specific towards Cdc42 in consistence with the literature. Kinases of the PAK family are prone to bind $Cdc42^{GTP\gamma S}$.

Interestingly, the comparison of the Rho GTPγS pull-downs to each other did not only reveal the specificity of proteins towards certain GTPases. Grb2 was enriched with $Rac1^{GTP\gamma S}$ (see Figure 3.14C) a finding that was not observed when comparing $Rac1^{GTP\gamma S}$ and $Rac1^{GDP}$. Grb2 has so far only been linked to Cdc42 in the literature (also found by LF-qGAP). In addition, the GEFs Dock1, Dock2, Dock3 and Dock4 were enriched with $Rac1^{GTP\gamma S}$, the GEFs Dock9, Dock10, Dock11 were enriched with $Cdc42^{GTP\gamma S}$. This is of interest because Dock1-4 contain an SH3 domain, whereas Dock9-11 do not. Trio, a GEF protein identified as $Rac1^{GDP}$-specific binder in the $Rac1^{GTP\gamma S}$ versus $Rac1^{GDP}$ pull-down, was now also found to bind $Rac1^{GTP\gamma S}$ when compared to $RhoA^{GTP\gamma S}$.

3.2.7 Cell type specificity of Rho interactions

LF-qGAP was introduced with the intention to take advantage of the broader expression profile of tissues compared to a single cell line. The overall number of interactions and their overlap between pull-downs from SILAC cell culture and label free brain lysates were compared in Venn diagrams (Figure 3.15).

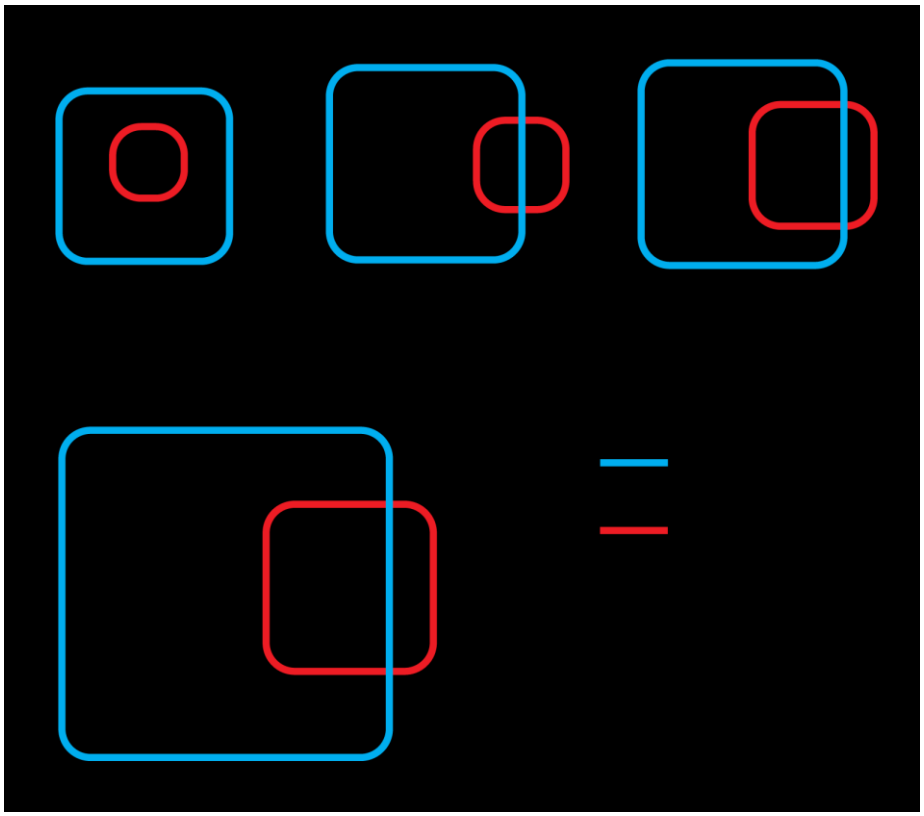

Figure 3.15: Venn diagram showing overlap between cell culture and tissue samples. Overlap of significant hits for the GDP and GTPγS pull-down are depicted for (A) the individual Rho GTPases and (B) the whole interactome. The size of the rectangle reflects the amount of interactors with the respective method. The number of overlapping proteins is written in *italics*. LF-qGAP identified for each Rho GTPase a higher number of interaction partners.

The identified binding partners for Rho GTPases in mouse brain mostly included those discovered in the cell culture experiments. Only 13 of 49 proteins (25% Figure 3.15 B) were identified specifically in SILAC-qGAP (e.g. BIN3, IQGAP1 and 2, Synaptojanin, Rap1gds). In most cases these SILAC-specific proteins were not identified in LF-qGAP at all (for instance BIN3) or did not possess enough quantification events (Synaptojanin2). As an exception IQGAP2 was quantified in all six Cdc42-cerebrum pull-downs but did not reveal any changes in intensity between $Cdc42^{GDP}$ and $Cdc42^{GTP\gamma S}$ experiments (see also discussion).

In general, we obtained more identified interactions for tissue samples (ratio 4:1), this can be explained by the different cell types and therefore more varied protein expression pattern of mouse brain compared to HeLa cells. It is important to note that more samples were taken for LF-qGAP (two triplicates, six samples in total) than for SILAC-qGAP (two samples). However, the total number of identified proteins was similar in LF- and SILAC-qGAP. Taken together, the data indicate that it is recommendable to work with complex tissues for interaction partner screening.

The three canonical GTPases were used for pull-down experiments with different subregions of the brain: hippocampus (Cdc42), cerebellum and remaining cerebrum (each with RhoA, Rac1 and Cdc42). Interestingly the tissues showed partly different binding profiles (Figure 3.16).

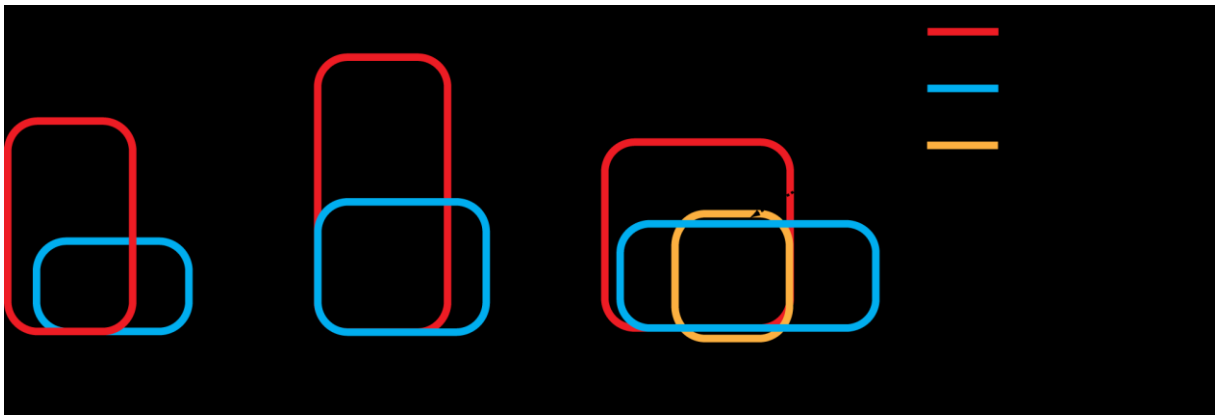

Figure 3.16: Venn diagram showing overlap of interaction partners between tissues for RhoA, Rac1 and Cdc42. The numbers of identified interactors for the respective Rho GTPase (GDP- and GTPγS-form) between the tissue types are compared. The size of the rectangle reflects the amount of interactors with the respective tissue. The number of overlapping proteins is written in *italics*.

Again, most of the tissue-specificities can be explained by missing presence or quantifications of the target in MS runs. The protein may not have been in the lysate at all or was not detected by mass

spectrometry. For example, the Rac1-Pak2 interaction is literature-described and was found for the cerebrum samples. In the Rac-cerebellum samples the protein Pak2 was not detected at all.

In contrast Cdc42$^{GTP\gamma S}$ was found to bind Dock9 from hippocampus samples but not from cerebrum and cerebellum samples despite its identification in all 12 sub pull-downs with even better intensities. More puzzling the Rac1$^{GTP\gamma S}$-Dock9 interaction was found in cerebrum and cerebellum samples.

Taken together, more interactors were identified with LF-qGAP compared to SILAC-qGAP. This is consistent with the idea that tissues contain more potential interaction partners than a cell line. In addition, it can be stated that differences in binding profiles between tissues were observed. In certain cases (Pak2, Dock9) a protein was present in several lysates, but interacted with Rho GTPases only in some of them.

3.3 Evaluation of alternative strategies for identification of Rho GTPase interactors

3.3.1 Triplicate label free experiment from cell culture

It was tested if pull-down with Rac1 from label free HeLa cells results in qualitatively and quantitatively comparable results compared to SILAC-qGAP. This could give clue if SILAC-labeling of cells is necessary after all. The successful application of LF-qGAP on a cell line would save time- and cost-intensive labeling. Therefore, the LF-qGAP approach was used to pull-down interaction partners of Rac1 $^{GTP\gamma S}$ and Rac1^{GDP}, similar to the experiments conducted with mouse brains.

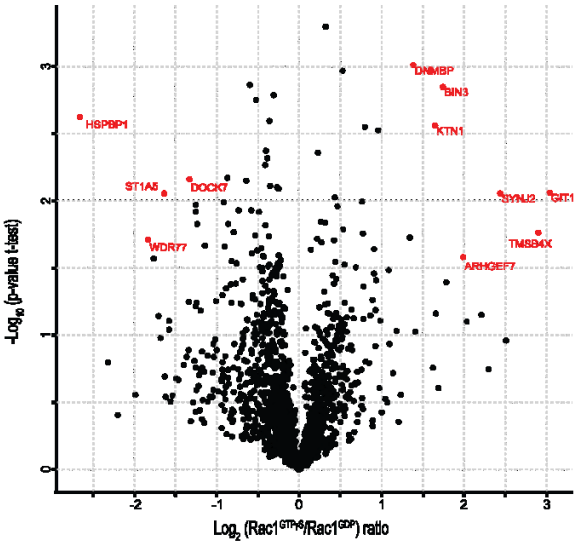

Figure 3.17: Rac1 interaction partners were identified by LF-qGAP from HeLa cells. Significant outliers are displayed with their official gene names and labeled in red. In total eleven significant interactors were found. Three of the eleven are listed in HIPPIE.

Eleven proteins were determined to be significant outliers. As a reminder: SILAC-qGAP led to the identification of 14 and LF-qGAP with mouse brains to the identification of 65 interaction partners of Rac1.

Four of the eleven interaction partners had been identified in Rac1 SILAC-qGAP as well (Bin3, Git1, Synaptojanin 2, Rho GEF 7). Furthermore, two proteins are known Rho-binders (Dock7, Dnmbp). Four of the remaining five proteins (HSPBP1, ST1A5, WDR77, and TMB4X) are not known to bind Rac1. Ktn1 (Kinectin) is a biological link of Rho GTPases to the microtubule system[249]. Kinectin is the only protein that is exclusively identified by LF-qGAP with HeLa cells. Three of the eleven interactors are listed in HIPPIE (Rho GEF 7, Ktn1, Synaptojanin 2). This results in an enrichment of: $p\ (X \geq 3) = 3.6 \cdot 10^{-4}$. Since Bin3, Git1, Dock7 and Dnmbp are very likely to interact with Rac1, the enrichment might be higher.

However, a substantial part of interaction partners identified with SILAC-qGAP could not be found with LF-qGAP in HeLa cells. Therefore SILAC-qGAP seems to be the more promising assay to identify interaction partners from a single cell line.

3.3.2 Immunoprecipitations with tagged CA/DN-variants from SILAC-cell culture

To identify protein-protein interactions by immunoprecipitation is a common alternative to pull-down experiments (see introduction)[202]. In the optimal case the protein of interest is precipitated at endogenous levels avoiding changes in transcription due to overexpression. Immunoprecipitation experiments can identify endogenous interactions, whereas during pull-down experiment the interactions forms in the lysate. Posttranscriptional modifications of the bait protein are not taken into account in pull-down experiments. The constitutively active (CA) and dominant negative (DN) forms of Rho GTPases contain point mutations that are either not able to hydrolyze GTP (CA) or to activate downstream effector proteins (DN).

It was tested if the CA- and DN-form are useful to mimic the GTP- and GDP-bound form of Rho GTPases in interaction studies. The transfection of cell lines with the CA- and DN-mutants of Rho GTPases would circumvent the laborious purification and loading of recombinant Rho GTPases. The CA- and DN-mutants have also been used in yeast-two hybrid interaction studies previously to mimic the GDP- and GTP-loading state[250].

Citrine-tagged CA- and DN-constructs of Rac1 and Cdc42 were transfected into SILAC labeled HeLa cells and immunoprecipitated (Figure 3.18).

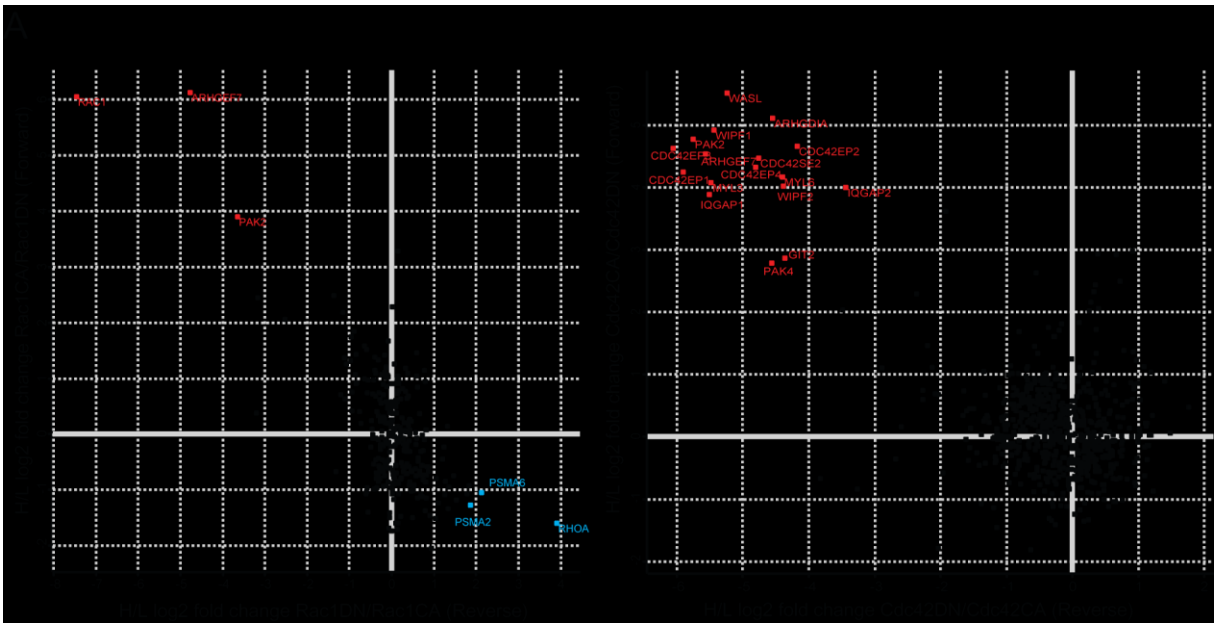

Figure 3.18: Immunoprecipitation of Citrine tagged Rho GTPases from H and L labeled HeLa cells. A) Rac1^{CA} against Rac1^{DN} B) Cdc42CA against Cdc42DN. Significant outliers are labeled in red. Noteworthy proteins are labeled in blue and explained in the text.

Immunoprecipitation of Rac1^{CA} against Rac1^{DN} resulted in three significant hits: Rac1, Rho GEF 7 (Arhgef7) and Pak2 (SILAC-qGAP identified 14 interaction partners for Rac1). Unexpectedly, Rac1 was 100-fold more present in the CA-experiment compared to the DN-immunoprecipitation (log_2 fold changes of 6 to 7). This is consistent with a lower fluorescence signal observed in Citrine-Rac1^{DN}-transfected cells before the experiment. Interestingly, the proteasomal subunits PSAM2/6 were enriched in the DN sample. Taken together it is possible, that Rac1^{DN} was degraded by the proteasome. This would point out, that Rac1^{DN} is not a good equivalent to Rac^{GDP}.

Immunoprecipitations of Cdc42$^{CA/DN}$ from SILAC-labeled HeLa cells resulted in 17 significant binders of the CA-mutant (SILAC-qGAP identified 26 interaction partners for Cdc42). All of them are literature-described or related to the actin cytoskeleton (Myl5/6). Astonishingly Rho GDI 1 (ARHGDIA) was a significant interaction partner of Cdc42^{CA}. Rho GDI 1 has been described to bind mostly to the GDP-bound form of Rho GTPases. For example the interaction of Rho GDI 1 with Cdc42$^{GTP\gamma S}$ has been shown to be only 10% efficient as the binding towards Cdc42$^{GDP\ 251}$. Therefore, it would have been expected that Rho GDI 1 is precipitated with Cdc42^{DN} and not with Cdc42^{CA}. It can be concluded, that the Cdc42^{DN} mutant is no biochemical equivalent for Cdc42^{GDP}.

It should also be noted that the reproducibility of CA/DN-IPs was much lower than for SILAC-qGAP experiments.

Altogether we found the mutated Rho GTPases (CA-/DN-mutants) to precipitate less interaction partners than SILAC-qGAP. The specificity of one identified interaction partners (Cdc42-Rho GDI 1) was contradictionary to the literature and we found evidence of degradation of Rac1^{DN}. It can be

concluded that the Rho GTPase mutants are no equivalent to the nucleotide-loaded form of GTPases. This is of importance because yeast two-hybrid is often performed with CA- and DN-constructs[250].

3.4 A network of Rho GTPase interaction partners

3.4.1 The interactome of Rho GTPases

The identified interactions of the six Rho GTPases were assembled into the first Rho GTPase interaction networks (Figure 3.19 and Figure 3.21). For the GTPγS-network 225 interactions were distributed on 146 proteins.

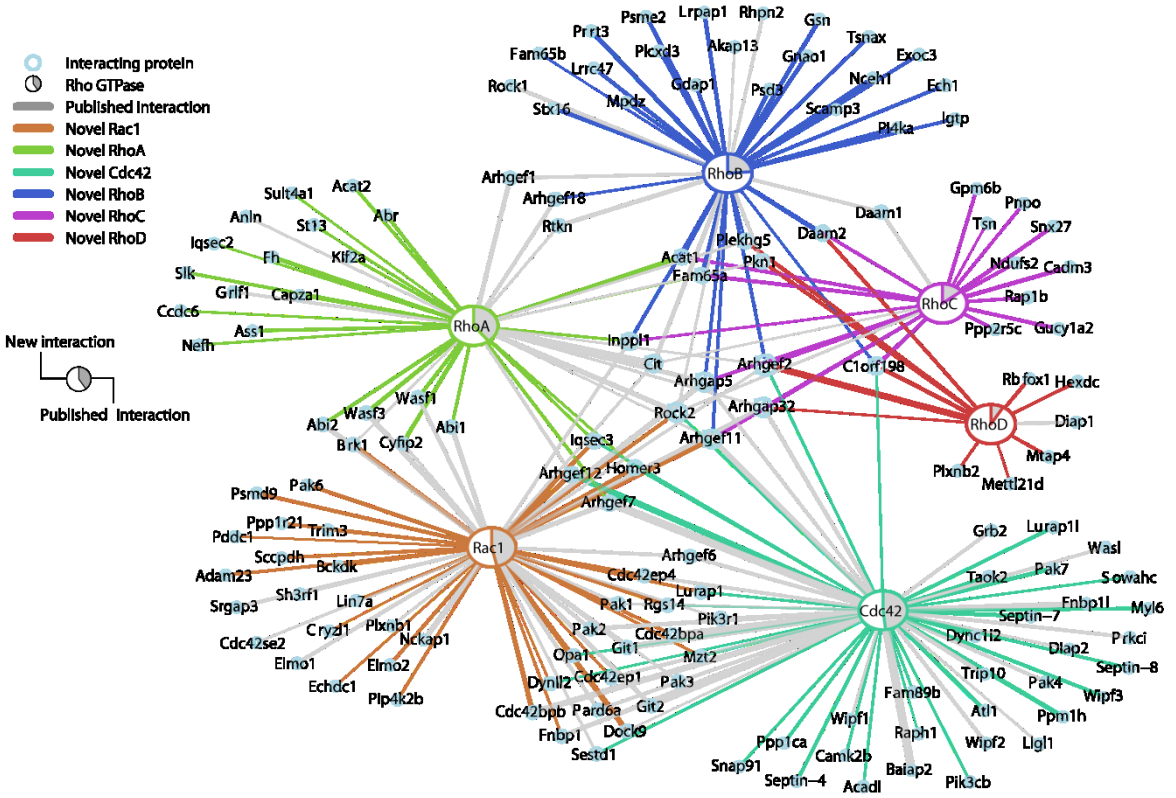

Figure 3.19: Interactome of Rho$^{GTP\gamma S}$ GTPases. Interacting proteins are symbolized by their official gene name. Edges are weighted according to the $\log_2$ fold changes between GTPγS and GDP pull-down. (Graphical display of results is a contribution from Dr. Henrik Zauber). Rho GTPases are symbolized by a pie chart according to the color in the legend. Grey area in the pie is equal to the percentage of interactions that was described somewhere in the literature (published interaction).

Most of the proteins (98 of 146) were specific interactors for one Rho GTPase. However, several proteins interacted with two or more Rho proteins (Table 3.7). Among the most promiscuous proteins were mainly Rho-regulating proteins (Rho GEF 2 and -11, Rho GAP 5 and -32).

Table 3.7: Number of interactions towards Rho GTPases in the GTPγS-network. The GTPγS-network consists of 146 proteins (plus six Rho GTPases). Most of the interactors (98) bound to a single Rho GTPase.

Number of Rho GTPases	1	2	3	4	5	6
Number of proteins	98	31	9	3	4	1

Rock2 was unexpectedly found not only to interact with RhoA, B and C, as previously described but also to Rac1 and Cdc42. These findings were supported by PLA experiments (Figure 3.13) and are further examined in section 3.2.6.

The largest overlap of interaction partners is observed between Rac1 and Cdc42. RhoA, RhoB and RhoC also seemingly share a subset of proteins. As these groups of proteins are evolutionary close together, we reasoned that the binding profile might reflect the evolutionary development of Rho GTPases. To support this thesis, the six Rho GTPases were clustered based on the $\log_2$ fold changes of their $Rho^{GTP\gamma S}$ interaction partners. In parallel the protein sequences of the six Rho GTPases were aligned (Figure 3.20).

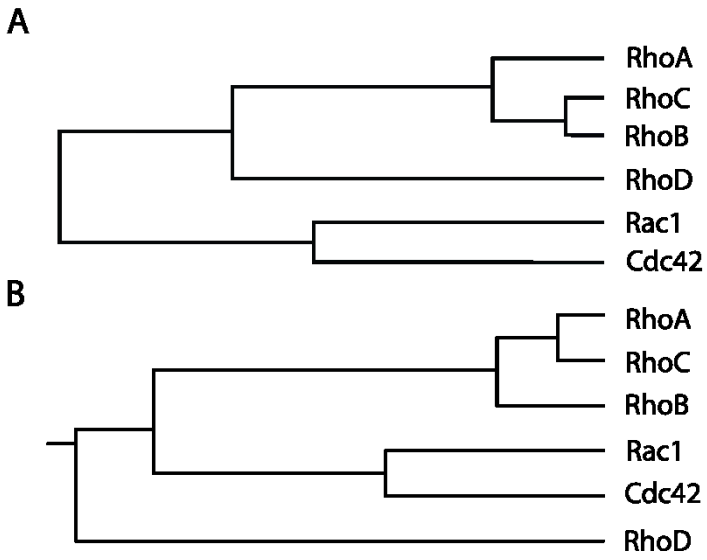

Figure 3.20: Relation between binding profiles and sequence alignment. A) Binding profiles of $Rho^{GTP\gamma S}$ were clustered with Perseus software considering the $\log_2$ fold changes. B) Unrooted tree based on alignment of protein sequences of the six Rho GTPases using the ClustalW online tool[226].

The results of hierarchical clustering and the sequence alignment are in accordance with each other: Rac1 and Cdc42 are closely related, as there is the Rho subgroup of RhoA, RhoB and RhoC. RhoD is evolutionary between the two groups. Within the Rho subgroup we found RhoC and RhoB most closely related whereas sequence alignment suggests a more close relationship between RhoA and RhoC.

The Rho^{GDP} interaction network reveals a lower level of overlapping interactions (Figure 3.21). Rho GDI 1 and Rho GEF 17 (Arhgef17) bind to three GTPases each. Rho GEF 17 is one of the few GEFs that exclusively binds to the GDP-bound form of Rho GTPases. Notably this protein does not contain a PH domain, which comes usually in tandem with the DH domain. Overlapping proteins between the Rho$^{GTP\gamma S}$ and the Rho^{GDP} network are the scaffold protein Baiap2 (binds to Cdc42$^{GTP\gamma S}$ and RhoD^{GDP}) and the metabolic protein Nceh1 (binds to RhoB$^{GTP\gamma S}$ and RhoA^{GDP}).

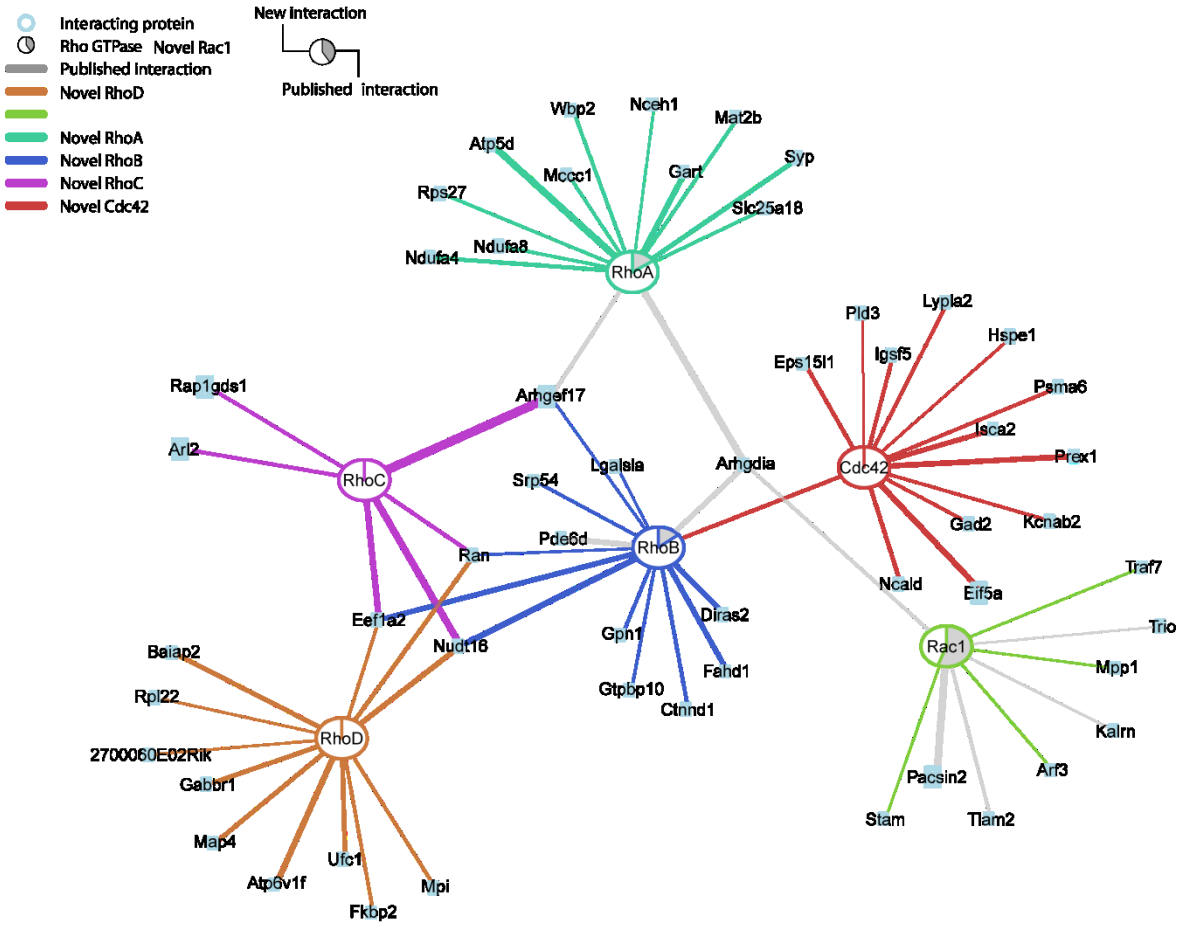

Figure 3.21: Interactome of Rho^{GDP} GTPases. Edges are weighted according to the $\log_2$ fold changes between GTPγS- and GDP-pull-down. (Graphical display of results is a contribution from Dr. Henrik Zauber). Proteins are labeled with their official gene name. Rho GTPases are symbolized by a pie chart according to the color in the legend. Grey area in the pie is equal to the percentage of interactions that was described somewhere in the literature (published interaction).

We expected that the Rho effector network could shed light on unknown functions of the Rho GTPases. For Cdc42$^{GTP\gamma S}$ interactors the terms 'establishment or maintenance of cell polarity' (3 proteins, p-value=$4.7 \cdot 10^{-3}$), 'cell division' (5, $1.4 \cdot 10^{-2}$) and for Rac1 $^{GTP\gamma S}$ interactors 'phagocytosis' (3, $1.1 \cdot 10^{-3}$) were enriched. These processes are linked with the respective GTPases since long[252,253].

In addition, we found apoptosis-related terms for RhoA and RhoB when we tested against a human background. In detail, interaction partners of RhoB$^{GTP\gamma S}$ were enriched in apoptosis-related terms like 'induction of apoptosis by extracellular signals' (5 proteins p-value= $5.8 \cdot 10^{-5}$), 'cell death' (8, $4.1 \cdot 10^{-4}$) or 'induction of apoptosis' (5, $3.5 \cdot 10^{-3}$). These terms had partly higher significance than terms that

are typical for Rho GTPases (e.g. ‘cytoskeleton organization’ with 5 proteins p-value= $1.5 \cdot 10^{-3}$). When the interaction partners of the GTPγS-forms of RhoD, RhoC, Rac1 and Cdc42 were tested no apoptosis-related terms were enriched. This is of special interest since RhoB has been linked to apoptosis and is target for anti-cancer drugs (see discussion).

It was also tested if specific biological functions could be assigned to the GDP-form of Rho proteins. However, enriched terms were either expected (‘regulation of Rho protein signal transduction’ with 5 proteins and p-value=$1.1 \cdot 10^{-4}$) or pointed on unspecific binding (‘guanyl nucleotide binding’ $1 \cdot 10^{-5}$).

4 Discussion

4.1 Development of qGAP

Rho GTPases are central regulators of the actin cytoskeleton[97]. In addition they regulate gene expression, polarity, cell division and other cellular processes[1,142]. Their ability to bind and hydrolyze GTP renders them flexible molecular switches. Their biological activities are mediated by a number of effector proteins[234,254]. Until now, studies mostly focused on the investigation of a single Rho-effector interaction. Thus, a comprehensive survey of Rho-binding partners has not been carried out yet. With the development of qGAP we aimed to establish an assay for the reliable identification of loading-state specific $Rho^{GDP/GTP\gamma S}$ interactors on the one hand and to obtain a global picture of the Rho interactome on the other hand. qGAP combines the classical pull-down approach with different strategies of quantitative mass spectrometry and is a new method in the large toolbox of q-AP-MS.

As a preparatory step the recombinant human Rho GTPases RhoA, Rac1, Cdc42, RhoB, RhoC, RhoD each with an N-terminal GST-tag were purified and loaded with nucleotides (see Figure 3.2). The purification of RhoA, Rac1 and Cdc42 yielded high amounts of protein (10 - 20 mg per litre culture medium). Purification of RhoB, RhoC and RhoD resulted in low amounts of protein (1-2 mg/l). One possible explanation for the low yield of RhoB and RhoC purification is low solubility due to phenylalanine 25 being exposed to the solvent, as observed for RhoA[229]. The introduction of the F25N mutation in RhoB and C likely would have increased the solubility and consequently the yields for RhoB and RhoC. However, low amounts of coupled Rho GTPases were sufficient for qGAP. Thus, RhoB and RhoC were used in their wildtype form. The purified human Rho GTPases were also used for experiments with mouse brains, since the sequences of human and mouse Rho proteins are almost identical (e.g. 99.5% for RhoA and 100% for Cdc42).

Comparison of different crosslinking strategies showed that crosslinking of Rho GTPases to N-hydroxysuccinimidyl (NHS)-sepharose results in the best overall identification of Rho interaction partners (see Figure 3.4) and in the highest reproducibility of the assay[202]. This finding is surprising since the small crosslinkers DMP and DSS are used as standard reagents for covalent crosslinking of antibodies in numerous publications[230]. In addition, the fusion-proteins bind in random orientation to the sepharose during NHS-coupling, whereas the binding of GST-Rho proteins towards glutathione sepharose allows for oriented binding followed by crosslinking with DSS or DMP. However, the small crosslinkers DSS and DMP may also bind to residues in the effector binding sites of Rho proteins. Thereby the binding sites might become inaccessible for effectors.

4.2 qGAP sensitively and specifically identifies Rho GTPase interaction partners

After developing qGAP, we used the assay to identify Rho interaction partners from cytoplasmic extracts from SILAC-labeled HeLa cells. 1,100 – 1,200 proteins were quantified in a typical experiment with label swap. We applied stringent criteria for the identification of outliers. More precisely, significance thresholds for both forward and reverse experiment were combined. In contrast, many other studies use arbitrary thresholds on the level of $\log_2$ fold changes. For the test set of RhoA, Rac1 and Cdc42, 49 significant outliers were identified. Thirty-two of these proteins (65.2%) are listed in the HIPPIE database[243]. The identified proteins were analyzed with the DAVID online tool for enrichment of biological processes[224]. The identified proteins possess molecular functions (GEF, GAP, DIA, scaffolds) that are closely related to Rho biology (see Table 3.1). Apart from one (thymidilate synthase), all proteins are linkable to Rho GTPase biology. This observation suggests that the vast majority of proteins identified by qGAP are true interaction partners of GTPases. Hypergeometric probability testing was employed to assess the significance of the enrichment of proteins listed as qGAP interaction partners in the HIPPIE data base (see Table 3.3). The enrichment was found to be highly significant with p-values of 10^{-8} (Rac1) to 10^{-35} (Cdc42). Taken together, qGAP is able to enrich Rho GTPase interaction partners from lysate of SILAC-labeled cells.

In the next step we extended qGAP towards lysates from mouse brains. Organs consist of numerous cell types and thus should contain a broader range of potential interaction partners than cell cultures. The label free approach is less cost-intensive and samples from any organism that has been sequenced can be screened. Five of the six investigated Rho GTPases have weak (Rac1), moderate (RhoA, Cdc42) or high (RhoB, RhoD) expression levels in different brain cell types[240]. According to the current knowledge, RhoC seems to be expressed mainly in macrophages or glandular cells[240]. LF-qGAP of RhoC from mouse lungs resulted in no significant hits (data not shown). This can be explained by the low amounts of lysate obtainable from this organ. Interestingly, we identified numerous interaction partners for RhoC in brain lysates including binding partners that are described in the literature. This means, that the bait protein does not necessarily need to be expressed in the cells that are investigated. Nevertheless, to reduce artifacts it is recommendable to use a cell line that expresses the protein of interest.

In total, 291 Rho interaction partners were identified for the six Rho GTPases, many of them repeatedly (in total 381 significant interactions) (see Figure 3.8 and Table 6.1). 60 of the 291 interactors (20.6%) are listed in HIPPIE (Table 3.4). Only considering the classical GTPases, the overlap is 51 of 188 (27.1%), which is still distinctively smaller than for SILAC-qGAP. That could either be interpreted by a lower specificity of LF-qGAP or by the identification of novel, unlisted Rho binding

partners in LF-qGAP. Detailed literature search revealed that in total 92 of 291 interactions (30.3%) can be linked to existing evidence[225].

The identified interaction partners were highly enriched in HIPPIE-listed Rho interaction partners (0.02 for RhoD to $7.3 \cdot 10^{-25}$ for Cdc42). Overall, the enrichment of interaction partners for the classical three Rho proteins was of higher significance than for the uncharted Rho GTPases.

This can be explained by the fact that for the classical Rho GTPases more interactions are listed in HIPPIE (482) than for the uncharted Rho GTPases (70). It is not expected that LF-qGAP selectively identifies more interaction partners for the classical GTPases. It would therefore be expected, that a database covering most biological interactions of RhoB, C and D would also lead to higher enrichment for these proteins. In reverse conclusion, many of the identified interactions for the uncharted Rho GTPases are expected to occur *in vivo* but have not been reported yet. To use an alternative standard beside the HIPPIE database, the enrichment of domains ("Interpro" terms) in LF-qGAP hits was tested (Table 3.5). This strategy investigates enrichment among hundreds of interpro-domains and is not influenced by the study bias. Indeed, the Rho-related PAK-box, DH domain, GEF domains and actin binding domains were found to be highly enriched. Notably, the SH3 domain was enriched as well (15 proteins, $4.8 \cdot 10^{-9}$).

In addition to direct interaction partners, qGAP identifies without doubt a high number of indirect interactions. First, these are complexes with defined biological function as the large WAVE and WASP complexes and the smaller MRCKα-Lurap1 and Par6-LLGL complexes, that were also identified with LF-qGAP. Second, there are numerous proteins from the actin cytoskeleton that may 'stick' to actin-binding components and are therefore enriched. For example, proteins of the septin family were identified to bind $Cdc42^{GTP\gamma S}$. Septins are cytoskeletal proteins that play a role in cytokinesis a process in which Cdc42 is also involved. Therefore, the interaction of Septins with Cdc42 could be indirect[255].

The method cannot distinguish between indirect and direct binding partners. Whether the identification of indirect binders represents rather an advantage or a drawback of qGAP depends on the scope of the researcher. We see qGAP as tool to explore Rho GTPase biology by identification of interacting proteins. Complementary approaches like isothermal titration calorimetry need to be used to test if the identified interactions are direct or indirect.

A large part (224 of 291, 77%) of the LF-qGAP interactions was GTPγS-specific (see Table 3.3 and Figure 3.21). This is in agreement with the GTP-bound form of the Rho GTPase representing the active state. Only nine of the GDP-specific interaction partners were described in the literature. This could either indicate that the false positive rate is higher in the group of GDP-specific interaction partners or that the biologic relevance of Rho^{GDP} proteins has been underestimated. Among the literature-overlap are GEF proteins (Rho GEF 17, Tiam2, Trio, Kalirin, Prex1), GDIs (Rho GDI 1, Pde6d)

and Pacsin2. Pacsin2 has recently been shown to bind via its SH3 domain to the hypervariable C-terminal region of Rac1[256]. We find proteins containing the SH3 domain strongly enriched in our data. Until now, it has been proposed that the SH3 domain in Rho-binding proteins links them to downstream effectors. Instead it could be possible that the SH3 domain offers an alternative binding site for Rho GTPases. SH3 domains bind to a PxxP amino acid motif. Rac1 contains a PNTP amino acid sequence at position 106 and a proline rich sequence at its carboxyl-terminus (CPPPV at residue 178) (C: cysteine, N: asparagine, P: proline, T: threonine, V: valine).

The GTPγS-specific interaction partners of RhoA, Rac1 and Cdc42 were checked in detail for links towards Rho biology (**Figure 3.9**). It was found that a large part of the interactions (45%) are known in the literature. For of 24.2% binding to Rho GTPases can be explained by known interactions leading to indirect binding or by the presence of a known GTPase-binding domain (CRIB, DH) or because a homolog of the protein is known to bind to the Rho GTPase. Cytoskeletal proteins (8.4%) are potentially indirectly binding to Rho GTPases as well. Thirty-two proteins show no obvious link to Rho GTPase biology (from a total of 158 $RhoA^{GTP\gamma S}$, $Rac1^{GTP\gamma S}$ and $Cdc42^{GTP\gamma S}$ binders). The 32 proteins are enriched in the terms 'phosphate metabolism' (5 proteins, p-value=0.03 with mouse genetic background), 'purine binding' (7, p-value=0.04), 'acetyl-CoA C-acetyltransferase activity' (2, p-value=0.004) and 'mitochondrion' (8, p-value=$1.6 \cdot 10^{-3}$). Proteins with phosphate/purine binding may be present in the $Rho^{GTP\gamma S}$ samples due to higher affinity towards GTPγS. Thus, they might represent false positives. The appearance of mitochondrial proteins is discussed later.

To ultimately evaluate the quality of LF-qGAP, the sensitivity and specificity were calculated and the reproducibility was estimated. In total, 8506 protein identifications (summed up over all experiments) were quantified with at least three events in either the GTPγS- or GDP-experiment. Altogether, 381 outliers were identified, 106 of them were part of the HIPPIE database as interactor of the respective Rho GTPase (true positives). Another 107 proteins that were not significant outliers were listed in HIPPIE (false negatives). This resulted in a sensitivity of 0.5 and a specificity of 0.97. Potential reasons for the sensitivity not being higher are missing or wrong entries in the standard database or technical deficits of LF-qGAP. It has already been mentioned that HIPPIE is incomplete and additional LF-qGAP significant interactors have been described in other literature sources to be Rho interactors. Taking these additional true positives into account the sensitivity increases to 0.59. However, the background was not checked for additional interaction partners. Therefore, speculations about the real sensitivity remain vague. Noteworthy, LF-qGAP performs better than yeast two-hybrid, for which false positive rates are estimated to be 70%[198].

It is also likely that false interactions are included in the HIPPIE reference. For example we identified the protein NONO as non-significant in our Rac1 pull-downs, but NONO is listed as an interaction

partner for Rac1 in HIPPIE. The protein NONO is a DNA/RNA-binding protein with no links to Rho GTPase biology. The interaction to Rac1 was found in yeast two-hybrid experiments, an no further validation experiments were performed for this interaction[257]. This makes it possible that the Rac1-NONO interaction is an incorrect entry in HIPPIE. On the other hand, some interactions were non-significant in LF-qGAP, but are by high chance binders for the respective Rho GTPase. For instance Dock1 (Dock180) was non-significant in two $Rac1^{GTP\gamma S}$ versus $Rac1^{GDP}$ experiments. With a total number of 50 identified peptides and a high overall intensity a proper quantification was ensured. Dock1 is a well described GEF for Rac1[59] and would have been expected to appear as a significant hit. Some possible biochemical and technical explanations for such a negative observation are discussed below.

First, a protein could bind to the GDP- and GTPγS-form of a Rho GTPase with the same affinity. This could be the case for both NONO and Dock1. These proteins would only be identified as significant binders if compared to a different control. Interestingly, when $Rac1^{GTP\gamma S}$ is compared to $RhoA^{GTP\gamma S}$ we find Dock1-4 as interaction partners of $Rac1^{GTP\gamma S}$, whereas Dock9-11 preferentially bind to $Cdc42^{GTP\gamma S}$ (Figure 3.14). All four Dock proteins that bind to Rac1 in a loading state independent manner contain SH3-domains, whereas the $Cdc42^{GTP\gamma S}$-specific Docks contain a PH domain instead (Figure 3.14D). This supports the possibility that nucleotide-unspecific binding could be mediated via the SH3 domain (see above). Second, a potential interaction partner could be unavailable to interact due to posttranslational modifications or strong binding towards another protein (e.g. the endogenous Rho protein) that blocks the binding site. Third, the interaction could be of low-affinity and transient. Finally, the label free quantification may not work precisely enough. For the label free approach, the protein intensities of numerous files (42 alone for the RhoA, Rac1 and Cdc42 experiments) need to be normalized. For the sake of completeness it shall be mentioned that the protein NONO was found in the protein background when Rac1 was compared to Cdc42 (log_2 fold change of -1.55 $Cdc42^{GTP\gamma S}$/ $Rac1^{GTP\gamma S}$).

It should also be noted that of the 552 HIPPIE-listed interactions for the six Rho GTPases some proteins were not identified at all. These proteins were either not present in the sample, did not have a reasonable number of quantification events or simply escaped detection. Considering these technical challenges, it is actually surprising that LF-qGAP was able to identify 60 (11%) of the 552 HIPPIE-listed interactions.

The reproducibility of LF-qGAP was estimated by clustering the 42 RhoA, Rac1 and Cdc42 pull-downs. The triplicates of each experiment clustered together in 13 of 14 cases. The only experiment that did not group as expected was the RhoA GDP replicate 1 from cortex. The first mass spectrometry run from this sample failed, so it was remeasured five days later with a slightly different setup (same

machine but different column). It seems that the different setup results in slight changes in the mass spectrometry analysis. These changes make the normalization of intensities more difficult. However, the overall results were not affected. This finding emphasizes the importance of running label free samples with identical setup. Nevertheless, the RhoA GDP replicate 1 from cortex did at least cluster with the other cortex samples. Since the grouping of samples by hierarchical clustering is almost equal to the experimental setup with triplicates, the reproducibility can be considered high.

In summary one can conclude that qGAP is able to identify proteins from a given lysate as Rho GTPase effectors that are 'biochemically available', meaning the binding site is free for binding and the effectors have a sufficiently high affinity towards the Rho GTPase. To differentiate between constitutive binding or nucleotide-specific binding it is advisable to add a further control, best another GTPase as shown for $Rac1^{GTP\gamma S}$ compared to $RhoA^{GTP\gamma S}$. Increasing the number of replicates would also help to increase the reliability of label free quantification.

4.3 qGAP in comparison to alternative strategies

With qGAP the first large-scale quantitative assay for the identification of nucleotide-specific Rho GTPase interaction partners has been established. Until now, systematic screening for binding partners of Rho GTPases was mainly done using the yeast two-hybrid assay. In a few studies, affinity purification followed by single protein detection or the ligand-overlay assay were used[258,259]. Studies based on the yeast two-hybrid assay supplied the scientific field with the identification of numerous potential interaction partners[210,260–262]. However, the reliability of identified interactions remained low due to the high intrinsic false positive rate of the assay and the uncommon subcellular localization of the Rho proteins. In yeast two-hybrid, the interaction between potential binding partners occurs within the yeast nucleus, whereas Rho GTPases evolve their biological function at the plasma membrane or in the cytosol. These could be the reasons why no survey study using yeast two-hybrid to identify Rho interaction partners has been published. Research papers using yeast two-hybrid focus on specific Rho-effector interactions often using constitutively active (CA) and dominant negative (DN) mutants of Rho proteins[263]. The CA-form is not able to hydrolyze GTP and the DN-form binds constitutively to a GEF molecule without further binding to effectors. These CA- and DN-mutants are not directly comparable with the GTP- and GDP-loaded form of Rho proteins as often suggested. This is seen in the present study (Results, 3.3.2): With the CA-form of Cdc42 the protein Rho GDI 1 was identified as a binder (see Figure 3.18A), but GDI 1 is known to interact with $Cdc42^{GDP}$ [237]. In addition, we found evidence for specific degradation of $Rac1^{DN}$. Rac1 was 100-fold more abundant in the CA- compared to the DN-immunoprecipitation (see Figure 3.18B). In the DN-

experiment, the proteasomal subunits PSMA2 and PSMA6 were enriched. These findings are surprising since the ubiquitination of $Rac1^{GTP}$ and Rac1-G12V (CA) have been described to be higher than for Rac1-T17N (DN)[264]. In any case, these data indicate that both forms are not directly equivalent to the nucleotide-loaded forms of GTPases. The drawbacks of the CA- and DN-mutants should not only be kept in mind for interaction studies with yeast two-hybrid or immunoprecipitations, but for any kind of biological study using them.

Affinity purification of differentially loaded Rho GTPases has been used previously to identify effectors[134]. This led to the discovery of several classical Rho binding proteins. In these experiments, large amounts of protein lysates were typically applied to affinity matrixes and the eluates were subjected to SDS-PAGE. In previous studies, the quantitative comparison between the GDP- and GTP-pull-down was often performed by visual examination of the stained gel only. Single bands were chosen for further investigation by cost- and time-intensive identification procedures. With this approach, low abundant proteins are expected to escape detection.

qGAP combines the advantages of the affinity-based enrichment of interaction partners from low amounts of source material (3 mouse brains delivered enough protein for pull-downs with 3 Rho GTPases) with the deep proteome-coverage of high sensitive mass spectrometric detection. The proteins are identified and quantified with a high degree of reliance allowing distinguishing the specific Rho binders from the protein background.

There is no published method that describes the systematic detection of Rho GTPase interactors from SILAC or label free samples to date. A method describing the application of SILAC to identify interaction partners of atypical Rho GTPases has been published[265]. However, atypical Rho GTPases do not hydrolyze bound GTP and the publication did not identify any interaction partners.

We sought to compare SILAC- and LF-qGAP by comparing the identified interaction partners (see 3.2.7). We found most SILAC-qGAP interactions were also identified by LF-qGAP. Of 49 SILAC-qGAP interactions 36 were identified by LF-qGAP as well: 20 of 26 (76.9%) for Cdc42, 7 of 14 (50%) for Rac1 and 9 of 9 (100%) for RhoA (see Figure 3.15). If only the HIPPIE-listed interaction partners are taken into account LF-qGAP identified 60 proteins, SILAC-qGAP 32 proteins and the overlap between them was 25 proteins. In general, proteins that were significant binding partners exclusively in LF-qGAP were not identified at all in SILAC-qGAP or did not have sufficient quantification. On the other hand, classical interaction partners as IQGAP1 and IQGAP2 were not Rac1 or Cdc42 specific interaction partners in brain lysates. IQGAP1 and BIN3 were not identified in any LF-qGAP experiment but have been reported to obtain detectable protein levels in cerebral endothelial cells and glial cells respectively[240]. The absence of those two proteins can be explained by technical reasons. The proteins may simply have escaped detection due to low abundance in brain cells. To our

astonishment IQGAP2 was identified in a Cdc42 LF-qGAP experiment as background protein with no clear tendency towards one of the two nucleotide forms. This could indicate that the interaction towards Cdc42 may be blocked and IQGAP2 regulates other GTPases in brain instead. In general, it can be assumed that protein ratios are determined much more precisely in SILAC because peptide peaks are compared within the same spectrum. In label free quantification, quantification is performed between two independently measured mass spectrometry experiments. It remains an exciting question whether pull-downs from SILAC-labeled mice result in the same binding profiles as LF-qGAP or even identify more effector proteins.

The advantages and limitations of qGAP can be summarized as follows: qGAP is able to identify Rho effector proteins from cell culture and label-free samples and distinguishes them from thousands of background proteins with high specificity, reproducibility and good sensitivity. qGAP is able to differentiate between Rho^{GDP}- and $Rho^{GTP\gamma S}$-binding partners better than immunoprecipitations with the CA- and DN-variants. qGAP is able to point to new interaction partners that can then be validated by other methods. The identification of new interaction partners can lead to the discovery of unknown Rho protein function. qGAP is able to identify constitutive binders if different Rho GTPases are compared. qGAP is applicable to other Ras GTPases, as shown for Arf6 (see Supplemental Data 6.1.1). However, it should be kept in mind that qGAP pulls down interaction partners from a cellular lysate. Posttranslational modifications on the Rho protein besides the nucleotide loading are not taken into account. The disintegration of the cell and cellular components may lead to biologically unspecific binding. Complexes that need an intact cell to form could also escape detection. Advantages and disadvantages of qGAP are summarized in Tble 4.1.

Table 4.1: Advantages and disadvantages of qGAP

qGAP	
Advantages	**Disadvantages**
• Identification of Rho^{GDP}- and $Rho^{GTP\gamma S}$-specific binders • Identification of constitutive binders (by comparison with additional GTPase) • Applicable for cell culture and complex tissues • Endogenous expression levels of proteins • Identification of indirect interactions and complexes • High specificity and reproducibility, good sensitivity • Applicable to other Ras GTPases	• Interactions form post-lysis • Complexes that need cellular environment could be missed • Direct and indirect interactions cannot be distinguished

4.4 A network of Rho GTPase interaction partners

We intended to establish qGAP to gain insights into Rho biology. Using qGAP with six different Rho GTPases, we identified 291 interaction partners. Some general assumptions on Rho biology can be derived from this Rho interactome. Some of the interactions also allows me to formulate hypothesis about their biological function. For validation, these hypotheses will have to be complemented with mechanistic studies.

In general it can be stated that the constructed Rho interaction network reflects Rho GTPase biology. Proteins binding the GTPγS-bound form are enriched in Rho-typical processes, domains and functions. In detail, we found proteins being enriched that are linked to specific Rho GTPase functions since a long time (Cdc42-cell polarity, Rac1-phagocytosis)[103,253]. Interestingly, the number of identified interaction partners differs strongly between the Rho GTPases. The 40 interaction partners we found for $Rac1^{GTP\gamma S}$ in the cerebrum experiment was the highest number of interactions in a single experiment, while the twelve interactors found for $RhoD^{GTP\gamma S}$ in the whole brain experiment was the lowest number. $Cdc42^{GTP\gamma S}$ was investigated in three experiments and has 60 interactions, the highest overall number of binding partners. The data is not sufficient to attribute any biological relevance to

the differences in the number of binding partners. It could be that investigation of different tissues leads to a higher number of interaction partners for RhoD and less interaction partners of Cdc42. It should only be remarked that, according to current knowledge, Cdc42 is involved in the broadest spectrum of biological processes among the Rho GTPases (e.g. actin remodeling, cell polarity, cell division). This could be reflected by a high number of interaction partners.

The interactors of the GDP-network are enriched in GEF proteins. No enrichment for further functions or processes was discovered. This could either mean that binders of the GDP-form have only regulatory functions like GEF/GDI as described in the literature. It could also be that enrichment studies are not sufficient to reveal additional biological functions of interactors of the GDP-form. Only two proteins, Rho GEF 17 (Arhgef17) and Rho GDI 1 (Arhgdia), were found to bind to all six GTPases in their GDP-bound state. This stands in strong contrast to the high overlap found among the interaction partners of the GTPγS-bound forms. The proteins Ran, Eef1a2 and Nudt16 interact with RhoB, RhoC and RhoD. These three proteins do not have any known link to Rho biology but show affinity towards guanyl nucleotides. Thus, it could be that the detected binding is an artifact.

In our experiments we discovered that eleven GEFs (Rho GEF 1, -2, -6, -7, -11, -12, -18, Abr, Plekhg5, Dock9 and Akap13) are more specific binders for the GTPγS-bound form of Rho GTPases than for the GDP-bound form. This was unexpected since GEFs bind and activate the GDP-form of Rho GTPases. These GEFs may bind the Rho proteins via another site than the DH domain or could be part of a protein complex and bind indirectly. Such large complexes may bind activated Rho proteins and keep them constantly in a GTP-bound state to ensure stability and activity of the complex.

An alternative explanation is the activation of one Rho GTPase by another. The cascade $Cdc42^{GTP}$→Rho GEF 6→$Rac1^{GDP}$ is an example for a successive activation of one Rho GTPase (Rac1) by a second GTPase (Cdc42)[209]. Our data indicate that such an activation cascade may represent a general scheme of Rho GTPase activation. Interestingly, the number of Rho GTPases a GEF binds to is different between the GTPγS- and the GDP-network. In the GDP-experiment five GEFs were interactors (Rho GEF 17, Prex1, Tiam2, Trio and Kalirin). Four of the five GDP-specific GEFs were binding only to one GTPase with Rho GEF 17 binding to three. In the GTPγS-experiments GEFs had several binding partners: Nine of eleven identified GEFs bound to two or more Rho GTPases. Altogether, this could mean that GEFs function as integrators for signals. They could mediate activation signals (from several Rho^{GTP} proteins) on a specific target. To validate this hypothesis, the targets of the GTP-specific GEFs need to be determined.

The interactome data could explain additional regulation mechanisms. We found two overlaps between the GTPγS- and the GDP-network. The adaptor protein BAIAP2 is binding to $Cdc42^{GTPγS}$ and $RhoD^{GDP}$ and the cholesterol ester hydrolase Nceh1 binds to $RhoB^{GTPγS}$ and $RhoA^{GDP}$. For the case of

RhoD^{GDP}-BAIAP2 binding one could discuss another example of a Rho GTPase being activated by another. BAIAP2 links membrane-bound small G-proteins to cytoplasmic effectors[212]. BAIAP2 is known to bind DIAPH1, a protein that was discovered with LF-qGAP as a RhoD$^{GTP\gamma S}$ binding partner. It is possible that RhoD^{GDP} stays in a complex with BAIAP2 and DIAPH1 and gets activated upon Cdc42-binding. That means that Cdc42^{GTP} would activate the RhoD^{GDP}-BAIAP2-DIAPH1 to RhoD^{GTP}-BAIAP2-DIAPH1 complex.

We found that the promiscuousness of Rho binding is higher than anticipated. One third of the identified proteins had interactions towards two or more Rho GTPases. Some of these interactions were expected (e.g. the binding of DAAM1 to RhoB and RhoC). However, some proteins showed binding towards several Rho GTPases that was not expected. Rock2 was described as a binding partner of RhoA[248] and later RhoB and RhoC. We found Rock2 also as binder of Rac1 and Cdc42. Moreover, we were able to validate these finding with proximity ligation assay. If the interaction is direct or indirect cannot be answered. The high number of number of overlapping interaction partners could be explained by several, not mutually exclusive hypothesis: Rho GTPases might have strongly overlapping functions that can be partly compensated by each other, Rho GTPases support an intense crosstalk, the regulation of Rho GTPases takes place on additional levels (e.g. localization and availability) and the affinity of an interactor towards the GTPases can be different. By comparing the GTPγS-bound pull-downs of the different Rho proteins to each other, it was shown that there is indeed an additional level of specificity: When RhoA$^{GTP\gamma S}$ was compared against Rac1$^{GTP\gamma S}$ and Cdc42$^{GTP\gamma S}$ the protein Rock2 was most specific for RhoA$^{GTP\gamma S}$ being in line with the literature data. We also found that there are proteins that seem to bind to both nucleotide-forms in equal manner (Grb2-Rac1).

The high overlap of interaction partners enabled us to cluster Rho GTPases according to their shared interactors. We found that the obtained dendrogram resembles to their evolutionary distance reflected by sequence similarity alignment. In hierarchical clustering, Rac1 and Cdc42 are closely related to each other and the Rho subfamily (RhoA, RhoB and RhoC) forms a group, whereas RhoD stands out. RhoC and RhoB show the closest relationship in clustering, whereas sequence alignment suggests a closer relation between RhoA and RhoC. This divergence can be explained by minor differences in the shared lysates used in RhoB and RhoC experiments and the lysate of the RhoA experiments. Alternatively, RhoB and RhoC may have more similar biological functions. The observation that Rac1 has the highest number of shared interactions (36) is also in line with the theory that recent Rho GTPases derive evolutionary from the ancestors of the Rac proteins.

Besides the overlap between the Rho GTPases, we observed unexpected overlap with binding partners of other Ras GTPases. The protein IQSEC3 was found to interact with RhoA$^{GTP\gamma S}$, Rac1$^{GTP\gamma S}$

and Cdc42$^{GTP\gamma S}$ and these interactions could be validated by PLA. With its SEC7 domain IQSEC3 functions as GEF for Arf1. IQSEC3 is predominantly expressed in neurons[266]. IQSEC3 has not been in the focus of research so far, but the family member IQSEC1 (BRAG2) plays a role in cell adhesion, a process that is often regulated by Rho GTPases[267]. It is tempting to speculate that the specificity of domains (DH, SEC7 or RasGAP) to their binding targets may be broader than previously thought. Another example from our data is the Ras association (RalGDS/AF-6) domain containing protein Raph1 that was pulled down with Cdc42$^{GTP\gamma S}$.

The observation of several mitochondrial proteins as significant interaction partners is most interesting since Rho GTPases are expected to be localized at the plasma membrane, at cytoskeletal structures or in the cytosol. However, previously it was shown that PAK5 binds to Rac1 and Cdc42, but continuously localizes to mitochondria to prevent apoptosis[268]. This shows that an interaction between Rho and mitochondrial proteins is indeed possible. As one example from the qGAP data, Opa1 was found to specifically bind Rac1 and Cdc42. Opa1 is a dynamin-like protein that regulates mitochondrial morphology and may be involved in the progression of apoptosis[269]. The interaction of Cdc42 with Opa1 was found in 3 of 3 experiments and the interaction of Rac1 with Opa1 was validated by PLA. This makes it likely that the Rac1 – Opa1 interaction takes place *in vivo*. Another example of a mitochondrial protein that was found and validated as interactor is ACAT1. ACAT1 was identified as binding partner of RhoA$^{GTP\gamma S}$ in SILAC- and LF-qGAP with high $\log_2$ fold changes and a high number of peptides. ACAT1, an acetyl-CoA acetyltransferase, has been recently identified by others as RhoA binding partner as well[134]. Taken together, Rho GTPases are seemingly able to interact with proteins that are located in the mitochondrion. It might be possible that Rho GTPases can enter the mitochondrion under certain conditions. More likely, Rho proteins could interact with mitochondrial proteins in the cytoplasm. Most mitochondrial proteins are encoded by genomic DNA, synthesized in the cytoplasm and targeted by signal sequences to the mitochondria. Rho GTPases may interact with these proteins during their way to the mitochondria. Alternatively, mitochondrial proteins may also be released from the organelle and interact afterwards with Rho GTPases. The release from the mitochondria could happen during apoptosis. The interaction of Rho proteins with mitochondrial proteins within the cytoplasm is supported by the experimental setup of SILAC-qGAP. Here, a cytoplasmic extract was prepared and ACAT1 interacted with RhoA$^{GTP\gamma S}$.

Finally, we hoped that binding profiles of RhoB, RhoC and RhoD would allow us to draw conclusions about their biologic function. We were most interested in similarities or differences compared to RhoA, Rac1 and Cdc42. As mentioned previously, we found processes enriched that are typically linked to Rho GTPases (Cdc42-cell division etc.). For RhoA and RhoB we found a clear enrichment of

apoptosis-related proteins. This is in line with RhoA being required for Ras-induced transformation of cells and for promotion of oncogenesis[270,271].

RhoB is present in two forms in the cell: Rho-GG (geranylgeranylation) localized on endosomes and Rho-FF (farnesylation) localized at the plasma membrane[272,273]. RhoB had been previously linked to stimulation of apoptosis, but clear mechanisms remained elusive[153,274,275]. In detail, RhoB was found to suppress tumor growth in mice[154] and RhoB deletion promotes tumor formation[20]. These pro-apoptotic effects separate RhoB clearly from RhoA and RhoC that promote Ras-induced transformation of cells[270,276]. Farnesyltransferase inhibitors (FTIs) were originally designed to block farnesylation of Ras. It was discovered, that the antiapoptotic impact of FTIs reaches above the effects of Ras farnesylation inhibition. Some of these effects were related to an increase of RhoB-GG causing a mislocalization of RhoB[277,278]. It was postulated that RhoB possibly competes for binding to Rho effector proteins and thereby disrupts proto-oncogenic signaling by RhoA/RhoC[279]. The mechanisms how RhoB affects apoptosis have not been decrypted yet. However, certain targets for RhoB have been suggested such as Cyclin B1[280,281].

The qGAP dataset contains eight proteins that are linked to apoptosis and that bind to $RhoB^{GTP\gamma S}$. These were Akap13, Rho GEF 2, Rho GEF 11, Rho GEF 18, Gelsolin, Plekhg5, Rhotekin and Rock1. In qGAP, the proteins Akap13, Gelsolin and Rock1 were specific to RhoB. The interactors Akap13 and Rock1 have been shown to bind RhoA in other publications[258,282]. Gelsolin is an actin-capping protein that has not been shown to bind Rho proteins[283]. Gelsolin prevents apoptosis by closing the mitochondrial voltage-dependent anion channel[284].

Interpretation of the LF-qGAP data about $RhoB^{GTP\gamma S}$ interacting proteins offers several ways how apoptosis can be regulated by RhoB. On one hand, RhoB may inhibit Gelsolin from its antiapoptotic function. This hypothesis could be tested by comparing the antitumorigenic effects of FTIs in cells with or without a Gelsolin knock-down. Alternatively to FTIs a constitutive active RhoB could be used.

On the other hand RhoB may function as competitive inhibitor to RhoA/RhoC-binding as previously suggested[279]. This hypothesis can be tested by performing pull-downs for $RhoA^{GTP\gamma S}$, $RhoB^{GTP\gamma S}$ and $RhoC^{GTP\gamma S}$ under the exactly same conditions. A higher affinity of the apoptosis-related proteins towards $RhoB^{GTP\gamma S}$ would indicate its potency to influence those pathways. Comparison of wildtype proteomes to RhoB-CA or RhoB knock-down proteomes could shed a light on RhoB expression targets. All experiments could be tested in mouse NIH3T3 cells, in which experiments on RhoB have been performed in studies[285].

In contrast to RhoA and RhoC, the protein RhoB is farnesylated at its carboxyl-terminus. Since the recombinant proteins are not expected to contain their carboxyl-terminal lipid moiety, it can be

deduced that this residue itself does not have a crucial influence on the interactions of RhoB. This observation is of medical interest since FTIs have been introduced recently for cancer treatment[275].

The identification of interaction partners for RhoA, Rac1, Cdc42, RhoB, RhoC and RhoD allowed us to obtain a global picture of the effector proteins of the Rho GTPases (Figure 3.19 and Figure 3.21), including a number of new interaction partners (Table 6.1). The interactome for the six Rho GTPases reflects two decades in Rho GTPase science.

5 Conclusions and Perspectives

Rho GTPases are central regulators of the actin cytoskeleton. Beyond this, they show influence on gene expression, cell division and other processes. The family of Rho GTPases can be classified into four classical subfamilies (Rho, Rac, Cdc42/TC10, RhoD/Rif) that are regulated by the GTP/GDP cycle and four atypical subfamilies. Among the classical Rho GTPases RhoA, Rac1 and Cdc42 have been studied most intensively. The functions of other family members, like RhoB, RhoC or RhoD, remained largely uncharacterized.

Despite their influence on a broad range of biological processes, a comprehensive analysis of the protein interaction network of Rho GTPases is so far missing. Moreover, the most used method for the identification of Rho GTPase binding partners in large scale manner, yeast two-hybrid, suffered high false positive rates. Alternatively, Rho GTPase interaction partners were identified by overlay assays or AP-MS with identification of a limited number of effectors.

With quantitative GTPase affinity purification (qGAP), we successfully established an assay for the reliable identification of Rho GTPase interactors. We used qGAP in combination with metabolic labeling, SILAC-qGAP and as label free approach, LF-qGAP. By using the comprehensive Human Integrated Protein-Protein Interaction rEference database (HIPPIE) as reference, we showed high enrichment of known Rho interaction partners within the identified qGAP interactors for both, SILAC-qGAP and LF-qGAP. These findings were supported by high enrichment of Rho effector domains. Moreover, the high quality of LF-qGAP data was supported by determining the sensitivity, specificity and reproducibility. Eleven out of twelve tested new interactions could be validated by an alternative approach, the proximity ligation assay in combination with the CNF toxins. This independent assay was also developed during this thesis. We conclude that qGAP is a versatile and reliable method for the identification of interaction partners for each of the two nucleotide states of Rho GTPases. LF-qGAP enables identification of Rho effector proteins from any tissue resource of any sequenced organism.

When the Rho^{GTP}, $Rac1^{GTP}$ and $Cdc42^{GTP}$ pull-downs were compared, it was revealed that some interaction partners (e.g. Rock2) bind to the GTPases with different affinities. These findings were consistent with literature data. In addition it was shown that a few interactors (e.g. Grb2) seem to bind constitutively. The constitutive binding could be mediated by other motifs than the classical effector binding sites on the Rho proteins. It could be that the SH3 domain on effector proteins is necessary for constitutive binding to Rho proteins.

The binding profiles obtained from LF-qGAP allowed us to construct interaction networks for both nucleotide forms. These interaction networks revealed a promiscuousness of binding partners

between Rho GTPases that was higher than anticipated. Interestingly, the GTP-interaction network reflected the evolutionary relationship between the Rho GTPases. It is exciting to speculate, that many biologically-relevant interactions may be hidden in the qGAP dataset. These could shed a new light on Rho influence on the metabolism (RhoA-ACAT1, Cdc42-Acadl), microtubule organization (Cdc42-Mzt2) or mitochondrial fission (Cdc42/Rac1-Mzt2). It is important to note, that in cooperation projects, qGAP has been successfully applied to other monomeric GTPases. Among them were members of the Arf-, Rab- and GIMAP-families. Lysates from various tissues have also been applied to the qGAP protocol.

By enrichment studies we found a high abundance of apoptosis-related proteins in the RhoB binding profile. RhoB had been linked to tumor suppression previously and with this, it stays in opposition to RhoA and RhoC. The current hypothesis claims that RhoB is a competitive inhibitor of RhoA/RhoC binding to pro-survival targets. To test this hypothesis, the binding-profiles of the GTP-bound RhoA/RhoB/RhoC can be compared. We would expect a stronger binding of apoptosis-related targets towards RhoB. We found the anti-apoptotic protein Gelsolin as additional link between RhoB and apoptosis-regulation. We suggest testing this hypothesis by investigating the impact of farnesyltransferase inhibitors onto tumorigenesis in Gelsolin knock down cells.

Altogether, with qGAP a valuable method for the identification of Rho GTPase effectors was established. Many novel interaction partners were identified and eleven out of twelve could be validated by an independent, newly developed assay. qGAP has high specificity (97%) and reproducibility and a good sensitivity (50%). The high quality of the data shows that qGAP is a powerful method to investigate Rho GTPase biology. The first systematic comparison of Rho GTPase effectors provides a rich resource for the community.

6 Supplemental Data

6.1 Additional applications of qGAP

6.1.1 SILAC-qGAP for identification of interaction partners of Arf6

The SILAC-qGAP of Arf6 was part of a collaboration with Prof. Udo Heinemann (Max-Delbrück Center for Molecular Medicine, 13125 Berlin). GST-Arf6 was purified and nucleotide-loaded by Harald Striegl.

Finally the qGAP-approach was broadened to additional sets of Ras GTPases. In a series of collaborations GTPases from the Rab, Arf, GIMAP and other families were tested with SILAC- and LF-qGAP. Arf6 regulates endocytic recycling and may modulate vesicle budding and uncoating within the Golgi apparatus[286]. GST-Arf6$^{GTP\gamma S}$ and -Arf6^{GDP} were used for screening with SILAC-qGAP (Figure 6.1: Figure 6.1).

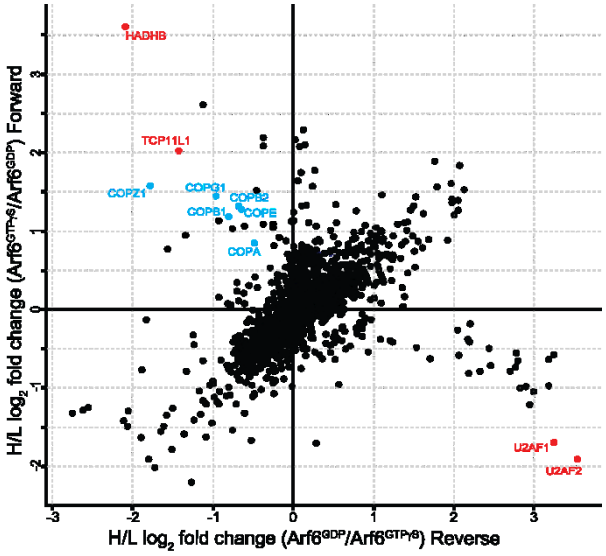

Figure 6.1: qGAP for Arf6 from SILAC-labeled cells. Cytoplasmic fractions of H and L labeled cells were used for pull-downs with the GTPγS- and GDP-form of Arf6. Significant outliers are marked in red, noteworthy proteins in blue.

Four proteins were significant outliers that are not known to bind Arf6. Interestingly, numerous components of the coatomer complex (COPA, COPB1, COPB2, COPE, COPG1 and COPZ1) are enriched with Arf6$^{GTP\gamma S}$. The coatomer is a protein complex coating COPI transport vesicles[287]. The coatomer is recruited by Arf GTPases. The results from SILAC-qGAP suggest that Arf6 is binding to the coatomer.

The presented example of Arf6 shall indicate to the reader that SILAC-qGAP is able to pull down interaction partners of other Ras superfamily members.

Table 6.1: List of all Rho GTPase interaction partners identified by qGAP

Table listing 291 protein protein-interactions between one of the six Rho GTPases RhoA, B, C, D, Rac1 or Cdc42 with the respective hit. Note that one hit (proteingroup) can contain several proteins due to shared peptides.

Peptides	Total number of identified peptides for the proteingroup.
Unique Peptides	Total number of identified unique peptides specificfor the proteingroup.
Sequence coverage [%]	Percentage of the sequence that is covered by the identified peptides of the best protein sequence contained in the group
PEP	Posterior error probability of the identification.
Major Protein ID	Uniprot identifier of the protein with the highest number of identified peptides
Protein names	Name(s) of the protein(s) contained within the group
Gene names	Name(s) of the genes(s) associated to the proteins(s) contained within the group.
GTPase	Rho GTPase with respective nucleotide state for which the interaction was found.
Interaction in HIPPIE	An' x' indicates that the interaction is listed in the HIPPIE database.
Interaction in literature	An 'x' indicates that the interaction is described in HIPPIE or somewhere else in the literature.

Gene names	GTPase	Peptides	Unique peptides	Sequence coverage [%]	PEP	Major Protein ID	Protein names	HIPPIE	Lite-rature
Eif5a;Eif5a2	$Cdc42^{GDP}$	5	5	56,5	2.70E-68	P63242	Eukaryotic translation initiation factor 5A-1;Eukaryotic translation initiation factor 5A-2		
Eps15l1	$Cdc42^{GDP}$	31	31	50,5	5.52E-255	Q60902	Epidermal growth factor receptor substrate 15-like 1		
Gad2	$Cdc42^{GDP}$	4	3	10,3	5.01E-79	P48320	Glutamate decarboxylase 2		
Hspe1	$Cdc42^{GDP}$	8	8	73,5	1.82E-86	Q4KL76	10 kDa heat shock protein, mitochondrial		
Igsf5;Pcp4	$Cdc42^{GDP}$	4	4	9,4	9.14E-66	D3YXH0	Purkinje cell protein 4		
Isca2	$Cdc42^{GDP}$	4	4	36,4	2.24E-211	Q9DCB8	Iron-sulfur cluster assembly 2 homolog, mitochondrial		
Kcnab2	$Cdc42^{GDP}$	8	8	27,5	5.53E-158	E0CXZ9	Voltage-gated potassium channel subunit beta-2		
Lypla2	$Cdc42^{GDP}$	7	7	39,4	1.99E-119	B1AV56	Acyl-protein thioesterase 2		
Ncald	$Cdc42^{GDP}$	7	4	47,2	0	Q91X97	Neurocalcin-delta		
Pld3	$Cdc42^{GDP}$	5	5	13,7	4.42E-22	O35405	Phospholipase D3		
Prex1	$Cdc42^{GDP}$	11	6	8,8	9.37E-37	Q69ZK0	Phosphatidylinositol 3,4,5-trisphosphate-dependent Rac exchanger 1 protein		
Psma6	$Cdc42^{GDP}$	5	5	26	2.23E-17	Q9QUM9	Proteasome subunit alpha type-6		
Acadl	$Cdc42^{GTP}$	16	16	41,9	0	P51174	Long-chain specific acyl-CoA dehydrogenase, mitochondrial		
Arhgap32	$Cdc42^{GTP}$	28	28	18,3	3.55E-253	Q811P8	Rho GTPase-activating protein 32	x	x
Arhgap5	$Cdc42^{GTP}$	48	48	43,2	0	E9PYT0	Rho GTPase-activating protein 5		x
Arhgef11	$Cdc42^{GTP}$	73	4	61,5	0	Q68FM7		x	x
Arhgef12	$Cdc42^{GTP}$	77	2	61,6	0	Q8R4H2	Rho guanine nucleotide exchange factor 12		
Arhgef2	$Cdc42^{GTP}$	47	47	55,8	0	Q60875	Rho guanine nucleotide exchange factor 2		
Arhgef6	$Cdc42^{GTP}$	23	8	38,7	0	F6WMJ3	Rho guanine nucleotide exchange	x	x

Gene names	GTPase	Peptides	Unique peptides	Sequence coverage [%]	PEP	Major Protein ID	Protein names	HIPPIE	Lite-rature
							factor 6		
Arhgef7	$Cdc42^{GTP}$	68	0	81,9	0	Q9ES28	Rho guanine nucleotide exchange factor 7	x	x
Atl1	$Cdc42^{GTP}$	6	6	14,5	9.21E-28	Q8BH66	Atlastin-1		
Baiap2	$Cdc42^{GTP}$	43	3	77,6	0	Q3UKP6	Brain-specific angiogenesis inhibitor 1-associated protein 2	x	x
C1orf198	$Cdc42^{GTP}$	12	12	62,7	7.31E-82	Q8C3W1	Uncharacterized protein C1orf198 homolog		
Camk2b	$Cdc42^{GTP}$	21	10	47,4	0	Q5SVJ0	Calcium/calmodulin-dependent protein kinase type II subunit beta		
Cdc42bpa	$Cdc42^{GTP}$	72	64	45,7	0	E9PVY0	Serine/threonine-protein kinase MRCK alpha	x	x
Cdc42bpb	$Cdc42^{GTP}$	105	96	63,9	0	Q7TT50	Serine/threonine-protein kinase MRCK beta	x	x
Cdc42ep1	$Cdc42^{GTP}$	14	13	39,1	6.04E-57	Q91W92	Cdc42 effector protein 1	x	x
Cdc42ep4	$Cdc42^{GTP}$	27	26	82,5	0	A2A6Q1	Cdc42 effector protein 4	x	x
Diap2;Diaph2	$Cdc42^{GTP}$	17	17	25,8	6.03E-135	E9Q4U7	Protein diaphanous homolog 2	x	x
Dock9	$Cdc42^{GTP}$	80	3	47,9	0	E9QMR2		x	x
Dync1i2	$Cdc42^{GTP}$	6	6	21,5	2.79E-145	A2BFF9	Cytoplasmic dynein 1 intermediate chain 2		
Dynll2	$Cdc42^{GTP}$	4	2	34,8	3.83E-26	B2KGQ2	Dynein light chain 2, cytoplasmic		
Fam89b	$Cdc42^{GTP}$	6	6	39,2	9.51E-65	Q9QUI1			
Fnbp1	$Cdc42^{GTP}$	21	21	44	1.70E-157	Q80TY0	Formin-binding protein 1	x	x
Fnbp1l	$Cdc42^{GTP}$	30	1	64,6	0	E9PUK3		x	x
Git1	$Cdc42^{GTP}$	52	2	81,6	0	Q68FF6	ARF GTPase-activating protein GIT1		x
Git2	$Cdc42^{GTP}$	29	4	53	0	E9PVA6			x
Grb2	$Cdc42^{GTP}$	16	16	68,7	1.76E-251	Q3U5I5	Growth factor receptor-bound protein 2	x	x
Homer3	$Cdc42^{GTP}$	26	25	79,7	1.53E-291	Q99JP6-2	Homer protein homolog 3		
Iqsec3	$Cdc42^{GTP}$	7	7	9,2	2.95E-149	Q3TES0	IQ motif and SEC7 domain-containing protein 3		
Llgl1	$Cdc42^{GTP}$	13	13	20	5.06E-68	Q80Y17	Lethal(2) giant larvae protein homolog 1		x
Lurap1	$Cdc42^{GTP}$	9	9	49,4	2.05E-58	A2A8F6	Leucine rich adaptor protein 1		
Lurap1l	$Cdc42^{GTP}$	7	7	33,9	2.18E-49	Q8K2P1	Leucine rich adaptor protein 1-like		
Myl6;Gm8894	$Cdc42^{GTP}$	9	9	60,3	1.71E-67	Q60605	Myosin light polypeptide 6		
Mzt2	$Cdc42^{GTP}$	3	3	44,7	1.85E-127	Q9CQ25	Mitotic-spindle organizing protein 2		
Opa1	$Cdc42^{GTP}$	50	50	57,8	0	P58281-2	Dynamin-like 120 kDa protein, mitochondrial;Dynamin-like 120 kDa protein, form S1		
Pak1	$Cdc42^{GTP}$	42	24	77,6	0	G5E884	Serine/threonine-protein kinase PAK 1	x	x
Pak2	$Cdc42^{GTP}$	27	15	62,2	0	Q8CIN4	Serine/threonine-protein kinase	x	x

Gene names	GTPase	Peptides	Unique peptides	Sequence coverage [%]	PEP	Major Protein ID	Protein names	HIPPIE	Lite-rature
							PAK 2;PAK-2p27;PAK-2p34		
Pak3	$Cdc42^{GTP}$	37	1	69,9	0	A3KGC1		x	x
Pak4	$Cdc42^{GTP}$	9	8	22,3	7.90E-93	Q8BTW9	Serine/threonine-protein kinase PAK 4		x
Pak7	$Cdc42^{GTP}$	8	7	17,2	4.51E-40	B1AYC2	Serine/threonine-protein kinase PAK 7		
Pard6a	$Cdc42^{GTP}$	7	5	32,1	1.77E-28	Q9Z101	Partitioning defective 6 homolog alpha	x	x
Pik3cb	$Cdc42^{GTP}$	11	11	15	4.68E-47	Q8BTI9	Phosphatidylinositol 4,5-bisphosphate 3-kinase catalytic subunit beta isoform		
Pik3r1	$Cdc42^{GTP}$	11	10	18,9	1.68E-62	P26450	Phosphatidylinositol 3-kinase regulatory subunit alpha	x	x
Ppm1h	$Cdc42^{GTP}$	16	16	37,8	3.19E-163	Q3UYC0	Protein phosphatase 1H		
Ppp1ca	$Cdc42^{GTP}$	9	4	29,7	7.06E-159	P62137	Serine/threonine-protein phosphatase PP1-alpha catalytic subunit;Serine/threonine-protein phosphatase		
Prkci	$Cdc42^{GTP}$	8	8	15,9	2.88E-96	Q5DTK3	Protein kinase C iota type	x	x
Raph1	$Cdc42^{GTP}$	8	8	16,8	5.88E-88	F2Z408			
Rgs14	$Cdc42^{GTP}$	12	12	29,3	5.51E-124	P97492	Regulator of G-protein signaling 14		
Rock2	$Cdc42^{GTP}$	78	71	55,5	0	F8VPK5	Rho-associated protein kinase 2		
Septin4	$Cdc42^{GTP}$	16	14	46,2	4.63E-106	P28661	Septin-4		
Septin7	$Cdc42^{GTP}$	22	20	58,6	0	E9Q9F5	Septin-7		
Septin8	$Cdc42^{GTP}$	18	12	59,3	0	B1AQZ0	Septin-8		
Sestd1	$Cdc42^{GTP}$	13	13	25,9	2.27E-102	Q80UK0	SEC14 domain and spectrin repeat-containing protein 1		
Snap91	$Cdc42^{GTP}$	16	14	28,2	0	Q61548	Clathrin coat assembly protein AP180		
Sowahc	$Cdc42^{GTP}$	8	8	23,8	2.55E-40	Q8C0J6	Ankyrin repeat domain-containing protein SOWAHC		
Taok2	$Cdc42^{GTP}$	9	9	12,9	3.03E-87	Q6ZQ29-2	Serine/threonine-protein kinase TAO2		
Trip10	$Cdc42^{GTP}$	20	20	41,6	0	Q8CJ53	Cdc42-interacting protein 4		x
Wasl	$Cdc42^{GTP}$	32	32	68,9	0	Q3TXX8	Neural Wiskott-Aldrich syndrome protein	x	x
Wipf1	$Cdc42^{GTP}$	6	6	18,5	8.13E-28	A2ATB9	WAS/WASL-interacting protein family member 1	x	x
Wipf2	$Cdc42^{GTP}$	29	29	78,9	0	Q6PEV3	WAS/WASL-interacting protein family member 2		x
Wipf3	$Cdc42^{GTP}$	17	17	50,9	0	P0C7L0	WAS/WASL-interacting protein family member 3		
Arf3;Arf1;Arf2	$Rac1^{GDP}$	10	6	65,2	0	P61205	ADP-ribosylation factor 3;ADP-ribosylation factor 1;ADP-ribosylation factor 2		
Arhgdia	$Rac1^{GDP}$	13	13	67,2	0	Q99PT1	Rho GDP-dissociation inhibitor 1	x	x
Kalrn	$Rac1^{GDP}$	34	2	16	0	A2CG49-7	Kalirin	x	x
Mpp1	$Rac1^{GDP}$	8	8	24,2	5.25E-37	P70290	55 kDa erythrocyte membrane		

Gene names	GTPase	Peptides	Unique peptides	Sequence coverage [%]	PEP	Major Protein ID	Protein names	HIPPIE	Lite-rature
							protein		
Pacsin2	$Rac1^{GDP}$	16	14	45,1	3.94E-169	Q3TDA7	Protein kinase C and casein kinase substrate in neurons protein 2		x
Stam	$Rac1^{GDP}$	3	3	12,8	1.07E-09	P70297	Signal transducing adapter molecule 1		
Tiam2	$Rac1^{GDP}$	14	13	12,9	4.42E-133	Q6ZPF3	T-lymphoma invasion and metastasis-inducing protein 2		x
Traf7	$Rac1^{GDP}$	4	4	8,4	1.32E-11	F8WJF7	E3 ubiquitin-protein ligase TRAF7		
Trio	$Rac1^{GDP}$	38	31	17,4	0	Q0KL02-4	Triple functional domain protein	x	x
Abi1	$Rac1^{GTP}$	20	15	44,1	0	B7ZCT9	Abl interactor 1		x
Abi2	$Rac1^{GTP}$	19	14	44,8	0	P62484	Abl interactor 2		x
Adam23	$Rac1^{GTP}$	5	5	9,9	6.05E-39	Q5SRA0	Disintegrin and metalloproteinase domain-containing protein 23		
Arhgap32	$Rac1^{GTP}$	28	28	18,3	3.55E-253	Q811P8	Rho GTPase-activating protein 32	x	x
Arhgap5	$Rac1^{GTP}$	48	48	43,2	0	E9PYT0	Rho GTPase-activating protein 5		x
Arhgef11	$Rac1^{GTP}$	73	4	61,5	0	Q68FM7			
Arhgef12	$Rac1^{GTP}$	77	2	61,6	0	Q8R4H2	Rho guanine nucleotide exchange factor 12		
Arhgef2	$Rac1^{GTP}$	47	47	55,8	0	Q60875	Rho guanine nucleotide exchange factor 2	x	x
Arhgef6	$Rac1^{GTP}$	23	8	38,7	0	F6WMJ3	Rho guanine nucleotide exchange factor 6		x
Arhgef7	$Rac1^{GTP}$	68	0	81,9	0	Q9ES28	Rho guanine nucleotide exchange factor 7	x	x
Bckdk	$Rac1^{GTP}$	4	4	11,7	2.43E-11	O55028	[3-methyl-2-oxobutanoate dehydrogenase [lipoamide]] kinase, mitochondrial		
Brk1	$Rac1^{GTP}$	12	12	88	0	Q91VR8	Protein BRICK1		
Cdc42bpa	$Rac1^{GTP}$	72	64	45,7	0	E9PVY0	Serine/threonine-protein kinase MRCK alpha		
Cdc42bpb	$Rac1^{GTP}$	105	96	63,9	0	Q7TT50	Serine/threonine-protein kinase MRCK beta		
Cdc42ep1	$Rac1^{GTP}$	14	13	39,1	6.04E-57	Q91W92	Cdc42 effector protein 1		
Cdc42ep4	$Rac1^{GTP}$	27	26	82,5	0	A2A6Q1	Cdc42 effector protein 4		
Cdc42se2	$Rac1^{GTP}$	2	2	66,7	6.77E-124	Q8BGH7	CDC42 small effector protein 2	x	x
Cit	$Rac1^{GTP}$	86	86	39,9	0	E9QL53	Citron Rho-interacting kinase	x	x
Cryzl1	$Rac1^{GTP}$	7	7	25,9	8.65E-32	Q921W4	Quinone oxidoreductase-like protein 1		
Cyfip2	$Rac1^{GTP}$	51	32	45,9	0	Q5SQX6	Cytoplasmic FMR1-interacting protein 2		x
Dock9	$Rac1^{GTP}$	80	3	47,9	0	E9QMR2			
Dynll2	$Rac1^{GTP}$	4	2	34,8	3.83E-26	B2KGQ2	Dynein light chain 2, cytoplasmic		
Echdc1	$Rac1^{GTP}$	14	14	57,8	4.17E-142	Q9D9V3	Ethylmalonyl-CoA decarboxylase		

Gene names	GTPase	Peptides	Unique peptides	Sequence coverage [%]	PEP	Major Protein ID	Protein names	HIPPIE	Lite-rature
Elmo1	$Rac1^{GTP}$	29	21	41	0	F8WIL9	Engulfment and cell motility protein 1	x	x
Elmo2	$Rac1^{GTP}$	32	24	45,3	0	Q8BHL5-2	Engulfment and cell motility protein 2		
Fnbp1	$Rac1^{GTP}$	21	21	44	1.70E-157	Q80TY0	Formin-binding protein 1		
Git1	$Rac1^{GTP}$	52	2	81,6	0	Q68FF6	ARF GTPase-activating protein GIT1		x
Git2	$Rac1^{GTP}$	29	4	53	0	E9PVA6			x
Homer3	$Rac1^{GTP}$	26	25	79,7	1.53E-291	Q99JP6-2	Homer protein homolog 3		
Inppl1	$Rac1^{GTP}$	17	17	22,8	2.52E-211	Q6P549	Phosphatidylinositol 3,4,5-trisphosphate 5-phosphatase 2		x
Iqsec3	$Rac1^{GTP}$	7	7	9,2	2.95E-149	Q3TES0	IQ motif and SEC7 domain-containing protein 3		
Lin7a	$Rac1^{GTP}$	9	5	44,6	4.83E-246	Q8JZS0	Protein lin-7 homolog A		
Lurap1	$Rac1^{GTP}$	9	9	49,4	2.05E-58	A2A8F6	Leucine rich adaptor protein 1		
Mzt2	$Rac1^{GTP}$	3	3	44,7	1.85E-127	Q9CQ25	Mitotic-spindle organizing protein 2		
Nckap1	$Rac1^{GTP}$	59	59	57,6	0	A2AS98	Nck-associated protein 1	x	x
Opa1	$Rac1^{GTP}$	50	50	57,8	0	P58281-2	Dynamin-like 120 kDa protein, mitochondrial;Dynamin-like 120 kDa protein, form S1		
Pak1	$Rac1^{GTP}$	42	24	77,6	0	G5E884	Serine/threonine-protein kinase PAK 1	x	x
Pak2	$Rac1^{GTP}$	27	15	62,2	0	Q8CIN4	Serine/threonine-protein kinase PAK 2;PAK-2p27;PAK-2p34	x	x
Pak3	$Rac1^{GTP}$	37	1	69,9	0	A3KGC1		x	x
Pak6	$Rac1^{GTP}$	3	2	6,7	3.85E-20	Q3ULB5	Serine/threonine-protein kinase PAK 6		
Pard6a	$Rac1^{GTP}$	7	5	32,1	1.77E-28	Q9Z101	Partitioning defective 6 homolog alpha	x	x
Pddc1	$Rac1^{GTP}$	4	4	28,2	4.90E-26	Q8BFQ8	Parkinson disease 7 domain-containing protein 1		
Pik3r1	$Rac1^{GTP}$	11	10	18,9	1.68E-62	P26450	Phosphatidylinositol 3-kinase regulatory subunit alpha	x	x
Pip4k2b	$Rac1^{GTP}$	9	6	26,7	4.99E-79	Q3UJ95	Phosphatidylinositol 5-phosphate 4-kinase type-2 beta		
Plxnb1	$Rac1^{GTP}$	5	5	5,2	1.07E-64	Q8CJH3	Plexin-B1	x	x
Ppp1r21	$Rac1^{GTP}$	14	14	26,5	2.90E-148	Q3TDD9	Protein phosphatase 1 regulatory subunit 21		
Psmd9	$Rac1^{GTP}$	4	4	23,9	4.02E-14	Q9CR00	26S proteasome non-ATPase regulatory subunit 9		
Rgs14	$Rac1^{GTP}$	12	12	29,3	5.51E-124	P97492	Regulator of G-protein signaling 14		
Rock2	$Rac1^{GTP}$	78	71	55,5	0	F8VPK5	Rho-associated protein kinase 2		
Sccpdh	$Rac1^{GTP}$	3	3	16,3	6.72E-142	Q8R127	Saccharopine dehydrogenase-like oxidoreductase		
Sestd1	$Rac1^{GTP}$	13	13	25,9	2.27E-102	Q80UK0	SEC14 domain and spectrin repeat-containing protein 1		x
Sh3rf1	$Rac1^{GTP}$	4	4	7,8	9.27E-23	Q69ZI1	E3 ubiquitin-protein ligase SH3RF1	x	x
Srgap3	$Rac1^{GTP}$	5	5	6,6	2.97E-36	F8VPQ4	SLIT-ROBO Rho GTPase-activating		x

Gene names	GTPase	Peptides	Unique peptides	Sequence coverage [%]	PEP	Major Protein ID	Protein names	HIPPIE	Lite-rature
							protein 3		
Trim3	$Rac1^{GTP}$	17	17	27,7	5.31E-281	Q9R1R2	Tripartite motif-containing protein 3		
Wasf1	$Rac1^{GTP}$	24	24	50,6	0	Q8R5H6	Wiskott-Aldrich syndrome protein family member 1	x	x
Wasf3	$Rac1^{GTP}$	15	15	40,5	0	Q8VHI6	Wiskott-Aldrich syndrome protein family member 3		x
Arhgdia	$RhoA^{GDP}$	13	13	67,2	0	Q99PT1	Rho GDP-dissociation inhibitor 1	x	x
Arhgef17	$RhoA^{GDP}$	19	19	13	0	Q80U35	Rho guanine nucleotide exchange factor 17		x
Atp5d	$RhoA^{GDP}$	4	4	41,1	3.47E-234	Q4FK74	ATP synthase subunit delta, mitochondrial		
Gart	$RhoA^{GDP}$	6	6	10,7	2.90E-171	Q64737	Trifunctional purine biosynthetic protein adenosine-3;Phosphoribosylamine--glycine ligase;Phosphoribosylformylglycinamidine cyclo-ligase;Phosphoribosylglycinamide formyltransferase		
Mat2b	$RhoA^{GDP}$	5	5	17,1	4.70E-23	Q99LB6	Methionine adenosyltransferase 2 subunit beta		
Mccc1	$RhoA^{GDP}$	9	9	22,5	3.78E-68	Q99MR8	Methylcrotonoyl-CoA carboxylase subunit alpha, mitochondrial		
Nceh1	$RhoA^{GDP}$	5	5	27,2	2.86E-46	Q8BLF1	Neutral cholesterol ester hydrolase 1		
Ndufa4	$RhoA^{GDP}$	8	8	86,6	2.75E-74	Q62425	NADH dehydrogenase [ubiquinone] 1 alpha subcomplex subunit 4		
Ndufa8	$RhoA^{GDP}$	7	7	50	3.31E-72	Q9DCJ5	NADH dehydrogenase [ubiquinone] 1 alpha subcomplex subunit 8		
Rps27;Gm17241	$RhoA^{GDP}$	3	1	29,8	1.40E-61	Q6ZWU9	40S ribosomal protein S27		
Slc25a18	$RhoA^{GDP}$	6	3	17,5	6.53E-28	Q9DB41	Mitochondrial glutamate carrier 2		
Syp	$RhoA^{GDP}$	5	1	24,5	1.43E-46	F8WGK2			
Wbp2	$RhoA^{GDP}$	4	4	18,8	2.26E-19	E9Q1S7	WW domain-binding protein 2		
Abi1	$RhoA^{GTP}$	20	15	44,1	0	B7ZCT9	Abl interactor 1		
Abi2	$RhoA^{GTP}$	19	14	44,8	0	P62484	Abl interactor 2		
Abr	$RhoA^{GTP}$	10	9	21,7	1.91E-44	Q5SSL4-2	Active breakpoint cluster region-related protein		
Acat1	$RhoA^{GTP}$	32	32	84	0	Q8QZT1	Acetyl-CoA acetyltransferase, mitochondrial		
Acat2;Acat3	$RhoA^{GTP}$	6	6	17,4	3.04E-12	Q8CAY6	Acetyl-CoA acetyltransferase, cytosolic		
Anln	$RhoA^{GTP}$	11	11	12,4	1.83E-88	Q8K298	Actin-binding protein anillin		x
Arhgap32	$RhoA^{GTP}$	28	28	18,3	3.55E-253	Q811P8	Rho GTPase-activating protein 32	x	x
Arhgap5	$RhoA^{GTP}$	48	48	43,2	0	E9PYT0	Rho GTPase-activating protein 5		x
Arhgef1	$RhoA^{GTP}$	33	33	46,2	0	Q61210-5	Rho guanine nucleotide exchange factor 1	x	x
Arhgef11	$RhoA^{GTP}$	73	4	61,5	0	Q68FM7		x	x

Gene names	GTPase	Peptides	Unique peptides	Sequence coverage [%]	PEP	Major Protein ID	Protein names	HIPPIE	Lite-rature
Arhgef12	$RhoA^{GTP}$	77	2	61,6	0	Q8R4H2	Rho guanine nucleotide exchange factor 12	x	x
Arhgef18	$RhoA^{GTP}$	20	20	27,6	2.32E-182	Q6P9R4	Rho guanine nucleotide exchange factor 18	x	x
Arhgef2	$RhoA^{GTP}$	47	47	55,8	0	Q60875	Rho guanine nucleotide exchange factor 2	x	x
Arhgef7	$RhoA^{GTP}$	68	0	81,9	0	Q9ES28	Rho guanine nucleotide exchange factor 7		
Ass1	$RhoA^{GTP}$	2	2	11,2	5.20E-58	P16460	Argininosuccinate synthase		
Brk1	$RhoA^{GTP}$	12	12	88	0	Q91VR8	Protein BRICK1		x
Capza1	$RhoA^{GTP}$	7	4	32,4	5.87E-72	E9PWZ5	F-actin-capping protein subunit alpha-1		
Ccdc6	$RhoA^{GTP}$	2	2	7,2	1.40E-07	D3YZP9	Coiled-coil domain-containing protein 6		
Cit	$RhoA^{GTP}$	86	86	39,9	0	E9QL53	Citron Rho-interacting kinase	x	x
Cyfip2	$RhoA^{GTP}$	51	32	45,9	0	Q5SQX6	Cytoplasmic FMR1-interacting protein 2		
Fam65a	$RhoA^{GTP}$	19	18	24,9	1.27E-292	G5E8A2	Protein FAM65A		
Fh	$RhoA^{GTP}$	21	21	59,6	0	P97807	Fumarate hydratase, mitochondrial		
Grlf1;Arhgap35	$RhoA^{GTP}$	9	9	8,9	2.08E-90	B2RTN5	Rho GTPase-activating protein 35		x
Homer3	$RhoA^{GTP}$	26	25	79,7	1.53E-291	Q99JP6-2	Homer protein homolog 3		
Inppl1	$RhoA^{GTP}$	17	17	22,8	2.52E-211	Q6P549	Phosphatidylinositol 3,4,5-trisphosphate 5-phosphatase 2		
Iqsec2	$RhoA^{GTP}$	6	5	4,6	2.51E-56	E9QAD8	IQ motif and SEC7 domain-containing protein 2		
Iqsec3	$RhoA^{GTP}$	7	7	9,2	2.95E-149	Q3TES0	IQ motif and SEC7 domain-containing protein 3		
Kif2a	$RhoA^{GTP}$	8	8	16,3	2.76E-20	E0CZ72	Kinesin-like protein KIF2A		
Nefh	$RhoA^{GTP}$	11	8	12,8	3.45E-80	P19246	Neurofilament heavy polypeptide		
Pkn1	$RhoA^{GTP}$	18	18	23,7	1.90E-299	P70268-2	Serine/threonine-protein kinase N1	x	x
Plekhg5	$RhoA^{GTP}$	8	8	10,5	1.41E-66	Q66T02	Pleckstrin homology domain-containing family G member 5		x
Rock2	$RhoA^{GTP}$	78	71	55,5	0	F8VPK5	Rho-associated protein kinase 2	x	x
Rtkn	$RhoA^{GTP}$	12	12	35,6	0	Q8C6B2-2	Rhotekin	x	x
Slk	$RhoA^{GTP}$	10	10	11,8	3.75E-86	O54988	STE20-like serine/threonine-protein kinase		
St13	$RhoA^{GTP}$	7	7	20,5	1.04E-64	Q99L47	Hsc70-interacting protein		
Sult4a1	$RhoA^{GTP}$	5	5	21,1	1.05E-48	P63046	Sulfotransferase 4A1		
Wasf1	$RhoA^{GTP}$	24	24	50,6	0	Q8R5H6	Wiskott-Aldrich syndrome protein family member 1		
Wasf3	$RhoA^{GTP}$	15	15	40,5	0	Q8VHI6	Wiskott-Aldrich syndrome protein family member 3		
Arhgdia	$RhoB^{GDP}$	14	14	60,8	0	Q99PT1	Rho GDP-dissociation inhibitor 1	x	x
Arhgef1	$RhoB^{GDP}$	25	25	30	0	Q80U35-	Rho guanine nucleotide exchange		

Gene names	GTPase	Peptides	Unique peptides	Sequence coverage [%]	PEP	Major Protein ID	Protein names	HIPPIE	Lite-rature
7						2	factor 17		
Cdc42	$RhoB^{GDP}$	3	2	20,4	8.87E-37	P60766	Cell division control protein 42 homolog		
Ctnnd1	$RhoB^{GDP}$	6	6	6,8	3.95E-13	E9Q8Z8	Catenin delta-1		
Diras2	$RhoB^{GDP}$	9	9	45,2	1.17E-50	Q3UWU7	GTP-binding protein Di-Ras2		
Eef1a2	$RhoB^{GDP}$	46	25	71,5	0	P62631	Elongation factor 1-alpha 2;Elongation factor 1-alpha		
Fahd1	$RhoB^{GDP}$	3	3	20,7	2.05E-13	Q3UQY4	Acylpyruvase FAHD1, mitochondrial		
Gpn1	$RhoB^{GDP}$	5	5	18	1.10E-36	Q4VAB2	GPN-loop GTPase 1		
Gtpbp10	$RhoB^{GDP}$	6	6	22,4	4.44E-27	Q8K013	GTP-binding protein 10		
Lgalsla	$RhoB^{GDP}$	4	3	20,9	1.55E-14	Q8VED9	Galectin-related protein A		
Nudt16	$RhoB^{GDP}$	13	13	55,9	5.13E-199	Q6P3D0	U8 snoRNA-decapping enzyme		
Pde6d	$RhoB^{GDP}$	4	4	24,7	4.46E-11	O55057	Retinal rod rhodopsin-sensitive cGMP 3,5-cyclic phosphodiesterase subunit delta	x	x
Ran	$RhoB^{GDP}$	18	9	50	8.16E-280	P62827	GTP-binding nuclear protein Ran		
Srp54;Srp54c	$RhoB^{GDP}$	13	2	36,7	8.55E-41	P14576	Signal recognition particle 54 kDa protein		
Acat1	$RhoB^{GTP}$	24	24	64,9	0	Q8QZT1	Acetyl-CoA acetyltransferase, mitochondrial		
Akap13	$RhoB^{GTP}$	12	12	7,1	6.95E-44	E9Q474			x
Arhgap5	$RhoB^{GTP}$	23	23	19,6	1.10E-104	E9PYT0	Rho GTPase-activating protein 5		
Arhgef1	$RhoB^{GTP}$	49	49	52,9	0	E9PUF7	Rho guanine nucleotide exchange factor 1	x	x
Arhgef11	$RhoB^{GTP}$	80	6	56,6	0	Q68FM7			
Arhgef18	$RhoB^{GTP}$	24	23	29,4	5.22E-134	Q6P9R4	Rho guanine nucleotide exchange factor 18		
Arhgef2	$RhoB^{GTP}$	78	78	68,3	0	Q60875	Rho guanine nucleotide exchange factor 2		
C1orf198	$RhoB^{GTP}$	19	19	69,6	4.40E-187	Q8C3W1	Uncharacterized protein C1orf198 homolog		
Cit	$RhoB^{GTP}$	56	1	28,9	6.00E-276	E9QPY8	Citron Rho-interacting kinase	x	x
Daam1	$RhoB^{GTP}$	42	40	41,3	0	Q8BPM0	Disheveled-associated activator of morphogenesis 1	x	x
Daam2	$RhoB^{GTP}$	40	38	42,1	1.69E-201	Q80U19	Disheveled-associated activator of morphogenesis 2		
Ech1	$RhoB^{GTP}$	5	5	23,9	7.18E-14	O35459	Delta(3,5)-Delta(2,4)-dienoyl-CoA isomerase, mitochondrial		
Exoc3	$RhoB^{GTP}$	12	12	20,1	2.56E-40	Q6KAR6	Exocyst complex component 3		
Fam65a	$RhoB^{GTP}$	33	32	35,2	0	G5E8A2	Protein FAM65A		
Fam65b	$RhoB^{GTP}$	17	4	20,2	1.49E-70	Q80U16	Protein FAM65B		
Gdap1	$RhoB^{GTP}$	9	8	26	8.26E-34	O88741	Ganglioside-induced differentiation-associated protein 1		
Gnao1	$RhoB^{GTP}$	25	3	60,2	0	P18872	Guanine nucleotide-binding protein G(o) subunit alpha		
Gsn	$RhoB^{GTP}$	6	6	10,3	3.55E-48	A2AL35	Gelsolin		

Gene names	GTPase	Peptides	Unique peptides	Sequence coverage [%]	PEP	Major Protein ID	Protein names	HIPPIE	Lite-rature
Igtp	$RhoB^{GTP}$	6	6	20,8	3.48E-27	Q9DCE9			
Inppl1	$RhoB^{GTP}$	16	16	19,3	1.51E-55	Q6P549	Phosphatidylinositol 3,4,5-trisphosphate 5-phosphatase 2		
Lrpap1	$RhoB^{GTP}$	7	7	24,9	8.79E-20	F6SY09	Alpha-2-macroglobulin receptor-associated protein		
Lrrc47	$RhoB^{GTP}$	7	7	16,1	1.94E-52	E9PV22	Leucine-rich repeat-containing protein 47		
Mpdz	$RhoB^{GTP}$	13	13	8,9	1.65E-33	F8WGE8	Multiple PDZ domain protein		
Nceh1	$RhoB^{GTP}$	13	13	44,4	7.18E-146	Q8BLF1	Neutral cholesterol ester hydrolase 1		
Pi4ka	$RhoB^{GTP}$	22	22	16,2	4.64E-104	E9Q3L2			
Pkn1	$RhoB^{GTP}$	13	13	17,5	1.13E-110	P70268-2	Serine/threonine-protein kinase N1		x
Plcxd3	$RhoB^{GTP}$	8	8	40,5	3.10E-43	G3X9A7	PI-PLC X domain-containing protein 3		
Plekhg5	$RhoB^{GTP}$	30	30	29,6	2.14E-200	Q66T02	Pleckstrin homology domain-containing family G member 5		
Prrt3	$RhoB^{GTP}$	3	3	4,5	3.53E-23	Q6PE13	Proline-rich transmembrane protein 3		
Psd3	$RhoB^{GTP}$	5	5	16,2	6.19E-29	Q8C0E9	PH and SEC7 domain-containing protein 3		
Psme2	$RhoB^{GTP}$	5	4	27,2	5.84E-17	P97372	Proteasome activator complex subunit 2		
Rhpn2	$RhoB^{GTP}$	12	12	18,8	4.73E-24	Q8BWR8	Rhophilin-2	x	x
Rock1	$RhoB^{GTP}$	13	7	11,4	6.41E-34	P70335	Rho-associated protein kinase 1		x
Rock2	$RhoB^{GTP}$	65	59	43,8	0	E9PYM9	Rho-associated protein kinase 2		x
Rtkn	$RhoB^{GTP}$	4	4	12,4	8.62E-19	Q8C6B2	Rhotekin		x
Scamp3	$RhoB^{GTP}$	4	4	19,1	2.89E-113	Q3UXS0	Secretory carrier-associated membrane protein 3		
Stx16	$RhoB^{GTP}$	3	3	17,5	3.14E-90	E9QM25	Syntaxin-16		
Tsnax	$RhoB^{GTP}$	9	9	35,9	6.34E-100	Q9QZE7	Translin-associated protein X		
Arhgef17	$RhoC^{GDP}$	25	25	30	0	Q80U35-2	Rho guanine nucleotide exchange factor 17		
Arl2	$RhoC^{GDP}$	10	10	50,5	5.63E-128	Q9D0J4	ADP-ribosylation factor-like protein 2		
Eef1a2	$RhoC^{GDP}$	46	25	71,5	0	P62631	Elongation factor 1-alpha 2;Elongation factor 1-alpha		
Nudt16	$RhoC^{GDP}$	13	13	55,9	5.13E-199	Q6P3D0	U8 snoRNA-decapping enzyme		
Ran	$RhoC^{GDP}$	18	9	50	8.16E-280	P62827	GTP-binding nuclear protein Ran		
Rap1gds1	$RhoC^{GDP}$	27	27	59	0	E9Q912			
Acat1	$RhoC^{GTP}$	24	24	64,9	0	Q8QZT1	Acetyl-CoA acetyltransferase, mitochondrial		
Arhgap32	$RhoC^{GTP}$	31	31	21,4	1.83E-293	Q811P8	Rho GTPase-activating protein 32		
Arhgap5	$RhoC^{GTP}$	23	23	19,6	1.10E-104	E9PYT0	Rho GTPase-activating protein 5		
Arhgef11	$RhoC^{GTP}$	80	6	56,6	0	Q68FM7			

Gene names	GTPase	Peptides	Unique peptides	Sequence coverage [%]	PEP	Major Protein ID	Protein names	HIPPIE	Lite-rature
Arhgef2	$RhoC^{GTP}$	78	78	68,3	0	Q60875	Rho guanine nucleotide exchange factor 2		
C1orf198	$RhoC^{GTP}$	19	19	69,6	4.40E-187	Q8C3W1	Uncharacterized protein C1orf198 homolog		
Cadm3	$RhoC^{GTP}$	7	7	30,8	4.18E-203	Q99N28	Cell adhesion molecule 3		
Cit	$RhoC^{GTP}$	56	1	28,9	6.00E-276	E9QPY8	Citron Rho-interacting kinase	x	x
Daam1	$RhoC^{GTP}$	42	40	41,3	0	Q8BPM0	Disheveled-associated activator of morphogenesis 1	x	x
Daam2	$RhoC^{GTP}$	40	38	42,1	1.69E-201	Q80U19	Disheveled-associated activator of morphogenesis 2		
Fam65a	$RhoC^{GTP}$	33	32	35,2	0	G5E8A2	Protein FAM65A		
Gpm6b	$RhoC^{GTP}$	8	8	19,2	5.65E-114	A2AEG6	Neuronal membrane glycoprotein M6-b		
Gucy1a2	$RhoC^{GTP}$	11	11	26	7.47E-135	F8VQK3			
Inppl1	$RhoC^{GTP}$	16	16	19,3	1.51E-55	Q6P549	Phosphatidylinositol 3,4,5-trisphosphate 5-phosphatase 2		
Ndufs2	$RhoC^{GTP}$	5	5	12,1	9.01E-23	Q91WD5	NADH dehydrogenase [ubiquinone] iron-sulfur protein 2, mitochondrial		
Pnpo	$RhoC^{GTP}$	6	6	37,2	7.00E-27	Q91XF0	Pyridoxine-5-phosphate oxidase		
Ppp2r5c	$RhoC^{GTP}$	8	5	20,4	1.05E-33	Q60996	Serine/threonine-protein phosphatase 2A 56 kDa regulatory subunit gamma isoform		
Rap1b;Rap1a	$RhoC^{GTP}$	6	6	42,4	2.74E-53	Q52L50	Ras-related protein Rap-1b;Ras-related protein Rap-1A		
Rock2	$RhoC^{GTP}$	65	59	43,8	0	E9PYM9	Rho-associated protein kinase 2		x
Snx27	$RhoC^{GTP}$	11	8	29,1	1.62E-39	Q3UHD6	Sorting nexin-27		
Tsn	$RhoC^{GTP}$	6	6	46,1	3.88E-79	Q545E6	Translin		
2700060E02Rik	$RhoD^{GDP}$	8	8	47,1	7.68E-43	Q4VA29	UPF0568 protein C14orf166 homolog		
Atp6v1f	$RhoD^{GDP}$	4	4	32,8	1.89E-12	Q9D1K2	V-type proton ATPase subunit F		
Baiap2	$RhoD^{GDP}$	8	8	17	4.12E-18	B1AZ47	Brain-specific angiogenesis inhibitor 1-associated protein 2		
Eef1a2	$RhoD^{GDP}$	46	25	71,5	0	P62631	Elongation factor 1-alpha 2;Elongation factor 1-alpha		
Fkbp2	$RhoD^{GDP}$	3	3	24,3	2.40E-09	P45878	Peptidyl-prolyl cis-trans isomerase FKBP2;Peptidyl-prolyl cis-trans isomerase		
Gabbr1	$RhoD^{GDP}$	6	6	9,1	2.57E-66	Q9WV18	Gamma-aminobutyric acid type B receptor subunit 1		
Map4;Mtap4	$RhoD^{GDP}$	17	7	22,3	1.39E-98	P27546	Microtubule-associated protein 4;Microtubule-associated protein		
Mpi	$RhoD^{GDP}$	7	7	27,7	3.43E-94	Q3V100	Mannose-6-phosphate isomerase		
Nudt16	$RhoD^{GDP}$	13	13	55,9	5.13E-199	Q6P3D0	U8 snoRNA-decapping enzyme		
Ran	$RhoD^{GDP}$	18	9	50	8.16E-280	P62827	GTP-binding nuclear protein Ran		
Rpl22	$RhoD^{GDP}$	5	3	27,3	1.29E-16	P67984	60S ribosomal protein L22		
Ufc1	$RhoD^{GDP}$	4	4	34,1	4.32E-32	Q9CR09	Ubiquitin-fold modifier-conjugating enzyme 1		
Arhgap3	$RhoD^{GTP}$	31	31	21,4	1.83E-293	Q811P8	Rho GTPase-activating protein 32		

Gene names	GTPase	Peptides	Unique peptides	Sequence coverage [%]	PEP	Major Protein ID	Protein names	HIPPIE	Lite-rature
2									
Arhgef2	RhoD-^{GTP}	78	78	68,3	0	Q60875	Rho guanine nucleotide exchange factor 2		
C1orf198	RhoD-^{GTP}	19	19	69,6	4.40E-187	Q8C3W1	Uncharacterized protein C1orf198 homolog		
Daam2	RhoD-^{GTP}	40	38	42,1	1.69E-201	Q80U19	Disheveled-associated activator of morphogenesis 2		
Diap1;Diaph1	RhoD-^{GTP}	12	12	13,3	4.42E-36	E9PV41	Protein diaphanous homolog 1	x	x
Hexdc	RhoD-^{GTP}	8	8	24,9	4.60E-33	Q3U4H6-2	Hexosaminidase D		
Mettl21d	RhoD-^{GTP}	7	7	30,3	1.43E-172	Q8C436	Methyltransferase-like protein 21D		
Mtap4	RhoD-^{GTP}	5	3	72	1.32E-98	F6XPV7	Microtubule-associated protein		
Pkn1	RhoD-^{GTP}	13	13	17,5	1.13E-110	P70268-2	Serine/threonine-protein kinase N1		
Plekhg5	RhoD-^{GTP}	30	30	29,6	2.14E-200	Q66T02	Pleckstrin homology domain-containing family G member 5		
Plxnb2	RhoD-^{GTP}	14	14	10,8	5.08E-96	B2RXS4	Plexin-B2		
Rbfox1	RhoD-^{GTP}	12	2	29,7	5.60E-207	Q9JJ43-3	RNA binding protein fox-1 homolog 1		

Abbreviations/Units

A	Ampere
ABC	Ammonium bicarbonate
Amp	Ampicillin
BAR domain	Bin-Amphyphysin-Rvs domain
cf.	Confer
C-terminus	Carboxyl-terminus
CID	collision induced dissociation
CV	Column volume
dFCS	Dialyzed fetal calf serum
DMEM	Dulbecco's Modified Eagle Medium
DNA	Deoxyribonucleic acid
DTT	Dithiothreitol
EDTA	Ethylenediaminetetraacetic acid
EGTA	Ehtylene glycol tetraacetic acid
ESI	Electrospray ionization
FDR	False discovery rate
G domain	Guanine nucleotide binding domain
G protein	Guanine nucleotide binding protein
GAP	GTPase-activating protein
GDI	Guanine nucleotide dissociation inhibitor
GDP	Guanosine- 5 '-diphosphate
GEF	Guanine nucleotide exchange factor
GO	Gene ontology
GSH	Reduced glutathione
GTP	Guanosine- 5 '-triphosphate
GTP-γ-S	Guanosine- 5 '-O-[γ-thio]triphosphate
GST	Glutathione S-transferase
hrs	Hours
HCD	Higher-energy collisional dissociation
HEPES	4 -(2 -hydroxyethyl)- 1 -piperazineethanesulfonic acid
HPLC	High pressure liquid chromatography
Ig	Immunoglobulin
IP	Immunoprecipitation
IPTG	Isopropyl-β-D-thiogalactopyranosid
Kan	Kanamycin
kDa	Kilo-Dalton
LB medium	Lysogeny broth medium
LC-MS/MS	Liquid chromatography-tandem mass spectrometry
LTQ	Linear trap quadrupole
LysC	Lyslendopeptidase
MDC	Max-Delbrück-Centrum für Molekulare Medizin Berlin-Buch
MES	2-N-morpholinoethanesulfonic acid
µl	microliter
min	Minutes
MOPS	4-morpholinepropanesulfonic acid
m/z	Mass-to-charge ratio
mRNA	Messenger ribonucleic acid
MS	Mass spectrometry
nanoLC	Nanoflow liquid chromatography
N-terminus	Amino-terminus

NF-κB	Nuclear factor κB
OD_{600}	Optical density at 600 nanometer
Orbitrap	Orbital ion trap mass analyzer
PBS	Phosphate buffered saline
P-loop	Phosphate-binding loop
PCR	Polymerase chain reaction
PLA	Proximity ligation assay
PPI	Protein-protein interaction
ppm	Parts per million
PTM	Post-translational modification
q-AP-MS	Quantitative affinity purification followed by mass spectrometry
rpm	Revolutions per minute
RT	Room temperature
SDS	PAGE Sodiumdodecylsulfate polyacrylamide gel electrophoresis
SDS-PAGE	Sodium dodecyl sulfate-polyacrylamide gel electrophoresis
SEC	Size-exclusion chromatography
SILAC	Stable isotope labeling by amino acids in cell culture
STAGE tips	Stop-and-go extraction tips
TB	Terrific broth
TFA	Trifluoroacetic acid
Tris	Tris(hydroxymethyl)aminomethane
V	Volt
XIC	Extracted ion chromatogram

List of figures

List of tables

Bibliography

1. Etienne-Manneville, S. & Hall, A. Rho GTPases in cell biology. *Nature* **420,** 629–35 (2002).

2. Jaffe, A. B. & Hall, A. Rho GTPases: biochemistry and biology. *Annu. Rev. Cell Dev. Biol.* **21,** 247–269 (2005).

3. Ridley, A. J. Life at the leading edge. *Cell* **145,** 1012–1022 (2011).

4. Rossman, K. L., Der, C. J. & Sondek, J. GEF means go: turning on RHO GTPases with guanine nucleotide-exchange factors. *Nat. Rev. Mol. Cell Biol.* **6,** 167–80 (2005).

5. Bernards, A. & Settleman, J. GAP control: regulating the regulators of small GTPases. *Trends Cell Biol.* **14,** 377–385 (2004).

6. Garcia-Mata, R., Boulter, E. & Burridge, K. The "invisible hand": regulation of RHO GTPases by RHOGDIs. *Nat. Rev. Mol. Cell Biol.* **12,** 493–504 (2011).

7. Wennerberg, K., Rossman, K. L. & Der, C. J. The Ras superfamily at a glance. *J. Cell Sci.* **118,** 843–846 (2005).

8. Zerial, M. & McBride, H. Rab proteins as membrane organizers. *Nat. Rev. Mol. Cell Biol.* **2,** 107–117 (2001).

9. Colicelli, J. Human RAS superfamily proteins and related GTPases. *Sci. STKE signal Transduct. Knowl. Environ.* **2004,** RE13 (2004).

10. Espinosa, E. J., Calero, M., Sridevi, K. & Pfeffer, S. R. RhoBTB3: a Rho GTPase-family ATPase required for endosome to Golgi transport. *Cell* **137,** 938–48 (2009).

11. Bourne, H. R., Sanders, D. A. & McCormick, F. The GTPase superfamily: conserved structure and molecular mechanism. *Nature* **349,** 117–127 (1991).

12. Madaule, P. & Axel, R. A novel ras-related gene family. *Cell* **41,** 31–40 (1985).

13. Ridley, A. J. & Hall, A. The small GTP-binding protein Rho regulates the assembly of focal adhesions and actin stress fibers in response to growth-factors. *Cell* **70,** 389–399 (1992).

14. Ridley, A. J., Paterson, H. F., Johnston, C. L., Diekmann, D. & Hall, A. The small GTP-binding protein Rac regulates growthfactor induced membrane-ruffling. *Cell* **70,** 401–410 (1992).

15. Nobes, C. D. & Hall, A. Rho, rac, and cdc42 GTPases regulate the assembly of multimolecular focal complexes associated with actin stress fibers, lamellipodia, and filopodia. *Cell* **81,** 53–62 (1995).

16. Kozma, R., Ahmed, S., Best, A. & Lim, L. The Ras-related protein Cdc42Hs and bradykinin promote formation of peripheral actin microspikes and filopodia in Swiss 3T3 fibroblasts. *Mol. Cell. Biol.* **15,** 1942–1952 (1995).

17. Shinjo, K. *et al.* Molecular cloning of the gene for the human placental GTP-binding protein Gp (G25K): identification of this GTP-binding protein as the human homolog of the yeast cell-division-cycle protein CDC42. *Proc. Natl. Acad. Sci. U. S. A.* **87,** 9853–9857 (1987).

18. Heasman, S. J. & Ridley, A. J. Mammalian Rho GTPases: new insights into their functions from in vivo studies. *Nat. Rev. Mol. Cell Biol.* **9,** 690–701 (2008).

19. Ridley, A. J. Rho family proteins: coordinating cell responses. *Trends Cell Biol.* **11,** 471–477 (2001).

20. Liu, A.-X., Rane, N., Liu, J.-P. & Prendergast, G. C. RhoB Is Dispensable for Mouse Development, but It Modifies Susceptibility to Tumor Formation as Well as Cell Adhesion and Growth Factor Signaling in Transformed Cells. *Mol. Cell. Biol.* **21,** 6906–6912 (2001).

21. Hakem, A. *et al.* RhoC is dispensable for embryogenesis and tumor initiation but essential for metastasis. *Genes Dev.* **19,** 1974–1979 (2005).

22. Zalcman, G. *et al.* RhoGDI-3 is a new GDP dissociation inhibitor (GDI). Identification of a non-cytosolic GDI protein interacting with the small GTP-binding proteins RhoB and RhoG. *J. Biol. Chem.* **271,** 30366–30374 (1996).

23. Wheeler, A. P. & Ridley, A. J. Why three Rho proteins? RhoA, RhoB, RhoC, and cell motility. *Exp. Cell Res.* **301,** 43–49 (2004).

24. Eden, S., Rohatgi, R., Podtelejnikov, A. V, Mann, M. & Kirschner, M. W. Mechanism of regulation of WAVE1-induced actin nucleation by Rac1 and Nck. *Nature* **418,** 790–793 (2002).

25. Fiegen, D. *et al.* Alternative splicing of Rac1 generates Rac1b, a self-activating GTPase. *J. Biol. Chem.* **279,** 4743–4749 (2004).

26. Dorseuil, O., Reibel, L., Bokoch, G. M., Camonis, J. & Gacon, G. The Rac target NADPH oxidase p67phox interacts preferentially with Rac2 rather than Rac1. *J. Biol. Chem.* **271,** 83–88 (1996).

27. Werner, E. GTPases and reactive oxygen species: switches for killing and signaling. *J. Cell Sci.* **117,** 143–53 (2004).

28. Mira, J.-P., Benard, V., Groffen, J., Sanders, L. C. & Knaus, U. G. Endogenous, hyperactive Rac3 controls proliferation of breast cancer cells by a p21-activated kinase-dependent pathway. *Proc. Natl. Acad. Sci. U. S. A.* **97,** 185–189 (2000).

29. Katoh, H. *et al.* Small GTPase RhoG is a key regulator for neurite outgrowth in PC12 cells. *Mol. Cell. Biol.* **20,** 7378–7387 (2000).

30. Machesky, L. M. & Insall, R. H. Scar1 and the related Wiskott-Aldrich syndrome protein, WASP, regulate the actin cytoskeleton through the Arp2/3 complex. *Curr. Biol.* **8,** 1347–56 (1998).

31. Michaelson, D. *et al.* Differential localization of Rho GTPases in live cells: regulation by hypervariable regions and RhoGDI binding. *J. Cell Biol.* **152,** 111–26 (2001).

32. Tanabe, K. *et al.* The small GTP-binding protein TC10 promotes nerve elongation in neuronal cells, and its expression is induced during nerve regeneration in rats. *J. Neurosci.* **20,** 4138–4144 (2000).

33. Murphy, C. *et al.* Endosome dynamics regulated by a Rho protein. *Nature* **384,** 427–432 (1996).

34. Murphy, C. *et al.* Dual function of rhoD in vesicular movement and cell motility. *Eur. J. Cell Biol.* **80,** 391–398 (2001).

35. Ellis, S. & Mellor, H. The novel Rho-family GTPase rif regulates coordinated actin-based membrane rearrangements. *Curr. Biol.* **10,** 1387–1390 (2000).

36. Aspenström, P., Ruusala, A. & Pacholsky, D. Taking Rho GTPases to the next level: the cellular functions of atypical Rho GTPases. *Exp. Cell Res.* **313,** 3673–3679 (2007).

37. Aspenström, P., Fransson, A. & Saras, J. Rho GTPases have diverse effects on the organization of the actin filament system. *Biochem. J.* **377,** 327–337 (2004).

38. Foster, R. *et al.* Identification of a novel human Rho protein with unusual properties: GTPase deficiency and in vivo farnesylation. *Mol. Cell. Biol.* **16,** 2689–2699 (1996).

39. Nobes, C. D. *et al.* A new member of the Rho family, Rnd1, promotes disassembly of actin filament structures and loss of cell adhesion. *J. Cell Biol.* **141,** 187–197 (1998).

40. Li, X. *et al.* The Hematopoiesis-Specific GTP-Binding Protein RhoH Is GTPase Deficient and Modulates Activities of Other Rho GTPases by an Inhibitory Function. *Mol. Cell. Biol.* **22,** 1158–1171 (2002).

41. Shutes, A., Berzat, A. C., Cox, A. D. & Der, C. J. Atypical mechanism of regulation of the Wrch-1 Rho family small GTPase. *Curr. Biol.* **14,** 2052–2056 (2004).

42. Tao, W., Pennica, D., Xu, L., Kalejta, R. F. & Levine, A. J. Wrch-1, a novel member of the Rho gene family that is regulated by Wnt-1. *Genes Dev.* **15,** 1796–1807 (2001).

43. Ramos, S., Khademi, F., Somesh, B. P. & Rivero, F. Genomic organization and expression profile of the small GTPases of the RhoBTB family in human and mouse. *Gene* **298,** 147–157 (2002).

44. Hamaguchi, M. *et al.* DBC2, a candidate for a tumor suppressor gene involved in breast cancer. *Proc. Natl. Acad. Sci. U. S. A.* **99,** 13647–13652 (2002).

45. Venter, J. C. *et al.* The sequence of the human genome. *Science (80-.).* **291,** 1304–1351 (2001).

46. Peck, J., Douglas, G., Wu, C. H. & Burbelo, P. D. Human RhoGAP domain-containing proteins: structure, function and evolutionary relationships. *FEBS Lett.* **528,** 27–34 (2002).

47. Pan, J. Y. & Wessling-Resnick, M. GEF-mediated GDP/GTP exchange by monomeric GTPases: a regulatory role for Mg2+? *BioEssays news Rev. Mol. Cell. Dev. Biol.* **20,** 516–521 (1998).

48. Meller, N., Merlot, S. & Guda, C. CZH proteins: a new family of Rho-GEFs. *J. Cell Sci.* **118,** 4937–4946 (2005).

49. Eva, A., Vecchio, G., Rao, C. D., Tronick, S. R. & Aaronson, S. A. The predicted DBL oncogene product defines a distinct class of transforming proteins. *Proc. Natl. Acad. Sci. U. S. A.* **85,** 2061–2065 (1988).

50. Hart, M. J., Eva, A., Evans, T., Aaronson, S. A. & Cerione, R. A. Catalysis of guanine nucleotide exchange on the CDC42Hs protein by the dbl oncogene product. *Nature* **354,** 311–314 (1991).

51. Worthylake, D. K., Rossman, K. L. & Sondek, J. Crystal structure of the DH/PH fragment of Dbs without bound GTPase. *Struct. London Engl. 1993* **12,** 1078–1086 (2004).

52. Liu, X. *et al.* NMR structure and mutagenesis of the N-terminal Dbl homology domain of the nucleotide exchange factor Trio. *Cell* **95,** 269–277 (1998).

53. Vanni, C. *et al.* Phosphorylation-independent membrane relocalization of ezrin following association with Dbl in vivo. *Oncogene* **23,** 4098–4106 (2004).

54. Bellanger, J. M. *et al.* The Rac1- and RhoG-specific GEF domain of Trio targets filamin to remodel cytoskeletal actin. *Nat. Cell Biol.* **2,** 888–892 (2000).

55. Côté, J.-F. & Vuori, K. Identification of an evolutionarily conserved superfamily of DOCK180-related proteins with guanine nucleotide exchange activity. *J. Cell Sci.* **115,** 4901–4913 (2002).

56. Brugnera, E. *et al.* Unconventional Rac-GEF activity is mediated through the Dock180-ELMO complex. *Nat. Cell Biol.* **4,** 574–82 (2002).

57. Meller, N., Irani-Tehrani, M., Kiosses, W. B., Del Pozo, M. A. & Schwartz, M. A. Zizimin1, a novel Cdc42 activator, reveals a new GEF domain for Rho proteins. *Nat. Cell Biol.* **4,** 639–47 (2002).

58. Cheresh, D. A., Leng, J. & Klemke, R. L. Regulation of Cell Contraction and Membrane Ruffling by Distinct Signals in Migratory Cells. *J. Cell Biol.* **146,** 1107–1116 (1999).

59. Kiyokawa, E. *et al.* Activation of Rac1 by a Crk SH3-binding protein, DOCK180. *Genes Dev.* **12,** 3331–6 (1998).

60. Crespo, P., Schuebel, K. E., Ostrom, A. A., Gutkind, J. S. & Bustelo, X. R. Phosphotyrosine-dependent activation of Rac-1 GDP/GTP exchange by the vav proto-oncogene product. *Nature* **385,** 169–172 (1997).

61. Han, J. *et al.* Lck regulates Vav activation of members of the Rho family of GTPases. *Mol. Cell. Biol.* **17,** 1346–1353 (1997).

62. Aghazadeh, B., Lowry, W. E., Huang, X. Y. & Rosen, M. K. Structural basis for relief of autoinhibition of the Dbl homology domain of proto-oncogene Vav by tyrosine phosphorylation. *Cell* **102,** 625–633 (2000).

63. Tatsumoto, T., Xie, X., Blumenthal, R., Okamoto, I. & Miki, T. Human Ect2 Is an Exchange Factor for Rho Gtpases, Phosphorylated in G2/M Phases, and Involved in Cytokinesis. *J. Cell Biol.* **147,** 921–928 (1999).

64. Li, Z. *et al.* Directional sensing requires G beta gamma-mediated PAK1 and PIX alpha-dependent activation of Cdc42. *Cell* **114,** 215–227 (2003).

65. Obermeier, A. *et al.* PAK promotes morphological changes by acting upstream of Rac. *Eur. Mol. Biol. Organ. J.* **17,** 4328–4339 (1998).

66. Zhao, Z., Manser, E., Loo, T.-H. & Lim, L. Coupling of PAK-Interacting Exchange Factor PIX to GIT1 Promotes Focal Complex Disassembly. *Mol. Cell. Biol.* **20,** 6354–6363 (2000).

67. Buchsbaum, R. J., Connolly, B. A. & Feig, L. A. Interaction of Rac exchange factors Tiam1 and Ras-GRF1 with a scaffold for the p38 mitogen-activated protein kinase cascade. *Mol. Cell. Biol.* **22,** 4073–4085 (2002).

68. Cheng, L., Mahon, G. M., Kostenko, E. V & Whitehead, I. P. Pleckstrin homology domain-mediated activation of the rho-specific guanine nucleotide exchange factor Dbs by Rac1. *J. Biol. Chem.* **279,** 12786–93 ST – Pleckstrin homology domain–mediated (2004).

69. Lamarche, N. & Hall, A. GAPs for rho-related GTPases. *Trends Genet.* **10,** 436–440 (1994).

70. Boguski, M. S. & McCormick, F. Proteins regulating Ras and its relatives. *Nature* **366,** 643–654 (1993).

71. Rittinger, K., Walker, P. A., Eccleston, J. F., Smerdon, S. J. & Gamblin, S. J. Structure at 1.65 A of RhoA and its GTPase-activating protein in complex with a transition-state analogue. *Nature* **389,** 758–62 (1997).

72. Rittinger, K. *et al.* Crystal structure of a small G protein in complex with the GTPase-activating protein rhoGAP. *Nature* **388,** 693–697 (1997).

73. Nassar, N., Hoffman, G. R., Manor, D., Clardy, J. C. & Cerione, R. A. Structures of Cdc42 bound to the active and catalytically compromised forms of Cdc42GAP. *Nat. Struct. Biol.* **5,** 1047–1052 (1998).

74. Zheng, Y. *et al.* Biochemical comparisons of the Saccharomyces cerevisiae Bem2 and Bem3 proteins. Delineation of a limit Cdc42 GTPase-activating protein domain. *J. Biol. Chem.* **268,** 24629–24634 (1993).

75. Nakamura, T. *et al.* Grit, a GTPase-activating protein for the Rho family, regulates neurite extension through association with the TrkA receptor and N-Shc and CrkL/Crk adapter molecules. *Mol. Cell. Biol.* **22,** 8721–8734 (2002).

76. Tcherkezian, J. & Lamarche-Vane, N. Current knowledge of the large RhoGAP family of proteins. *Biol. cell under auspices Eur. Cell Biol. Organ.* **99,** 67–86 (2007).

77. Kozma, R., Ahmed, S., Best, A. & Lim, L. The GTPase-activating protein n-chimaerin cooperates with Rac1 and Cdc42Hs to induce the formation of lamellipodia and filopodia. *Mol. Cell. Biol.* **16,** 5069–5080 (1996).

78. Roof, R. W. *et al.* Phosphotyrosine (p-Tyr)-Dependent and -Independent Mechanisms of p190 RhoGAP-p120 RasGAP Interaction: Tyr 1105 of p190, a Substrate for c-Src, Is the Sole p-Tyr Mediator of Complex Formation. *Mol. Cell. Biol.* **18,** 7052–7063 (1998).

79. Ban, R., Irino, Y., Fukami, K. & Tanaka, H. Human mitotic spindle-associated protein PRC1 inhibits MgcRacGAP activity toward Cdc42 during the metaphase. *J. Biol. Chem.* **279,** 16394–16402 (2004).

80. Takai, Y., Kikuchi, A., Kawata, M., Yamamoto, K. & Hoshijima, M. Purification, characterization, and possible functions of small molecular weight GTP-binding proteins. *Am. J. Hypertens.* **3,** 220S–223S (1990).

81. DerMardirossian, C. & Bokoch, G. M. GDIs: central regulatory molecules in Rho GTPase activation. *Trends Cell Biol.* **15,** 356–363 (2005).

82. Fukumoto, Y. *et al.* Molecular cloning and characterization of a novel type of regulatory protein (GDI) for the rho proteins, ras p21-like small GTP-binding proteins. *Oncogene* **5,** 1321–1328 (1990).

83. Platko, J. V *et al.* A single residue can modify target-binding affinity and activity of the functional domain of the Rho-subfamily GDP dissociation inhibitors. *Proc. Natl. Acad. Sci. U. S. A.* **92,** 2974–2978 (1995).

84. Brunet, N., Morin, A. & Olofsson, B. RhoGDI-3 regulates RhoG and targets this protein to the Golgi complex through its unique N-terminal domain. *Traffic Copenhagen Denmark* **3,** 342–357 (2002).

85. Ren, X. D., Kiosses, W. B. & Schwartz, M. A. Regulation of the small GTP-binding protein Rho by cell adhesion and the cytoskeleton. *Eur. Mol. Biol. Organ. J.* **18,** 578–585 (1999).

86. Boulter, E. *et al.* Regulation of Rho GTPase crosstalk, degradation and activity by RhoGDI1. *Nat. Cell Biol.* **12,** 477–483 (2010).

87. Chianale, F. *et al.* Diacylglycerol kinase α mediates HGF-induced Rac activation and membrane ruffling by regulating atypical PKC and RhoGDI. *Proc. Natl. Acad. Sci. U. S. A.* **107,** 4182–4187 (2010).

88. Lin, Q., Fuji, R. N., Yang, W. & Cerione, R. A. RhoGDI is required for Cdc42-mediated cellular transformation. *Curr. Biol.* **13,** 1469–1479 (2003).

89. Tiedje, C., Sakwa, I., Just, U. & Höfken, T. The Rho GDI Rdi1 Regulates Rho GTPases by Distinct Mechanisms. *Mol. Biol. Cell* **19,** 2885–2896 (2008).

90. Togawa, A. *et al.* Progressive impairment of kidneys and reproductive organs in mice lacking Rho GDIalpha. *Oncogene* **18,** 5373–5380 (1999).

91. Silvius, J. R. & l'Heureux, F. Fluorimetric evaluation of the affinities of isoprenylated peptides for lipid bilayers. *Biochemistry* **33,** 3014–3022 (1994).

92. Ghomashchi, F., Zhang, X., Liu, L. & Gelb, M. H. Binding of prenylated and polybasic peptides to membranes: affinities and intervesicle exchange. *Biochemistry* **34,** 11910–11918 (1995).

93. Winter-vann, A. M. & Casey, P. J. Opinion - Post-prenylation-processing enzymes as new targets in oncogenesis. *Nat. Rev. Cancer* **5,** 405–412 (2005).

94. Boyartchuk, V. L., Ashby, M. N. & Rine, J. Modulation of Ras and a-factor function by carboxyl-terminal proteolysis [see comments]. *Science (80-.).* **275,** 1796–1800 (1997).

95. Dai, Q. *et al.* Mammalian prenylcysteine carboxyl methyltransferase is in the endoplasmic reticulum. *J. Biol. Chem.* **273,** 15030–15034 (1998).

96. Rolli-Derkinderen, M. *et al.* Phosphorylation of serine 188 protects RhoA from ubiquitin/proteasome-mediated degradation in vascular smooth muscle cells. *Circ. Res.* **96,** 1152–1160 (2005).

97. Hall, A. Rho GTPases and the actin cytoskeleton. *Science (80-.).* **279,** 509–514 (1998).

98. Ridley, A. J. Rho GTPases and cell migration. *J. Cell Sci.* **114,** 2713–2722 (2001).

99. Pruyne, D. & Bretscher, A. Polarization of cell growth in yeast. I. Establishment and maintenance of polarity states. *J. Cell Sci.* **113 (Pt 3,** 365–375 (2000).

100. Kemphues, K. PARsing embryonic polarity. *Cell* **101,** 345–348 (2000).

101. Gotta, M., Abraham, M. C. & Ahringer, J. CDC-42 controls early cell polarity and spindle orientation in C. elegans. *Curr. Biol.* **11,** 482–488 (2001).

102. Kay, A. J. & Hunter, C. P. CDC-42 regulates PAR protein localization and function to control cellular and embryonic polarity in C. elegans. *Curr. Biol.* **11,** 474–481 (2001).

103. Joberty, G., Petersen, C., Gao, L. & Macara, I. G. The cell-polarity protein Par6 links Par3 and atypical protein kinase C to Cdc42. *Nat. Cell Biol.* **2,** 531–539 (2000).

104. Qiu, R. G., Abo, A. & Steven Martin, G. A human homolog of the C. elegans polarity determinant Par-6 links Rac and Cdc42 to PKCzeta signaling and cell transformation. *Curr. Biol.* **10,** 697–707 (2000).

105. Lin, D. *et al.* A mammalian PAR-3-PAR-6 complex implicated in Cdc42/Rac1 and aPKC signalling and cell polarity. *Nat. Cell Biol.* **2,** 540–547 (2000).

106. Jacinto, A., Martinez-Arias, A. & Martin, P. Mechanisms of epithelial fusion and repair. *Nat. Cell Biol.* **3,** E117–E123 (2001).

107. Raich, W. B., Agbunag, C. & Hardin, J. Rapid epithelial-sheet sealing in the Caenorhabditis elegans embryo requires cadherin-dependent filopodial priming. *Curr. Biol.* **9,** 1139–1146 (1999).

108. Vasioukhin, V., Bauer, C., Yin, M. & Fuchs, E. Directed actin polymerization is the driving force for epithelial cell-cell adhesion. *Cell* **100,** 209–19 (2000).

109. Kuroda, S., Fukata, M., Nakagawa, M. & Kaibuchi, K. Cdc42, Rac1, and their effector IQGAP1 as molecular switches for cadherin-mediated cell-cell adhesion. *Biochem. Biophys. Res. Commun.* **262,** 1–6 (1999).

110. Malliri, A., Van Es, S., Huveneers, S. & Collard, J. G. The Rac exchange factor Tiam1 is required for the establishment and maintenance of cadherin-based adhesions. *J. Biol. Chem.* **279,** 30092–30098 (2004).

111. Yamanaka, T. *et al.* PAR-6 regulates aPKC activity in a novel way and mediates cell-cell contact-induced formation of the epithelial junctional complex. *Genes to cells devoted to Mol. Cell. Mech.* **6,** 721–731 (2001).

112. Rojas, R., Ruiz, W. G., Leung, S.-M., Jou, T.-S. & Apodaca, G. Cdc42-dependent Modulation of Tight Junctions and Membrane Protein Traffic in Polarized Madin-Darby Canine Kidney Cells. *Mol. Biol. Cell* **12,** 2257–2274 (2001).

113. Gao, L., Joberty, G. & Macara, I. G. Assembly of epithelial tight junctions is negatively regulated by Par6. *Curr. Biol.* **12,** 221–225 (2002).

114. Ridley, A. J. *et al.* Cell migration: integrating signals from front to back. *Science (80-.).* **302,** 1704–1709 (2003).

115. Abercrombie, M., Heaysman, J. E. & Pegrum, S. M. The locomotion of fibroblasts in culture. IV. Electron microscopy of the leading lamella. *Exp. Cell Res.* **67,** 359–367 (1971).

116. Friedl, P. & Gilmour, D. Collective cell migration in morphogenesis, regeneration and cancer. *Nat. Rev. Mol. Cell Biol.* **10,** 445–457 (2009).

117. Mullins, R. D., Heuser, J. A. & Pollard, T. D. The interaction of Arp2/3 complex with actin: Nucleation, high affinity pointed end capping, and formation of branching networks of filaments. *Proc. Natl. Acad. Sci. U. S. A.* **95,** 6181–6186 (1998).

118. Campellone, K. G. & Welch, M. D. A nucleator arms race: cellular control of actin assembly. *Nat. Rev. Mol. Cell Biol.* **11,** 237–251 (2010).

119. Chandra Roy, B., Kakinuma, N. & Kiyama, R. Kank attenuates actin remodeling by preventing interaction between IRSp53 and Rac1. *J. Cell Biol.* **184,** 253–267 (2009).

120. Chesarone, M. A., DuPage, A. G. & Goode, B. L. Unleashing formins to remodel the actin and microtubule cytoskeletons. *Nat. Rev. Mol. Cell Biol.* **11,** 62–74 (2010).

121. Gupton, S. L. & Gertler, F. B. Filopodia: the fingers that do the walking. *Sci. STKE signal Transduct. Knowl. Environ.* **2007,** re5 (2007).

122. Machesky, L. M. & Li, A. Fascin: Invasive filopodia promoting metastasis. *Commun. Integr. Biol.* **3,** 263–270 (2010).

123. Johnston, S. A., Bramble, J. P., Yeung, C. L., Mendes, P. M. & Machesky, L. M. Arp2/3 complex activity in filopodia of spreading cells. *BMC Cell Biol.* **9,** 65 (2008).

124. Takenawa, T. & Suetsugu, S. The WASP-WAVE protein network: connecting the membrane to the cytoskeleton. *Nat. Rev. Mol. Cell Biol.* **8,** 37–48 (2007).

125. Mellor, H. The role of formins in filopodia formation. *Biochim. Biophys. Acta* **1803,** 191–200 (2010).

126. Ladoux, B. & Nicolas, A. Physically based principles of cell adhesion mechanosensitivity in tissues. *Rep. Prog. Phys.* **75,** 116601 (2012).

127. Sahai, E. & Marshall, C. J. RHO-GTPases and cancer. *Nat. Rev. Cancer* **2,** 133–142 (2002).

128. Albanese, C. *et al.* Transforming p21ras mutants and c-Ets-2 activate the cyclin D1 promoter through distinguishable regions. *J. Biol. Chem.* **270,** 23589–97 (1995).

129. King, A. J. *et al.* The protein kinase Pak3 positively regulates Raf-1 activity through phosphorylation of serine 338. *Nature* **396,** 180–3 (1998).

130. Frost, J. A. *et al.* Cross-cascade activation of ERKs and ternary complex factors by Rho family proteins. *EMBO J.* **16,** 6426–38 (1997).

131. Diekmann, D., Abo, A., Johnston, C., Segal, A. W. & Hall, A. INTERACTION OF RAC WITH P67(PHOX) AND REGULATION OF PHAGOCYTIC NADPH OXIDASE ACTIVITY. *Science (80-.).* **265,** 531–533 (1994).

132. Illenberger, D. *et al.* Stimulation of phospholipase C-beta2 by the Rho GTPases Cdc42Hs and Rac1. *Eur. Mol. Biol. Organ. J.* **17,** 6241–6249 (1998).

133. Weernink, P. A. O. *et al.* Activation of type I phosphatidylinositol 4-phosphate 5-kinase isoforms by the Rho GTPases, RhoA, Rac1, and Cdc42. *J. Biol. Chem.* **279,** 7840–7849 (2004).

134. Kato, K. *et al.* The inositol 5-phosphatase SHIP2 is an effector of RhoA and is involved in cell polarity and migration. *Mol. Biol. Cell* **23,** 2593–604 (2012).

135. Olson, M. F., Ashworth, A. & Hall, A. An essential role for Rho, Rac, and Cdc42 GTPases in cell cycle progression through G1. *Science (80-.).* **269,** 1270–1272 (1995).

136. Yamamoto, M. *et al.* ADP-ribosylation of the rhoA gene product by botulinum C3 exoenzyme causes Swiss 3T3 cells to accumulate in the G1 phase of the cell cycle. *Oncogene* **8,** 1449–1455 (1993).

137. Westwick, J. K. *et al.* Rac regulation of transformation, gene expression, and actin organization by multiple, PAK-independent pathways. *Mol. Cell. Biol.* **17,** 1324–1335 (1997).

138. Wittmann, T. & Waterman-Storer, C. M. Cell motility: can Rho GTPases and microtubules point the way? *J. Cell Sci.* **114,** 3795–3803 (2001).

139. Yasuda, S. *et al.* Cdc42 and mDia3 regulate microtubule attachment to kinetochores. *Nature* **428,** 767–771 (2004).

140. Glotzer, M. Animal cell cytokinesis. *Annu. Rev. Cell Dev. Biol.* **17,** 351–386 (2001).

141. Iden, S. & Collard, J. G. Crosstalk between small GTPases and polarity proteins in cell polarization. *Nat. Rev. Mol. Cell Biol.* **9,** 846–59 (2008).

142. Vega, F. M. & Ridley, A. J. Rho GTPases in cancer cell biology. *FEBS Lett.* **582,** 2093–2101 (2008).

143. Qiu, R. G., Chen, J., McCormick, F. & Symons, M. A role for Rho in Ras transformation. *Proc. Natl. Acad. Sci. U. S. A.* **92,** 11781–11785 (1995).

144. Qiu, R. G., Chen, J., Kirn, D., McCormick, F. & Symons, M. An essential role for Rac in Ras transformation. *Nature* **374,** 457–459 (1995).

145. Qiu, R. G., Abo, A., McCormick, F. & Symons, M. Cdc42 regulates anchorage-independent growth and is necessary for Ras transformation. *Mol. Cell. Biol.* **17,** 3449–3458 (1997).

146. Kamai, T., Arai, K., Tsujii, T., Honda, M. & Yoshida, K. Overexpression of RhoA mRNA is associated with advanced stage in testicular germ cell tumour. *BJU Int.* **87,** 227–231 (2001).

147. Van Golen, K. L., Wu, Z. F., Qiao, X. T., Bao, L. W. & Merajver, S. D. RhoC GTPase, a novel transforming oncogene for human mammary epithelial cells that partially recapitulates the inflammatory breast cancer phenotype. *Cancer Res.* **60,** 5832–5838 (2000).

148. Lin, R., Bagrodia, S., Cerione, R. & Manor, D. A novel Cdc42Hs mutant induces cellular transformation. *Curr. Biol.* **7,** 794–797 (1997).

149. Worthylake, R. A., Lemoine, S., Watson, J. M. & Burridge, K. RhoA is required for monocyte tail retraction during transendothelial migration. *J. Cell Biol.* **154,** 147–160 (2001).

150. Adamson, P., Etienne, S., Couraud, P. O., Calder, V. & Greenwood, J. Lymphocyte migration through brain endothelial cell monolayers involves signaling through endothelial ICAM-1 via a rho-dependent pathway. *J. Immunol.* **162,** 2964–2973 (1999).

151. Soede, R. D., Zeelenberg, I. S., Wijnands, Y. M., Kamp, M. & Roos, E. Stromal cell-derived factor-1-induced LFA-1 activation during in vivo migration of T cell hybridoma cells requires Gq/11, RhoA, and myosin, as well as Gi and Cdc42. *J. Immunol.* **166,** 4293–4301 (2001).

152. Clark, E. A., Golub, T. R., Lander, E. S. & Hynes, R. O. Genomic analysis of metastasis reveals an essential role for RhoC. *Nature* **406,** 532–5. (2000).

153. Huang, M. & Prendergast, G. C. RhoB in cancer suppression. *Histol. Histopathol.* **21,** 213–8 (2006).

154. Chen, Z. *et al.* Both farnesylated and geranylgeranylated RhoB inhibit malignant transformation and suppress human tumor growth in nude mice. *J. Biol. Chem.* **275,** 17974–8 (2000).

155. Adnane, J., Muro-Cacho, C., Mathews, L., Sebti, S. M. & Muñoz-Antonia, T. Suppression of rho B expression in invasive carcinoma from head and neck cancer patients. *Clin. Cancer Res.* **8,** 2225–32 (2002).

156. Aktories, K., Barbieri, J. T. & Baribieri, J. T. Bacterial Cytotoxins: Targeting Eukaryotic Switches. *Nat. Rev. Microbiol.* **3,** 397–410 (2005).

157. Aktories, K. Bacterial protein toxins that modify host regulatory GTPases. *Nat. Rev. Microbiol.* **9,** 487–498 (2011).

158. Just, I. *et al.* Glucosylation of Rho proteins by Clostridium difficile toxin B. *Nature* **375,** 500–503 (1995).

159. Aktories, K., Wilde, C. & Vogelsgesang, M. Rho-modifying C3-like ADP-ribosyltransferases. *Rev. Physiol. Biochem. Pharmacol.* **152,** 1–22 (2004).

160. Schmidt, G. *et al.* Gln 63 of Rho is deamidated by Escherichia coli cytotoxic necrotizing factor-1. *Nature* **387,** 725–9 (1997).

161. Flatau, G. *et al.* Toxin-induced activation of the G protein p21 Rho by deamidation of glutamine. *Nature* **387,** 729–733 (1997).

162. Han, X., Aslanian, A. & Yates 3rd, J. R. Mass spectrometry for proteomics. *Curr Opin Chem Biol* **12,** 483–490 (2008).

163. Aebersold, R. & Mann, M. Mass spectrometry-based proteomics. *Nature* **422,** 198–207 (2003).

164. Rappsilber, J., Ishihama, Y. & Mann, M. Stop and go extraction tips for matrix-assisted laser desorption/ionization, nanoelectrospray, and LC/MS sample pretreatment in proteomics. *Anal Chem* **75,** 663–670 (2003).

165. Fenn, J. B., Mann, M., Meng, C. K., Wong, S. F. & Whitehouse, C. M. Electrospray ionization for mass spectrometry of large biomolecules. *Science (80-.).* **246,** 64–71 (1989).

166. Zubarev, R. A. & Makarov, A. Orbitrap Mass Spectrometry. *Anal. Chem.* (2013). doi:10.1021/ac4001223

167. Perry, R. H., Cooks, R. G. & Noll, R. J. Orbitrap mass spectrometry: instrumentation, ion motion and applications. *Mass Spectrom. Rev.* **27,** 661–699 (2008).

168. Hu, Q. *et al.* The Orbitrap: a new mass spectrometer. *J. mass Spectrom. JMS* **40,** 430–443 (2005).

169. Makarov, A. Electrostatic axially harmonic orbital trapping: a high-performance technique of mass analysis. *Anal. Chem.* **72,** 1156–62 (2000).

170. Makarov, A., Denisov, E., Lange, O. & Horning, S. Dynamic range of mass accuracy in LTQ Orbitrap hybrid mass spectrometer. *J. Am. Soc. Mass Spectrom.* **17,** 977–982 (2006).

171. Makarov, A. *et al.* Performance evaluation of a hybrid linear ion trap/orbitrap mass spectrometer. *Anal. Chem.* **78,** 2113–20 (2006).

172. Michalski, A. *et al.* Mass spectrometry-based proteomics using Q Exactive, a high-performance benchtop quadrupole Orbitrap mass spectrometer. *Mol. Cell. proteomics MCP* **10,** M111.011015 (2011).

173. Steen, H. & Mann, M. The ABC's (and XYZ's) of peptide sequencing. *Nat. Rev. Mol. Cell Biol.* **5,** 699–711 (2004).

174. Ross, P. L. *et al.* Multiplexed protein quantitation in Saccharomyces cerevisiae using amine-reactive isobaric tagging reagents. *Mol. Cell. proteomics MCP* **3,** 1154–1169 (2004).

175. Gygi, S. P. *et al.* Quantitative analysis of complex protein mixtures using isotope-coded affinity tags. *Nat. Biotechnol.* **17,** 994–999 (1999).

176. Sury, M. D., Chen, J. X. & Selbach, M. The SILAC fly allows for accurate protein quantification in vivo. *Mol Cell Proteomics* **9,** 2173–2183 (2010).

177. Bantscheff, M., Schirle, M., Sweetman, G., Rick, J. & Kuster, B. Quantitative mass spectrometry in proteomics: a critical review. *Anal. Bioanal. Chem.* **389,** 1017–31 (2007).

178. Cox, J. & Mann, M. MaxQuant enables high peptide identification rates, individualized p.p.b.-range mass accuracies and proteome-wide protein quantification. *Nat Biotechnol* **26,** 1367–1372 (2008).

179. Cox, J. *et al.* A practical guide to the MaxQuant computational platform for SILAC-based quantitative proteomics. *Nat Protoc* **4,** 698–705 (2009).

180. Cox, J. *et al.* Andromeda: a peptide search engine integrated into the MaxQuant environment. *J. Proteome Res.* **10,** 1794–805 (2011).

181. Käll, L., Storey, J. D., MacCoss, M. J. & Noble, W. S. Assigning significance to peptides identified by tandem mass spectrometry using decoy databases. *J. Proteome Res.* **7,** 29–34 (2008).

182. Elias, J. E. & Gygi, S. P. Target-decoy search strategy for increased confidence in large-scale protein identifications by mass spectrometry. *Nat Methods* **4,** 207–214 (2007).

183. Käll, L., Storey, J. D., MacCoss, M. J. & Noble, W. S. Posterior error probabilities and false discovery rates: two sides of the same coin. *J. Proteome Res.* **7,** 40–4 (2008).

184. Käll, L., Storey, J. D. & Noble, W. S. Non-parametric estimation of posterior error probabilities associated with peptides identified by tandem mass spectrometry. *Bioinformatics* **24,** i42–8 (2008).

185. Selbach, M. *et al.* Widespread changes in protein synthesis induced by microRNAs. *Nature* **455,** 58–63 (2008).

186. Bonaldi, T. *et al.* Combined use of RNAi and quantitative proteomics to study gene function in Drosophila. *Mol. Cell* **31,** 762–72 (2008).

187. Stelzl, U. & Wanker, E. E. The value of high quality protein-protein interaction networks for systems biology. *Curr Opin Chem Biol* **10,** 551–558 (2006).

188. Krogan, N. J. *et al.* Global landscape of protein complexes in the yeast Saccharomyces cerevisiae. *Nature* **440,** 637–643 (2006).

189. Gavin, A.-C. *et al.* Proteome survey reveals modularity of the yeast cell machinery. *Nature* **440,** 631–636 (2006).

190. Rigaut, G. *et al.* A generic protein purification method for protein complex characterization and proteome exploration. *Nat Biotechnol* **17,** 1030–1032 (1999).

191. Söderberg, O. *et al.* Direct observation of individual endogenous protein complexes in situ by proximity ligation. *Nat. Methods* **3,** 995–1000 (2006).

192. Gu, G. J. *et al.* Protein tag-mediated conjugation of oligonucleotides to recombinant affinity binders for proximity ligation. *N. Biotechnol.* **30,** 144–52 (2013).

193. Christensen, J. J., Izatt, R. M. & Eatough, D. Thermodynamics of Metal Cyanide Coordination. V. Log K, ΔH°, and ΔS° Values for the Hg 2+ -CN- System. *Inorg. Chem.* **4,** 1278–1280 (1965).

194. Freyer, M. W. & Lewis, E. A. Isothermal titration calorimetry: experimental design, data analysis, and probing macromolecule/ligand binding and kinetic interactions. *Methods Cell Biol.* **84,** 79–113 (2008).

195. Truong, K. & Ikura, M. The use of FRET imaging microscopy to detect protein-protein interactions and protein conformational changes in vivo. *Curr. Opin. Struct. Biol.* **11,** 573–8 (2001).

196. Fields, S. & Song, O. A novel genetic system to detect protein-protein interactions. *Nature* **340,** 245–246 (1989).

197. Yu, H. Y. *et al.* High-quality binary protein interaction map of the yeast interactome network. *Science (80-.).* **322,** 104–110 (2008).

198. Deane, C. M., Salwiński, Ł., Xenarios, I. & Eisenberg, D. Protein interactions: two methods for assessment of the reliability of high throughput observations. *Mol. Cell. proteomics MCP* **1,** 349–356 (2002).

199. Smith, G. P. Filamentous fusion phage: novel expression vectors that display cloned antigens on the virion surface. *Science (80-.).* **228,** 1315–1317 (1985).

200. Gingras, A.-C. C., Gstaiger, M., Raught, B. & Aebersold, R. Analysis of protein complexes using mass spectrometry. *Nat Rev Mol Cell Biol* **8,** 645–654 (2007).

201. Vermeulen, M., Hubner, N. C. & Mann, M. High confidence determination of specific protein-protein interactions using quantitative mass spectrometry. *Curr Opin Biotechnol* **19,** 331–337 (2008).

202. Paul, F. E., Hosp, F. & Selbach, M. Analyzing protein-protein interactions by quantitative mass spectrometry. *Methods San Diego Calif* **54,** 387–395 (2011).

203. Köcher, T. & Superti-furga, G. Mass spectrometry – based functional proteomics : from molecular machines to protein networks. *Nat. Methods* **4,** 807–815 (2007).

204. Thakur, S. S. *et al.* Deep and Highly Sensitive Proteome Coverage by LC-MS/MS Without Prefractionation. *Mol. Cell. proteomics MCP* **10,** M110.003699 (2011).

205. Selbach, M. *et al.* Host cell interactome of tyrosine-phosphorylated bacterial proteins. *Cell Host Microbe* **5,** 397–403 (2009).

206. Selbach, M. & Mann, M. Protein interaction screening by quantitative immunoprecipitation combined with knockdown (QUICK). *Nat Methods* **3,** 981–983 (2006).

207. Hart, M. J. *et al.* Cellular transformation and guanine nucleotide exchange activity are catalyzed by a common domain on the dbl oncogene product. *J. Biol. Chem.* **269,** 62–65 (1994).

208. Burbelo, P. D. *et al.* p190-B, a new member of the Rho GAP family, and Rho are induced to cluster after integrin cross-linking. *J. Biol. Chem.* **270,** 30919–30926 (1995).

209. Baird, D., Feng, Q. & Cerione, R. A. The Cool-2/alpha-Pix protein mediates a Cdc42-Rac signaling cascade. *Curr. Biol.* **15,** 1–10 (2005).

210. Madaule, P. *et al.* A novel partner for the GTP-bound forms of rho and rac. *FEBS Lett.* **377,** 243–248 (1995).

211. Reid, T. *et al.* Rhotekin, a new putative target for Rho bearing homology to a serine/threonine kinase, PKN, and rhophilin in the rho-binding domain. *J. Biol. Chem.* **270,** 7359–7364 (1995).

212. Miki, H., Yamaguchi, H., Suetsugu, S. & Takenawa, T. IRSp53 is an essential intermediate between Rac and WAVE in the regulation of membrane ruffling. *Nature* **408,** 732–5 (2000).

213. Vaqué, J. P. *et al.* A genome-wide RNAi screen reveals a Trio-regulated Rho GTPase circuitry transducing mitogenic signals initiated by G protein-coupled receptors. *Mol. Cell* **49,** 94–108 (2013).

214. Delprato, A. Topological and functional properties of the small GTPases protein interaction network. *PLoS One* **7,** e44882 (2012).

215. Sambrook, J., Fritsch, E. F. & Maniatis, T. *Molecular Cloning: A Laboratory Manual. Cold Spring Harbor laboratory press*. *New York* 931–957 (Cold Spring Harbor, 1989).

216. PREMIER Biosoft. at <http://www.premierbiosoft.com/>

217. Tucker, J. *et al.* Expression of p21 proteins in Escherichia coli and stereochemistry of the nucleotide-binding site. *EMBO J.* **5,** 1351–8 (1986).

218. Lenzen, C., Cool, R. H. & Wittinghofer, A. Analysis of intrinsic and CDC25-stimulated guanine nucleotide exchange of p21ras-nucleotide complexes by fluorescence measurements. *Methods Enzymol.* **255,** 95–109 (1995).

219. Bradford, M. M. A rapid and sensitive method for the quantitation of microgram quantities of protein utilizing the principle of protein-dye binding. *Anal. Biochem.* **72,** 248–54 (1976).

220. Gasteiger, E. *et al. The Proteomics Protocols Handbook*. *Digestion* 571–607 (Humana Press, 2005). doi:10.1385/1592598900

221. Ishihama, Y., Rappsilber, J., Andersen, J. S. & Mann, M. Microcolumns with self-assembled particle frits for proteomics. *J Chromatogr A* **979,** 233–239 (2002).

222. Kelstrup, C. D., Young, C., Lavallee, R., Nielsen, M. L. & Olsen, J. V. Optimized Fast and Sensitive Acquisition Methods for Shotgun Proteomics on a Quadrupole Orbitrap Mass Spectrometer. *J. Proteome Res.* (2012). doi:10.1021/pr3000249

223. Tusher, V. G., Tibshirani, R. & Chu, G. Significance analysis of microarrays applied to the ionizing radiation response. *Proc. Natl. Acad. Sci. U. S. A.* **98,** 5116–21 (2001).

224. Huang, D. W., Sherman, B. T. & Lempicki, R. A. Systematic and integrative analysis of large gene lists using DAVID bioinformatics resources. *Nat. Protoc.* **4,** 44–57 (2009).

225. Magrane, M. & Consortium, U. UniProt Knowledgebase: a hub of integrated protein data. *Database (Oxford).* **2011,** bar009 (2011).

226. Larkin, M. A. *et al.* Clustal W and Clustal X version 2.0. *Bioinformatics* **23,** 2947–8 (2007).

227. Goody, R. S. & Eckstein, F. Thiophosphate analogs of nucleoside di- and triphosphates. *J. Am. Chem. Soc.* **93,** 6252–6257 (1971).

228. Cherfils, J. *et al.* Crystal structures of the small G protein Rap2A in complex with its substrate GTP, with GDP and with GTPgammaS. *EMBO J.* **16,** 5582–91 (1997).

229. Self, A. J. & Hall, A. [1] Purification of recombinant Rho/Rac/G25K from Escherichia coli. *Methods Enzymol.* **256,** 3–10 (1995).

230. De Ruiter, G. A., Smid, P., Schols, H. A., Van Boom, J. H. & Rombouts, F. M. Detection of fungal carbohydrate antigens by high-performance immunoaffinity chromatography using a protein A column with covalently linked immunoglobulin G. *J. Chromatogr.* **584,** 69–75 (1992).

231. Frost, R. G., Monthony, J. F., Engelhorn, S. C. & Siebert, C. J. Covalent immobilization of proteins to N-hydroxysuccinimide ester derivatives of agarose. Effect of protein charge on immobilization. *Biochim. Biophys. Acta* **670,** 163–9 (1981).

232. Gottlieb, A. B., Seide, R. K. & Kindt, T. J. Quantitative determination of allotypic and idiotypic markers with antisera coupled to N-hydroxysuccinimide-activated sepharose. *J. Immunol.* **114,** 51–4 (1975).

233. Ong, S. E. & Mann, M. A practical recipe for stable isotope labeling by amino acids in cell culture (SILAC). *Nat Protoc* **1,** 2650–2660 (2006).

234. Bustelo, X. R., Sauzeau, V. & Berenjeno, I. M. GTP-binding proteins of the Rho/Rac family: regulation, effectors and functions in vivo. *Bioessays* **29,** 356–70 (2007).

235. Park, S.-S. *et al.* Effective correction of experimental errors in quantitative proteomics using stable isotope labeling by amino acids in cell culture (SILAC). *J. Proteomics* **75,** 3720–32 (2012).

236. Hill, C. S., Wynne, J. & Treisman, R. The Rho family GTPases RhoA, Racl , and CDC42Hsregulate transcriptional activation by SRF. *Cell* **81,** 1159–1170 (1995).

237. Adra, C. N. *et al.* Identification of a novel protein with GDP dissociation inhibitor activity for the ras-like proteins CDC42Hs and rac I. *Genes. Chromosomes Cancer* **8,** 253–61 (1993).

238. Kruger, M. *et al.* SILAC mouse for quantitative proteomics uncovers kindlin-3 as an essential factor for red blood cell function. *Cell* **134,** 353–364 (2008).

239. Hubner, N. C. *et al.* Quantitative proteomics combined with BAC TransgeneOmics reveals in vivo protein interactions. *J Cell Biol* **189,** 739–754 (2009).

240. Uhlen, M. *et al.* Towards a knowledge-based Human Protein Atlas. *Nat. Biotechnol.* **28,** 1248–50 (2010).

241. Tan, I., Yong, J., Dong, J. M., Lim, L. & Leung, T. A tripartite complex containing MRCK modulates lamellar actomyosin retrograde flow. *Cell* **135,** 123–36 (2008).

242. Medina, F. *et al.* Activated RhoA is a positive feedback regulator of the Lbc family of Rho guanine nucleotide exchange factor proteins. *J. Biol. Chem.* **288,** 11325–33 (2013).

243. Schaefer, M. H. *et al.* HIPPIE: Integrating protein interaction networks with experiment based quality scores. *PLoS One* **7,** e31826 (2012).

244. Coll, P. M., Rincon, S. A., Izquierdo, R. A. & Perez, P. Hob3p, the fission yeast ortholog of human BIN3, localizes Cdc42p to the division site and regulates cytokinesis. *EMBO J.* **26,** 1865–77 (2007).

245. Weibrecht, I. *et al.* Proximity ligation assays: a recent addition to the proteomics toolbox. *Expert Rev. Proteomics* **7,** 401–9 (2010).

246. Lockman, H. A., Gillespie, R. A., Baker, B. D. & Shakhnovich, E. Yersinia pseudotuberculosis produces a cytotoxic necrotizing factor. *Infect. Immun.* **70,** (2002).

247. Sun, Y.-J. *et al.* Solo/Trio8, a membrane-associated short isoform of Trio, modulates endosome dynamics and neurite elongation. *Mol. Cell. Biol.* **26,** 6923–35 (2006).

248. Leung, T., Manser, E., Tan, L. & Lim, L. A novel serine/threonine kinase binding the Ras-related RhoA GTPase which translocates the kinase to peripheral membranes. *J. Biol. Chem.* **270,** 29051–4 (1995).

249. Vignal, E., Blangy, A., Martin, M., Gauthier-Rouvière, C. & Fort, P. Kinectin is a key effector of RhoG microtubule-dependent cellular activity. *Mol. Cell. Biol.* **21,** 8022–34 (2001).

250. Jaffe, A. B., Aspenstrom, P. & Hall, A. Human CNK1 Acts as a Scaffold Protein, Linking Rho and Ras Signal Transduction Pathways. *Mol. Cell. Biol.* **24,** 1736–1746 (2004).

251. Sasaki, T., Kato, M. & Takai, Y. Consequences of weak interaction of rho GDI with the GTP-bound forms of rho p21 and rac p21. *J. Biol. Chem.* **268,** 23959–63 (1993).

252. Ridley, A. J. Rho-related proteins: actin cytoskeleton and cell cycle. *Curr. Opin. Genet. Dev.* **5,** 24–30 (1995).

253. Niedergang, F. & Chavrier, P. Regulation of phagocytosis by Rho GTPases. *Curr. Top. Microbiol. Immunol.* **291,** 43–60 (2005).

254. Bishop, A. L. & Hall, A. Rho GTPases an their effector proteins. *Biochem. J.* **348,** 241–255 (2000).

255. Zhu, M. *et al.* Septin 7 interacts with centromere-associated protein E and is required for its kinetochore localization. *J. Biol. Chem.* **283,** 18916–25 (2008).

256. De Kreuk, B.-J. *et al.* The F-BAR domain protein PACSIN2 associates with Rac1 and regulates cell spreading and migration. *J. Cell Sci.* **124,** 2375–88 (2011).

257. Bandyopadhyay, S. *et al.* A human MAP kinase interactome. *Nat. Methods* **7,** 801–5 (2010).

258. Ishizaki, T. *et al.* The small GTP-binding protein Rho binds to and activates a 160 kDa Ser/Thr protein kinase homologous to myotonic dystrophy kinase. *EMBO J.* **15,** 1885–93 (1996).

259. Manser, E. *et al.* Diversity and versatility of GTPase activating proteins for the p21rho subfamily of ras G proteins detected by a novel overlay assay. *J. Biol. Chem.* **267,** 16025–8 (1992).

260. Swiercz, J. M., Kuner, R., Behrens, J. & Offermanns, S. Plexin-B1 Directly Interacts with PDZ-RhoGEF/LARG to Regulate RhoA and Growth Cone Morphology. *Neuron* **35,** 51–63 (2002).

261. Chang, L., Adams, R. D. & Saltiel, A. R. The TC10-interacting protein CIP4/2 is required for insulin-stimulated Glut4 translocation in 3T3L1 adipocytes. *Proc. Natl. Acad. Sci. U. S. A.* **99,** 12835–40 (2002).

262. Watanabe, N. *et al.* p140mDia, a mammalian homolog of Drosophila diaphanous, is a target protein for Rho small GTPase and is a ligand for profilin. *EMBO J.* **16,** 3044–56 (1997).

263. Aspenström, P. & Olson, M. F. Yeast two-hybrid system to detect protein-protein interactions with Rho GTPases. *Methods Enzymol.* **256,** 228–41 (1995).

264. Lynch, E. A., Stall, J., Schmidt, G., Chavrier, P. & D'Souza-Schorey, C. Proteasome-mediated degradation of Rac1-GTP during epithelial cell scattering. *Mol. Biol. Cell* **17,** 2236–42 (2006).

265. Montani, L., Bausch-Fluck, D., Domingues, A. F., Wollscheid, B. & Relvas, J. B. Identification of new interacting partners for atypical Rho GTPases: a SILAC-based approach. *Methods Mol. Biol.* **827,** 305–17 (2012).

266. Hattori, Y. *et al.* Identification of a neuron-specific human gene, KIAA1110, that is a guanine nucleotide exchange factor for ARF1. *Biochem. Biophys. Res. Commun.* **364,** 737–742 (2007).

267. Dunphy, J. L. *et al.* The Arf6 GEF GEP100/BRAG2 regulates cell adhesion by controlling endocytosis of beta1 integrins. *Curr. Biol.* **16,** 315–20 (2006).

268. Cotteret, S., Jaffer, Z. M., Beeser, A. & Chernoff, J. p21-Activated kinase 5 (Pak5) localizes to mitochondria and inhibits apoptosis by phosphorylating BAD. *Mol. Cell. Biol.* **23,** 5526–39 (2003).

269. Ishihara, N., Fujita, Y., Oka, T. & Mihara, K. Regulation of mitochondrial morphology through proteolytic cleavage of OPA1. *EMBO J.* **25,** 2966–77 (2006).

270. Khosravi-Far, R., Solski, P. A., Clark, G. J., Kinch, M. S. & Der, C. J. Activation of Rac1, RhoA, and mitogen-activated protein kinases is required for Ras transformation. *Mol. Cell. Biol.* **15,** 6443–53 (1995).

271. Pruitt, K. & Der, C. J. Ras and Rho regulation of the cell cycle and oncogenesis. *Cancer Lett.* **171,** 1–10 (2001).

272. Adamson, P., Marshall, C. J., Hall, A. & Tilbrook, P. A. Post-translational modifications of p21rho proteins. *J. Biol. Chem.* **267,** 20033–8 (1992).

273. Adamson, P., Paterson, H. F. & Hall, A. INtracellular localization of the P21rho proteins. *J. Cell Biol.* **119,** (1992).

274. Prendergast, G. C. Actin' up: RhoB in cancer and apoptosis. *Nat. Rev. Cancer* **1,** 162–168 (2001).

275. Fritz, G. & Kaina, B. Rho GTPases: promising cellular targets for novel anticancer drugs. *Curr. Cancer Drug Targets* **6,** 1–14 (2006).

276. Ridley, A. J. Rho proteins and cancer. *Breast Cancer Res. Treat.* **84,** 13–9 (2004).

277. Du, W., Lebowitz, P. F. & Prendergast, G. C. Cell growth inhibition by farnesyltransferase inhibitors is mediated by gain of geranylgeranylated RhoB. *Mol. Cell. Biol.* **19,** 1831–40 (1999).

278. Du, W. & Prendergast, G. C. Geranylgeranylated RhoB mediates suppression of human tumor cell growth by farnesyltransferase inhibitors. *Cancer Res.* **59,** 5492–6 (1999).

279. Zeng, P.-Y., Rane, N., Du, W., Chintapalli, J. & Prendergast, G. C. Role for RhoB and PRK in the suppression of epithelial cell transformation by farnesyltransferase inhibitors. *Oncogene* **22,** 1124–34 (2003).

280. Kamasani, U. *et al.* Cyclin B1 is a critical target of RhoB in the cell suicide program triggered by farnesyl transferase inhibition. *Cancer Res.* **64,** 8389–96 (2004).

281. Kamasani, U. & Liu, A. Genetic Response to Farnesyltransferase Inhibitors: Proapoptotic Targets of RhoB. *Cancer Biol. Ther.* **2,** 271–278 (2003).

282. Diviani, D., Soderling, J. & Scott, J. D. AKAP-Lbc anchors protein kinase A and nucleates Galpha 12-selective Rho-mediated stress fiber formation. *J. Biol. Chem.* **276,** 44247–57 (2001).

283. Lind, S. E. & Janmey, P. A. Human plasma gelsolin binds to fibronectin. *J. Biol. Chem.* **259,** 13262–6 (1984).

284. Kusano, H. *et al.* Human gelsolin prevents apoptosis by inhibiting apoptotic mitochondrial changes via closing VDAC. *Oncogene* **19,** 4807–14 (2000).

285. Mazières, J. *et al.* Geranylgeranylated, but not farnesylated, RhoB suppresses Ras transformation of NIH-3T3 cells. *Exp. Cell Res.* **304,** 354–64 (2005).

286. Prigent, M. *et al.* ARF6 controls post-endocytic recycling through its downstream exocyst complex effector. *J. Cell Biol.* **163,** 1111–21 (2003).

287. Cosson, P. & Letourneur, F. Coatomer interaction with di-lysine endoplasmic reticulum retention motifs. *Science* **263,** 1629–31 (1994).

Curriculum Vitae

For reasons of data protection, the curriculum vitae is not included in the online version.

Aus datenschutzrechtlichen Gründen entfällt der Lebenslauf in der Online-Version.

Publications

Published articles

- Welcker JE, Hernandez-Miranda LR, **Paul FE**, Jia S, Ivanov A, Selbach M, Birchmeier C.
  Insm1 controls development of pituitary endocrine cells and requires a SNAG domain for function and for recruitment of histone-modifying factors.
  Development **140,** 4947–58 (2013).

- **Paul FE**, Hosp F, Selbach M.
  Analyzing protein-protein interactions by quantitative mass spectrometry.
  Methods San Diego Calif **54,** 387–395 (2011).

- Grossmann KS, Wende H, **Paul FE**, Cheret C, Garratt AN, Zurborg S, Feinberg K, Besser D, Schulz H, Peles E, Selbach M, Birchmeier W, Birchmeier C.
  The tyrosine phosphatase Shp2 (PTPN11) directs Neuregulin-1/ErbB signaling throughout Schwann cell development.
  Proc. Natl. Acad. Sci. U. S. A. **106,** 16704–9 (2009).

- Selbach M, **Paul FE**, Brandt S, Guye P, Daumke O, Backert S, Dehio C, Mann M.
  Host cell interactome of tyrosine-phosphorylated bacterial proteins.
  Cell Host Microbe **5,** 397–403 (2009).

Manuscripts under editorial consideration

- **Paul FE**, Zauber H, Daumke O, Selbach M
  Quantitative GTPase affinity purification identifies Rho family interaction partners

Acknowledgement

During the time at the Max-Delbrück-Centrum I received a lot of support from people that helped me to develop myself as a scientist and to master this thesis.

First cheers go to **Prof. Matthias Selbach**. After we met in the MPI for Biochemistry he became my most important scientific mentor. I especially want to thank him for educating me in technical and scientific ways through the last years. Most important for me was to understand how a 'scientist thinks', meaning the design of experiments and the critical discussion and presentation of results. In addition, I want to thank him for the topic of this thesis and the possibility to gain an insight into the world of mass spectrometry.

Next, I want to thank **Prof. Udo Heinemann** for accepting supervision for my thesis at Freie Universität Berlin. **Prof. Oliver Daumke** was my most important cooperation partner in the last years, he and his group helped with protein purification, enzymes and a lot of input. The technical realization of experiments was supported by **Martha Hergeselle**, **Christian Sommer** and **Sabine Werner**. The 'know-how' of these three was an important help for the PLA experiments, protein purification and general mass spectrometric analysis.

A lot of thanks go to **Dr. Eva Rosenbaum**, **Dr. Katrin Eichelbaum**, **Rebecca Eccles**, **Dr. Henrik Zauber** and **Dr. Claudio Shah** for critically discussing the manuscript of the thesis and providing me with ideas for formulating the scientific outcome. Dr. Henrik Zauber contributed two figures to this thesis (Figure 3.20, Figure 3.21).

Prof. Anne Ridley and **Dr. Oliver Rocks** contributed with constructs and valuable scientifc discussion. I am deeply obliged to my cooperation partners **Dr. Katja Grossmann**, **Dr. Jochen Welcker** and **Prof. Carmen Birchmeier**. Many thanks go to the BIMSB and all its members. I want to thank **Prof. Kris Gunsalus** and **Prof. Fabio Piano** for giving me the opportunity to learn about the C. elegans system in their lab in New York and for disscusing the in vivo IP project.

A lot of thanks go to the MDC in general and specifically to the graduate school of the very professional Molecular Cell Biology program and the administration. I want to thank for continued funding and for the opportunity to take part in additional courses and lectures.

A lot of other scientists and friends (significant overlap) were involved in creation of my PhD thesis. Special thanks go to the Selbach lab members and visitors of the last years: **Liffey**, **Marie**, **Katrin**, **Sharbani**, **Christian**, **Björn**, **Thiess**, **Fabian**, **Jimmy**, **Erik**, **Murat**, **Henrik**, **Đorđe** and **Piotr**. I realized that I spent most of the last years with you people, starting from the famous Monday morning seminar (don't fall asleep, Christian), the ritual every day lunch (no second too late), high level fights for the 'inteligent statement'- redflag, a vivid music exchange in the lab (louder, please) and dry ice experiments (fortunately all ten fingers are still present, Erik and Đorđe). We also shared the rather tough moments in a scientists life: not always optimally running machines that could have won the nobel prize for unexpectedly opening a black hole in which prestigious samples disappeared, successful projects ('offgel' – a little machine that sometimes appears in my worst nightmares, what do you think about it, Liffey?), contaminations in the worm culture (nobody works more clean than you, Jimmy) and an office that anticipated climate change and prepared us for living in the Sahara

(condolences go to Liffey, Marie, Christian, Thiess, Fabian and Björn). The effects of this heat shock were often counteracted by spending endless days in the ms dungeons, aka fridge (very big thanks to Christian for endless patience). However, we knew how to make life more comfortable (e.g. by carrying a sofa from Schöneberg to Buch, do you remember, Erik?). To compensate for these challenges neurons were stimulated with pulses of coffein and EtOH (LiChrosolv/Russian Standard grade or Rakia, thanks to Đorđe or Caipi, p.a. in der Hafenbar mit Thiess).

Apart from our lab the MDC became a place in which I did not only spent a lot of time, but which I also learnt to love. Many memories will remain – the organization of the PhD retreat 2009, the organization of two Checkup parties, endless beer hours, shared lunch breaks and coffee hours and of course some unforgetable kite holidays – **Claudio**, **FloM**, **Eva**, **Guschdl**, **Jule**, **Kathrin** and **many more** – we had a great time!

Many thanks to the friends with whom I spent so much time in the last years, either in Berlin or during travels in Asia and who supported me so much – **Tobi** & **Anne**, **Christian** & **Lotta**, **Dušica**. Greetings also to the old Tübingen crew – **Dirk**, **Freddy**, **Oswin**, **Björn** and **Chris**.

Great thanks go to the masters of the administration **Petra**, **Jennifer**, **Sabine** and **Sonja** for taking care of all the small and big issues of German bureaucracy.

Last but not least to mention, my close family supported me through all the years namely my parents **Rosa** and **Rudi** and my brother **Alex**. Without your help this thesis would not have been created.

Declaration

I hereby declare, the present thesis “Developing quantitative GTPase affinity purification (qGAP) to identify interaction partners of Rho GTPases” is my own work and effort. It has not been submitted to any other university for any award. Where other sources of information have been used, they have been acknowledged.

Berlin, January 2014

Florian Paul